Adaptive NK cell Memory and Nucleosome Interference:
Two Tales of the Ly49 Receptor Family

by

Andrew Wight

A thesis submitted in partial fulfillment of the requirements
for a Doctorate of Philosophy in Immunology

Department of Biochemistry, Microbiology, and Immunology
Faculty of Medicine
University of Ottawa

Supervisor
Dr. Andrew P. Makrigiannis

Co-supervisor
Dr. Subash Sad

Abstract

Ly49 receptors are the canonical natural killer cell class-I major histocompatibility complex receptors expressed in mice. They have a well-defined role in natural killer cell self/non-self discrimination and in the developmental licensing of functional natural killer cells. In this thesis, I report two novel aspects of Ly49 receptor biology. First, I show that their expression may be regulated by specific nucleosome occupancy on AML-1 binding sites within the distal Ly49 promoter. This finding sheds light on a potential regulatory pathway that has thus far been unexplored in studies of the Ly49 receptor family, and highlights the Ly49 family as an ideal model system in which to study the impact of nucleosome occupancy in general. Second, I show that Ly49 receptors have a central and indispensable role in the emerging phenomenon known as adaptive natural killer cell memory. Natural killer cells have recently been observed displaying adaptive, long-lived, antigen specific memory responses comparable to T cell memory responses, but no explanatory mechanism has been discovered to describe how adaptive memory is possible in these 'innate' immune cells. Using Ly49-deficient mice, I show that the inhibitory, self-specific Ly49 receptors Ly49C and Ly49I are required for adaptive memory responses to chemical haptens or protein antigens. Moreover, I show that Ly49C/I binding capabilities are required during all stages of the memory response, as is antigen presentation in the context of class I major histocompatibility complex, again analogous to T cell memory responses. I present initial findings implicating these Ly49 receptors as key components of the antigen recognition process itself, and propose a mechanism based in evolutionarily ancient immunology to explain how this specificity could arise. Finally, I demonstrate that Ly49-dependent natural killer cell memory is capable of mediating powerful anti-cancer vaccination effects using an aggressive model of melanoma. Together, these findings in Ly49 family expression regulation and its functional role in adaptive NK cell responses open several new avenues of study in Ly49 receptor biology and natural killer cell immunology.

It is a precondition of being a conformist that the conformist not know that he is merely conforming. Once he comes to know that, the glass of conformity is fractured and the damage is irreparable. It cannot be reassembled using the techniques of restoration and renovation, but must rather be melted down in the fire and created all over again.

- Abu Hamad al-Ghazali

Acknowledgements

First, I extend my thanks and appreciation to Dr. Andrew Makrigiannis, my mentor and supervisor these past years. You took a huge risk when I landed in your office and said I wanted to study NK cell memory—an impossible phenotype without a shred of an explanatory mechanism—but thanks to your guidance and support, it paid off. For everything you've taught me, and everything we've created together, thank you.

I also thank Dr. Subash Sad for his generous support in the last years of my research. You went above and beyond in helping me to complete my work, even going so far as opening your lab to me when I needed space to finish my studies. Words cannot express my gratitude.

I thank Dr. Mir Munir Rahim—your patience, wisdom, and expertise were crucial to every part of this thesis, which could not have happened without you there to guide me. For teaching me so much about science—and incidentally, so much about sushi—thank you.

I thank all of my fellow lab mates in both Dr. Makrigiannis and Dr. Sad's lab. Megan, Ahmad, Elias, Mike, Angela, Haggag, Pati, Kim, Norah, Ardeshir, Stephanie, David, Dikchha, and Emmanuelle—you have been a second family to me throughout these projects, and every word of this thesis is steeped in your help, support, and encouragement. Thank you.

I thank Drs. Angela Crawley and Nadine Wiper-Bergeron, for their support along with Dr. Sad as my advisory committee. You helped me to navigate the transition to a PhD student, and provided an abundance of support and encouragement. I never dreaded a single TAC meeting, but instead looked forward to our yearly discussions with excitement. Thank you.

I thank Drs. Ilya Ioshikhes and Doo Yang—what began as a curious look at Ly49 promoters became a fruitful collaboration, which would not have happened without your generous supply of bioinformatics knowledge and tools. It was great working with you.

I thank Dr. Mona Nemer, and everyone in her lab. You did more than just provide ear-measuring calipers (though I am very appreciative that you did that!), you were my friends, my support, my collaborators, and my 'lab-away-from-lab'. Thank you.

I thank Dr. Holly Orlando, Marie Bedard, Tami Janveau, and everyone at ACVS. You taught me essential mouse skills, and allowed me to participate in animal ethics on an impactful level. Thank you.

I thank Drs. Vera Tang, Marc-Andre Langlois, and Lionel Filion. Your care and guidance has helped me hone my skills at all of immunology, not just flow cytometry. Thank you.

I thank Fay and Victoria, and everyone at the graduate studies office. I wasn't always the easiest student to work with, and your patience and assistance when I was faced with bureaucratic tangles was every bit as important to this work as the scientific support I have received. Thank you.

Finally, I thank my family, especially my parents and my wife Irenee. I have weathered the storms of this research on the rock of love and support that you have provided; you are every bit as present in this work as I am. From the bottom of my heart, thank you.

Contents

List of Abbreviations

%GC	Percent guanine-cytosine content
AIDS	Acquired immunodeficiency syndrome
AML-1	Acute myeloid leukemia factor 1
ANOVA	Analysis of variance
AP-1	Activator protein 1
ATAC-Seq	Assay for transposase-accessible chromatin and sequencing
B cell	Bursa cell
B16F10	B16 melanoma, sub-line F10
BCR	B cell receptor
BED	Browser extensible data
bp	Base-pairs
C/EBP	CCAAT/enhancer binding protein
CD	Cluster of differentiation (followed by a number)
c-ETS	Avian erythroblastosis virus oncogene homologue 1
ChIP	Chromatin immunoprecipitation
Clr	C-type lectin receptor
CMV	Cytomegalovirus
CpG	Cytosine-phosphate-Guanine
CXCR6	Chemokine receptor with CXC motif number 6
DAP12	DNAX-activation protein 12
DMEM	Dulbecco's modified Eagle's medium
DNA	Deoxyribonucleic acid
DNA-PKcs	DNA-dependent protein kinase, catalytic subunit
DNFB	2,4-dinitrofluorobenzene
dsRNA	double-stranded RNA
Eat-2	EWS/FLI1-activated transcript 2
Egr-1 & -2	Early growth response 1 & 2
ELISA	Enzyme-linked immunoadsorbant assay
F(ab')$_2$	Fragment antigen-binding, including hinge region, bi-valent (of an antibody)
FACS	Fluorescence-activated cell sorting
FasL	FAS cell surface death receptor Ligand
FBS	Fetal bovine serum
Fc	Fragment crystalizable (of an antibody)
FcεRγ1	Fc epsilon receptor gamma 1
FIMO	Find individual motif occurrence
Fu/HC	Fusability/histocompatibility locus
g-	FcεRγ1-negative NK cells

gamma-H2AX	S139-phosphorylated H2A histone family member X
GATA3	GATA-binding factor 3
GEO	Gene expression omnibus
GM-CSF	Granulocyte/monocyte colony stimulating factor
H&E	Hematoxylin and Eosin stain
H-2	Histocompatibility locus 2 (followed by gene and/or haplotype designation)
H3K9Ac	Histone subunit 3, Lysine 9 acetylation
HEPES	(4-(2-hydroxyethyl)-1-piperazineethanesulfonic acid
HIV	Human immunodeficiency virus
HLA	Human leukocyte antigen
HSP60	Heat-shock protein 60
IFNγ	Interferon gamma
IgG & IgE	Immunoglobulin G & E
Ik-3	Ikaros-family zinc finger-containing protein 3
IL	Interleukin (followed by a number)
Irf-1	Interferon regulatory factor 1
ITAM	Immunoreceptor tyrosine-based activating motif
Itg	Ly49I-transgenic
ITIM	Immunoreceptor tyrosine-based inhibitory motif
kb	kilobase
KIR	Killer-cell immunoglobulin-like receptor
Lck	Lymphocyte-specific protein tyrosine kinase
LFA-1	Lymphocyte function-associated antigen 1
L-selectin	Leukocyte selectin
Ly49	Lymphocyte antigen 49
Ly49KD	Ly49 knock-down
Lyf-1	Lymphoid transcription factor 1
MCMV	Mouse CMV
MHC-I & -II	Major histocompatibility complex I & II
MNase	Micrococcal nuclease
MNase-Seq	MNase sequencing
MZF-1	Myeloid zinc-finger-containing factor 1
NF-AT	Nuclear factor of activated T cells
NFκB	Nuclear factor kappa-B
NK cell	Natural Killer cell
NK1.1	NK antigen 1, variant 1 (antibody)
NKC	NK gene cluster
NKG2	NK gene family 2 (followed by a letter designation)
NKp46	NK protein of 46 kilodaltons

NKR-P1	NK receptor P1 (followed by a letter designation)
NK-T	Natural killer T cell
Oct-1	Octamer-binding transcription factor 1
Ova-I	SIINFEKL peptide
Ova-II	ISQAVHAAHAEINEAGR peptide
OXA	Oxazolone
PBS	Phosphate-buffered saline
piRNA	Piwi-interacting RNA
PLoS	Public library of science
Pro1 & 2	Promoters 1 & 2
PWM	Position-weight matrix
qPCR	quantitative polymerase chain reaction
RAG	Recombination-activating gene
RMA	RMA-sub-line of EL4 cells
RMA-S	(NK)-susceptible RMA
RNA	Ribonucleic acid
RNA-Seq	RNA-sequencing
SCID	Severe combined immunodeficiency disorder
SDS-PAGE	Sodium dodecyl sulfate-protein acrylamide gel electrophoresis
SH2	Src homology 2 domain
SHIP	SH2 domain-containing inositol 5'-phosphatase
SHP	SH2 domain-containing phosphatase
Sp1	Specificity protein 1
STAT3	Signal transducer and activator of transcription 3
Syk	Spleen tyrosine kinase
T cell	Thymus cell
Tal-1a	Tarsal-less 1A-like factor
TAP	Transporter associated with antigen processing
TATA	TA-repeat-rich sequence
TB	Tuberculosis
TBP	TATA-like binding protein
TCR	T cell receptor
TFBS	Transcription factor binding site
Thy1	Thymus cell antigen 1
TNF	Tumour necrosis factor
TRAIL	Tumor necrosis factor apoptosis-inducing ligand

List of Figures

1: Introduction

1.1: Conventional Natural Killer Cell Biology

1.1.1: Natural killer cells

Natural killer (NK) cells are a key cytotoxic component of the first-line immune defense against viruses and tumours. These cells are part of the innate lymphoid group of lymphocytes[1]. As innate immune cells, NK cells can participate in immune responses by reacting to danger signals, such as type I interferons secreted by virus-infected cells or interleukin 12 (IL-12) produced by activated myeloid cells, and pathogenic molecular patterns, such as unmethylated CpG-rich DNA sequences or double-stranded RNA molecules[2,3]. NK cells can also express a number of activating receptors for specific pathogenic ligands, such as Ly49H which allows for direct recognition of mouse cytomegalovirus (MCMV) by interacting with the viral protein m157[4].

Like their adaptive counterpart, the cytotoxic $CD8^+$ T cell, NK cells typically respond to nascent tumours or intracellular pathogens such as viruses. NK cell responses are therefore intended to kill offending self-cells. Upon activation, the NK cell has numerous mechanisms to kill its target, including crosslinking target cell death domain-containing receptors such as FasL and TRAIL[5] and release of cytotoxic granules. These granules contain perforin—a protein that creates pores in the target cell's membrane—and granzymes, which enter the perforin-created pores and directly activate executioner caspases, leading to cell death independent of an intact cell death pathway in the target[6].

In addition to its cytotoxic effects, the NK cell can secrete immune modulating cytokines when activated, including antiviral proteins such as interferon gamma (IFNγ)[7], inflammatory

mediators such as tumor necrosis factor (TNF)[8], and immune recruiting factors such as granulocyte/monocyte colony-stimulating factor (GM-CSF)[9]. The specific cytokines produced by the NK cell will depend on the quality of the activation signals received by the cell; however, IFNγ is the classic NK cell cytokine and is produced in response to a wide variety of activating signals[7]. IFNγ is the master regulator of the type I immune response, which is the immune response needed to clear intracellular infections and to kill mutated self-cells. IFNγ recruits and activates monocytes and T cells, increases transcription of type I response genes such as IL-12, promotes B cell class-switching to favour IgG antibodies over IgE, increases expression of antigen presenting and T cell-activating genes such as the major histocompatibility complexes and co-stimulatory B7 genes, and suppresses the activity of IL-4, preventing the immune system from polarizing to type 2 responses during a type 1 response[7]. Through its IFNγ expression, the NK cell can orchestrate an entire type 1 immune response.

Although NK cells can participate in this classic type of innate immune response, where inflammatory cytokines and danger signals induce a potent cellular response, the NK cell is unique in that it can also perform its cytotoxic and immunomodulatory functions in the apparent absence of any inflammatory or activating signals. This natural cytotoxicity allows the NK cell to respond to virus infections and cancerous transformations before they have gotten bad enough to induce danger signals, and so exists as one of the most potent tools available to the immune system for preserving homeostasis and performing preventative immune surveillance. To achieve this sub-inflammatory recognition, the NK cell expresses a battery of activating and inhibitory receptors. Some of the activating receptors recognize signs of infection, such as Ly49H recognizing the cytomegalovirus ligand m157[4] or NKp46 reacting to the complement cascade[10]. Others, however, detect signs of cellular stress, such as NKG2D, which recognizes fragments of

proteins including those interacting with the chaperone protein HSP60, indicative of a higher than normal level of misfolded proteins in the target cell[11].

Conversely, the inhibitory NK cell receptors recognize health markers. The most famous of these are the Ly49 family receptors in mice, or their functional equivalent, the killer-cell immunoglobulin-like receptor (KIR) family in humans. Inhibitory Ly49 or KIR proteins recognize class I major histocompatibility complex (MHC-I) molecules on their target, and interpret robust MHC-I expression as a sign of health[12,13]. Similarly, many subsets of cells express the C-type lectin receptor (Clr) family of molecules, which are detected by inhibitory NKR-P1 receptors and also interpreted as health markers[14]. By balancing the inhibitory signals received through these receptors with the strength of the activating signals received through their activating receptors, NK cells are able to make intelligent decisions about the degree of health or disease a in potential target cell and respond correctly.

1.1.2: The Missing-Self Hypothesis

This ability for NK cells to kill targets based on their 'lack of health' (rather than the more typical 'presence of disease' model used by most immune cells) is summarized in the missing-self hypothesis of NK function[15]. According to the missing-self hypothesis, an important role for NK cells is to detect the loss of MHC-I. $CD8^+$ T cells are powerful components of the immune system, but their ability to recognize and eliminate a target cell is entirely dependent on that target expressing and presenting antigen in the context of MHC-I. An efficient evasion strategy against $CD8^+$ T cells, then, is to suppress expression of MHC-I, making the cell immune to conventional $CD8^+$ T cell recognition. The NK cell is believed to maintain selective pressure on MHC-I expression by recognizing a loss of MHC-I expression—a 'missing-self' signal—ultimately killing the MHC-I-deficient cell.

This hypothesis is borne out by a number of experimental results with NK cells. NK cells *in vitro* or *in vivo* cannot efficiently kill a lymphoma cell line called RMA, but a variant of this cell line that lacks MHC-I expression—called RMA-S—is readily eliminated[15–17]. Similarly, spleen cells from MHC-I-deficient animals are rejected by the NK cells from MHC-I-sufficient hosts[18]. In one example from a real disease setting, mouse cytomegalovirus (MCMV), which suppresses MHC-I expression on its host, has evolved an MHC-I mimic that can prevent NK cell missing-self recognition, ultimately preventing infected mice from clearing the virus[19]. Some mice, however, have reacted by evolving an NK cell activating receptor that specifically recognizes this mimic, making these mice resistant to MCMV infection. Finally, tumours from mice with NK cells that can't perform missing-self recognition have been observed to reduce MHC-I expression, as predicted by the missing-self hypothesis[20].

1.1.3: The Ly49 receptor family

In mice, the receptors responsible for this MHC-I-based missing-self recognition belong to the Ly49 family of c-type lectin-like receptors. Each Ly49 receptor consists of an intracellular domain, a transmembrane region, a flexible stalk, and a lectin-like head domain[21]. To date, all Ly49 family members are reported to exist as homodimers. With the exception of Ly49B, which is markedly dissimilar from the other Ly49 receptors and is not expressed on NK cells, the Ly49 receptors are all encoded by seven-to-eight exon genes (called *klra*) that are arranged end-to-end in about 500 kb of the NK gene cluster (NKC) on mouse chromosome 6[22]. Based on structural and functional similarities, these *Klra* genes and the Ly49 receptors they encode are classed into three groups. Inhibitory Ly49 receptors form the largest group; these receptors possess a long, immunoreceptor tyrosine-based inhibitory motif (ITIM)-containing cytoplasmic tail, and generally recognize MHC-I as discussed above. Activating Ly49 receptors possess a short

cytoplasmic tail, and instead of a signaling platform, have charged residues in their transmembrane domains that allow association with and signaling through immunoreceptor tyrosine-based activating motif (ITAM)-containing adaptor proteins like DAP12[23]. Some of these activating receptors recognize viral mimics of MHC-I, such as Ly49H recognizing MCMV's m157 protein. Finally, *Klra* pseudogenes do not encode protein.

The inhibitory Ly49 receptors are highly diverse in terms of binding specificity, cell surface expression, and even the number and types present within a given organism's genome. This complexity is necessary to keep up with their binding partner, the extremely polymorphic and polygenic MHC-I family of proteins. Because each organism inherits a unique set of MHC-I molecules derived from both of its parents, a broad array of Ly49 receptors must also be inherited such that each expressed MHC-I molecules drawn from the myriad possibilities can be recognized by at least one Ly49. In the wild, this means that each mouse has a unique set of Ly49 receptors, much like their unique MHC-I. Each inbred laboratory mouse strain, however, has a defined Ly49 haplotype, consisting of as few as six or as many as twenty-one unique *Klra* genes. Studying the various laboratory haplotypes has revealed several interesting features of the Ly49 gene family. The first is the presence of framework genes: to date, all mouse haplotypes analyzed appear to possess genes encoding Ly49A and Ly49C (*Klra1* & *Klra3*), followed by a variable region, then Ly49G and Ly49I (*Klra7* & *Klra9*), another variable region, and finally Ly49E and Ly49Q (*Klra5* & *Klra17*)[24]. This structure and arrangement is illustrated in Figure 1.

They also each possess a remarkable two-promoter system, in which promoter 1 is bi-directional and dictates the lifelong expression state of the Ly49 in each NK cell, while promoter 2 is responsible for the mature expression of the receptor, once allowed to do so by promoter 1[25,26]. This complex promoter system will be discussed below in more detail, but is mentioned

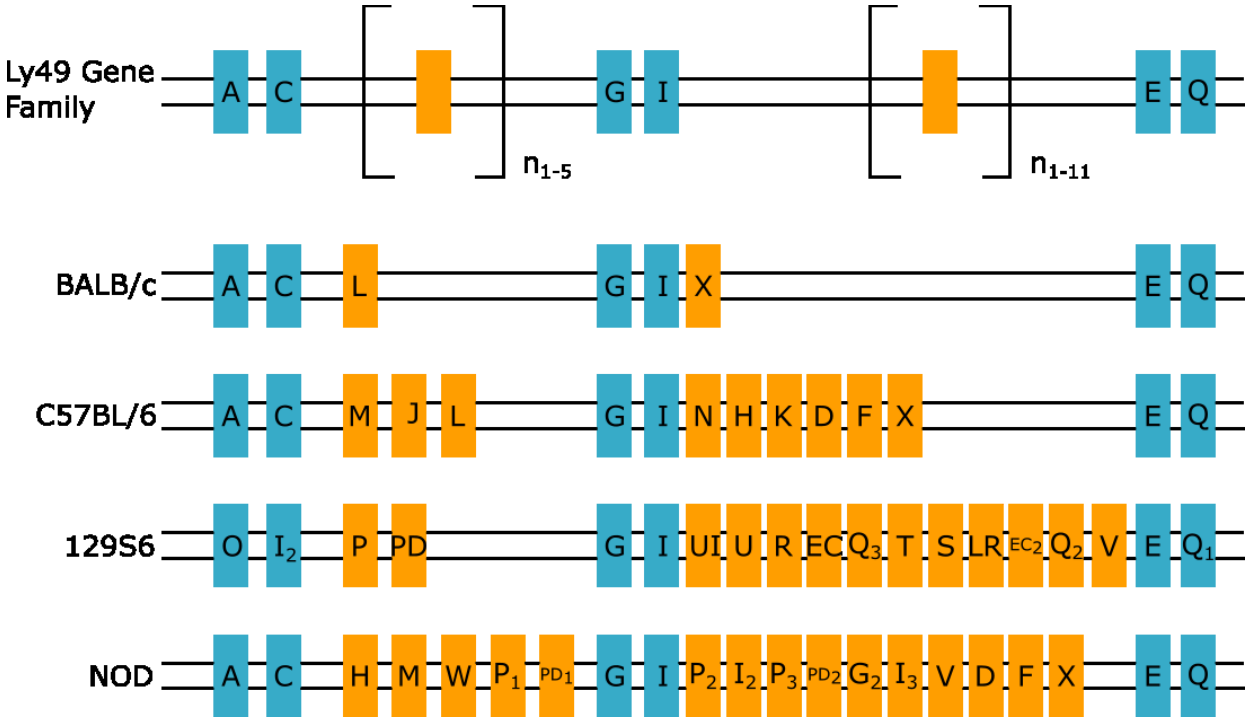

Figure 1: Diagram of *Klra* gene family arrangement. All known Ly49 haplotypes follow the general arrangement shown on top: two framework *Klra* (Encoding Ly49A and C), followed by a variable region of 1-5 genes, then two more framework genes (G and I), another variable region of 1-11 genes, then the final two framework genes (E and Q). Four example laboratory haplotypes are indicated. Note that the Ly49A and C receptors in the 129S6 mouse are named Ly49O and I_2, respectively.

here to discuss another feature of the Ly49 family of receptors. Human NK cells do not express Ly49 receptors. Instead, human NK cells use killer-cell immunoglobulin-like receptors (KIR) to mediate missing-self reactions. In an impressive feat of convergent evolution, however, the immunoglobulin KIR and the lectin-like Ly49—two structurally and evolutionarily unrelated families—have remarkable functional homology. Both families have inhibitory members that signal through ITIMs and activating members that signal through ITAM-containing adaptor proteins. Both are encoded by genes that are all present together in one gene cluster, arranged end-to-end, and organized into a framework-variable-framework-variable-framework pattern[27]. Finally, both make use of a two-promoter system where one promoter is a bi-directional 'on/off' switch and the other is a mono-directional driver of mature expression; however, in the human KIR, it is promoter 2 that acts as this bi-directional switch, while in the mouse Ly49, it is promoter 1[28]. Still, to see such similar features arise in such different gene families suggests important underlying functions to each.

1.1.4: Ly49 signal transduction

As mentioned above, Ly49 receptors are divided into activating or inhibitory receptors. This division is made based on the type of down-stream signaling events that occur upon receptor ligation, and more specifically upon whether the receptor in question possesses an immunotyrosine-receptor inhibitory motif (ITIM) or whether it associates with immunotyrosine-receptor activating motif (ITAM)-containing proteins[29,30]. Activating receptors were initially identified as lacking an ITIM and consequentially not able to be phosphorylated[29]. These were later found to associate with DAP12—an ITAM-containing adaptor protein—for signaling purposes by forming a non-covalent bond using a charged asparagine in their transmembrane domain[23,31]. This association with DAP12 allows for downstream signaling through the tyrosine

kinase Syk, ultimately leading to the gene transcription and calcium mobilization that allows the NK cell to perform its effector functions[32].

Conversely, inhibitory receptors possess an ITIM on their long cytoplasmic tails, which is phosphorylated by Src-family kinases such as Lck[33] when these receptors are crosslinked[29] and which then recruits the protein tyrosine phosphatases SH2 domain-containing phosphatase 1 (SHP-1), SHP-2, and SH2-containing inositol phosphatase (SHIP)[34,35]. Of the three, SHP-1 appears to be the canonical downstream mediator of inhibitory Ly49 signaling, and was found to directly dephosphorylate early mediators of activating NK cell signal transduction, interrupting the activating signals and preventing NK cell activation[36].

Because of these signaling mechanisms, inhibitory Ly49 signals are generally dominant over activating signals[37]. This is both due to the ability of SHP-1 to interrupt activating signal transduction very early in the process, and because the inhibitory receptors can occlude activating mediators such as Lck for their own use[33]. However, a powerful activating signal still has the potential to 'outrun' the inhibitory signaling, leading to the NK cell's ability to evaluate not only the presence of an activating signal but its relative strength compared to inhibitory health signals. Nevertheless, the dominant nature of the inhibitory signaling can result in difficulties in clearing virus infected cells that express activating viral ligands but also health markers such as MHC-I. This is exemplified in cases such as influenza[38] or cytomegalovirus[39,40] infections where NK cells that lack functional inhibitory receptors are more protective than their inhibitory receptor-expressing counterparts. The need for this population that does not express inhibitory receptors is one of the reasons behind the stochastic expression of Ly49 receptors, as will be discussed below.

1.1.5: Stochastic expression and the bi-directional promoter

Successful missing-self recognition depends on the stochastic expression of Ly49 and KIR, which is driven by the complex bi-directional two promoter system found in both of these gene families. This is because MHC-I's extreme polygenic and polymorphic nature presents some unique challenges to the Ly49 or KIR families. Above, the missing-self hypothesis was presented as a way to explain how NK cells keep selection pressure on pathogens to retain MHC-I expression, so that MHC-I can still present antigens to T cells. However, each MHC-I molecule has different affinities for different antigens, such that a given antigen would only be presented by a subset of available MHC-I molecules[41]. Therefore, a more refined evasion strategy from a virus or tumour would be to inhibit expression of the optimal MHC-I molecule, preventing efficient antigen presentation to T cells as before, while retaining the other, irrelevant MHC-I molecules on the cell surface to satisfy the missing-self recognition of an NK cell. One example of this strategy is HIV, which has been shown to suppress expression of HLA-A and HLA-B MHC-I molecules, but not HLA-C or HLA-E[42].

To prevent this potential evasion mechanism, NK cells express their Ly49 receptors (or KIR) stochastically, such that each NK cell will express anywhere from 0 to 6 specific Ly49 receptors[25,43]. In this way, there are potentially hundreds of Ly49-defined sub-populations of NK cells within a given immune system: for example, one sub-population of cells would express Ly49A, Ly49C, and Ly49H; another would express only Ly49C; yet another would consist of cells that don't express any; and so on. In this way, if a virus was to suppress only the optimal MHC-I, there exists a sub-population of NK cells for whom that was the only MHC-I they could recognize, and they will perform missing-self recognition and viral elimination as expected. That is to say, if a virus infecting a (wild-type, outbred) mouse removed expression of the MHC-I

molecule H-2K^{b} and left H-2D^{d} intact, any NK cells that expressed Ly49G would successfully be inhibited by this residual H-2D^{d} expression, but any NK cells that expressed Ly49C and not Ly49G would ignore the H-2D^{d} (since they lack a receptor capable of recognizing it) and only detect the loss of the Ly49C ligand, H-2K^{b}.

The bidirectional promoter in Ly49 and KIR genes is the key to this stochastic expression. Early in an NK cell's development, each Ly49 is either activated or not based on the bi-directional promoter 1 (Pro1). When the transcription machinery assembles on Pro1, if it assembles in the forward orientation, the helicase activity of this initial transcription is hypothesized to remove an as-yet unidentified repressor complex from Pro2[25,26]. This opening of Pro2 will then allow the constitutive Pro2 to drive expression of that Ly49 receptor for the rest of the NK cell's life. Conversely, if the initial transcription machinery happens to assemble in the reverse direction, Pro2 is never opened and that specific Ly49 receptor is not expressed. What effects lock Pro1 into this reverse orientation, preventing a reverse Pro1 from ever becoming a forward Pro1, are not currently known, but the result is that this probabilistic decision to either express a given Ly49 or not is stable over the life of the NK cell, but each NK cell independently determines its own Ly49 receptor expression profile during development[44].

A closer look at the mouse bi-directional promoter (diagrammed in Figure 2) reveals how this stochastic decision is made on a molecular level. The promoter consists of two TATA-like elements, one at the 5' end and one at the 3' end. Each TATA-like element is surrounded by CCAAT/enhancer binding protein (C/EBP) sites, and these two TATA+C/EBP zones are separated by a central, regulatory c-ETS/NFκB/AML-1/NFκB binding area. Each *Klra* gene has this same basic promoter structure, and careful mutational studies have revealed the role of each

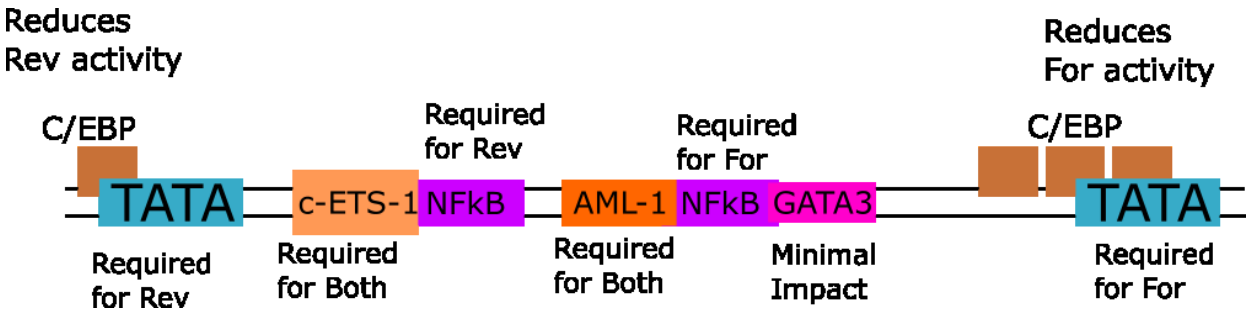

Figure 2: *Klra* promoter 1 is a bidirectional probabilistic switch. The *Klra* promoter 1 consists of a 5' TATA-like element with a C/EBP site, a regulatory region consisting of a c-ETS-1 binding site followed by an AML-1 site flanked by two NFκB sites and then a GATA3 site, then a 3' TATA-like element with three C/EBP sites. Each of promoter 1 reverse and promoter 1 forward consists of the appropriate TATA-like element and the nearest NFκB site; these factors stochastically assemble on the promoter in either the forward or the reverse direction, determining the Ly49 expression state of the cell in question. The c-ETS-1 and AML-1 sites appear to be necessary for the promoter to function in either direction, while the GATA3 site apparently has minimal function, as expression is not lost in either direction upon GATA3 site mutation. The C/EBP sites near each TATA-like element reduce (but do not eliminate) the binding ability of the nearest TATA, tuning the probabilities of whether the complex will assemble in either the forward or reverse direction.

element within it[25]. The central AML-1 and c-ETS elements are absolutely required for the function of the promoter—loss of either completely inactivates both directions of the promoter. Each TATA-like element and its corresponding nearest NFκB element is necessary for one direction of transcription: loss of the 5' TATA-like element prevents reverse transcription, while loss of the 3' prevents forward. Thus, once the promoter is opened by AML-1, the TATA-like binding protein (TBP) assembles on one of the two TATA-like elements based on random affinity binding, driving transcription in the appropriate direction.

The C/EBP binding sites appear to adjust the overall affinity of their TATA-like element. This accounts for the expression patterns observed for various Ly49 receptors. For example, Ly49G is expressed on roughly 50% of NK cells, indicating that the affinity of each of the TATA-like elements for TBP is relatively equal in Ly49G's promoter[45]. Conversely, Ly49F is only very rarely expressed, indicating that the 3' TATA-like element in this promoter has lower affinity than the 5'[46]. Again based on the above mutational studies, this affinity is inversely correlated with the strength of the C/EBP binding sites, suggesting that they are interfering with the TBP binding. This also allows for relatively straightforward evolutionary tuning of Ly49 expression: if, for example, Ly49F were to become selectively advantageous due to an emerging pathogen, loss-of-function mutations in Ly49F's 3' C/EBP binding sites would be sufficient to increase its expression in the overall NK cell pool.

KIRs, too, have a bi-directional promoter giving rise to stochastic expression of each receptor on each NK cell; however, the bi-directional promoter is downstream of the constitutive forward promoter in these receptors, and so their mechanism of action is believed to be somewhat different. Rather than forward expression removing a repressor element, KIRs are believed to be inhibited by the reverse transcription creating double-stranded RNA molecules

with the constitutive forward expression of the upstream promoter. These dsRNA molecules are processed into a 28 bp small RNA that resembles the piRNA elements that silence transposons; this 28 bp small RNA was required for KIR silencing[47]. Conversely, forward transcription from the downstream promoter does not conflict with the constitutive upstream promoter, and so the gene is transcribed.

Promoter 2 (or promoter 1 in KIR)—and the putative promoter 3—is a much more straightforward, conventional, mono-directional promoter that appears to be responsible for the constitutive expression of those genes selected by promoter 1[48]. The strongest evidence for this fact is that transcripts originating from promoter 1 are only detected in developing NK cells, while transcripts originating from promoter 2 (or 3) are abundant in mature NK cells. Some recent work has called this into question, presenting qPCR results detecting transcripts originating from promoter 1 in mature NK cells[49]. This was a surprising finding, especially since the report indicated that neither of the two TATA-like elements in promoter 1 are required for this mature promoter 1-driven expression. Indeed, more recent evidence has failed to reproduce much of this study, instead confirming earlier reports that promoter 1 is active in developing NK cells and not in mature NK cells, and that it does not play a role in enhancing Ly49 expression off of promoter 2, once promoter 2 is active[50].

In general, the bidirectional promoter leads to stochastic Ly49 expression and the 'product rule' of Ly49 expression: the probability of any two Ly49 receptors being co-expressed is the product of each individual Ly49's expression probability[44]. That is, if Ly49G is expressed on 50% of NK cells, and Ly49F on 2%, then about 1% of the NK cells will co-express Ly49G and Ly49F. The noted exception to this, however, is activating Ly49 receptors. Ly49D and Ly49H, the two activating receptors in the C57BL/6 mouse, have been shown to be co-expressed

at a higher-than-expected level, and tend to do so on NK cells lacking NKG2A expression[51]. Why this is the case is still not clear, but the activating receptors have been shown to be expressed later in NK development than the inhibitory receptors, and so may have fundamentally different processes regulating their expression[51].

1.1.6: NK cell licensing

Stochastic Ly49 and KIR transcription solves one problem with missing-self recognition, but it introduces another. Stochastic expression means that a number of NK cells will not express any Ly49 receptors capable of recognizing self-MHC-I. Indeed, in a C57BL/6 mouse, the only self-reactive Ly49 receptors are Ly49C and Ly49I[52,53]: roughly 50% of the NK cells in these mice do not express either Ly49C/I, and so do not recognize self-MHC-I[54]. If these cells were allowed to be fully functional, they would recognize every other cell as a missing-self target, since they cannot detect self at all, and would cause rampant autoimmunity. Obviously, this doesn't happen; it is prevented through a process called NK cell education or NK cell licensing[55]. While the mechanisms of licensing are still not fully understood, it can be thought of as a requirement for NK cells to 'prove' that they can successfully be inhibited by self signals. If the NK cell is self-inhibitable, it is licensed to perform missing-self reactions; if it is not, it remains unlicensed and will not perform missing-self rejection[55–57]. This was classically demonstrated in mice lacking MHC-I. NK cells from these mice do not reject MHC-I-deficient targets, despite being otherwise normal NK cells with normal Ly49 expression and the ability to kill viruses, provided there is a danger signal present[57]. Because these NK cells have never been licensed to MHC-I, they simply cannot participate in missing-self rejection.

Several models have arisen to explain how NK licensing might function[58]. The arming model proposes that inhibitory signals during NK development impact that NK cell's gene

expression, such that the more inhibitory signals that are received, the more active that NK cell becomes. The converse model, NK disarming, has also been proposed: in it, NK cells are initially highly active, but a rash of activating signals in the absence of inhibitory signaling exhausts the uninhibitable NK cells, leaving only the licensed, self-recognizing NK cells as fully functional. More recent work has found evidence for a third model, known as the rheostat model, which states that however NK licensing works, it is not a one-time event during NK development, but rather a constant adjustment in the NK cell's activation threshold based on the inhibitory and activating signals that NK receives throughout its life[59–61]. This is supported by adoptive transfer experiments. For example, NK cells from MHC-I-deficient mice are not MHC-I licensed; however, upon adoptive transfer to MHC-I-sufficient hosts, these mature unlicensed NK cells will become licensed (provided they express Ly49 receptors capable of recognizing the new host's MHC-I)[62].

One problem with all of these models is that they suggest that unlicensed NK cells are less functional than licensed NK cells. Again, this is true in the context of missing-self reactions: mice with only unlicensed NK cells, either through an MHC-I or an Ly49 deficiency, are not able to reject MHC-I-deficient target cells. However, more recent work from several groups has shown that unlicensed NK cells are as good or better than licensed NK cells at killing many viruses, provided these NK cells have some method other than loss of MHC-I to detect the virus (such as Ly49H recognizing m157 directly)[38–40]. This could indicate that the various models of NK licensing are all incorrect, although it could also indicate that the underlying model is correct, but inflammatory cytokine signaling in the context of a virus infection is sufficient to overcome any inherent defect in the unlicensed NK cells. Another issue with licensing is that there is as-yet no explanatory mechanism behind how it functions. A recent report found that the

activating NK cell receptor DNAM1 has an expression pattern that perfectly correlates with an NK cell's licensing status—that is, unlicensed cells have very low DNAM1 expression, licensed cells have very high DNAM1, and as a cell gains or loses licensing during an adoptive transfer experiment, it gains or loses DNAM1 as well[63]. This appeared to have somewhat solved the NK licensing puzzle, presenting a model where DNAM1 rapidly co-localizes with open LFA-1 in forming an immune synapse and allows for efficient NK cell activation. Licensed cells, with higher DNAM1 expression, would be more responsive to this DNAM1/LFA-1 partnership, and unlicensed cells would not. Unfortunately, a more recent report has since shown that while DNAM1 does indeed correlate with licensing status, mice lacking DNAM1—either through genetic ablation or antibody depletion—are fully able to perform missing-self rejection of RMA-S or MHC-I-negative splenocytes, the hallmark of licensed NK cells[64]. NK cell licensing remains a mystery for the time being, although for the purposes of this thesis, it is sufficient to know that licensing exists and that, in a C57BL/6 mouse, it is primarily mediated by Ly49C and Ly49I.

1.1.7: MHC-I and its receptors

Thus far, MHC-I has been considered mainly in its interactions with Ly49. However, this protein complex sits at the center of antigen-specific recognition, a role that will be briefly explored here. As was previous alluded, the MHC-I molecules' primary role in immunity is to present a peptide snapshot of all the protein products being produced by a cell, by presenting short, 8 or 9 amino acid-long peptide samples derived from proteasome processing of defective translation products[65]. These small peptides are imported into the endoplasmic reticulum by the Transporter associated with Antigen Processing (TAP). With the help of tapasin and several chaperones, the peptide is loaded into a nascent MHC-I molecule, which is then transported through the Golgi complex to the cell surface[66]. Alternatively, though a process that is not

completely understood, proteins that have been phagocytosed—which are normally presented on the class II major histocompatibility complex as a snapshot of what has been present at the site of an immune affront—can instead be loaded into the MHC-I complex; this is known as cross-presentation[67–69].

Regardless of how the peptide arrived into the MHC-I binding cleft, it is presented to passing T cells that interact with the cell in question. Under steady-state conditions, the presented peptides will be from normal, healthy cells, which should not have a T cell clone capable of recognizing them. In the case of a virus infection or a heavy mutational load associated with cancer, however, foreign peptides will be presented in the cleft and will be recognized by a $CD8^+$ T cell, which will then eliminate the target cell. This recognition is performed by the T cell's T cell receptor (TCR), which interacts directly with the peptide and the region of the MHC-I around the peptide binding cleft[70]. The accessory molecule CD8 also engages the MHC-I protein away from the peptide binding region, and serves to stabilize the interaction[71]. This is diagrammed in figure 3A.

Using their Ly49 receptors, NK cells also recognize MHC-I. Unlike the TCR, however, Ly49 does not engage MHC-I at the peptide binding cleft, but rather below it, similar to where CD8 binds[72,73] (figure 3B). Originally, this gave rise to the belief that NK cells were not able to sense the peptide sequence presented in MHC-I. More recently, however, Ly49 receptors have been shown to be somewhat peptide selective[74]. In particular, instead of recognizing the direct peptide sequence like a TCR, Ly49C appears to distinguish peptides only based on their sequence at amino acids 2 and 3[75]. How this is the case when Ly49C does not interact with any peptide residues is currently unknown, but there is some suggestion that the different binding properties of a peptide based on residues 2 and 3 have subtle allosteric effects on other regions of

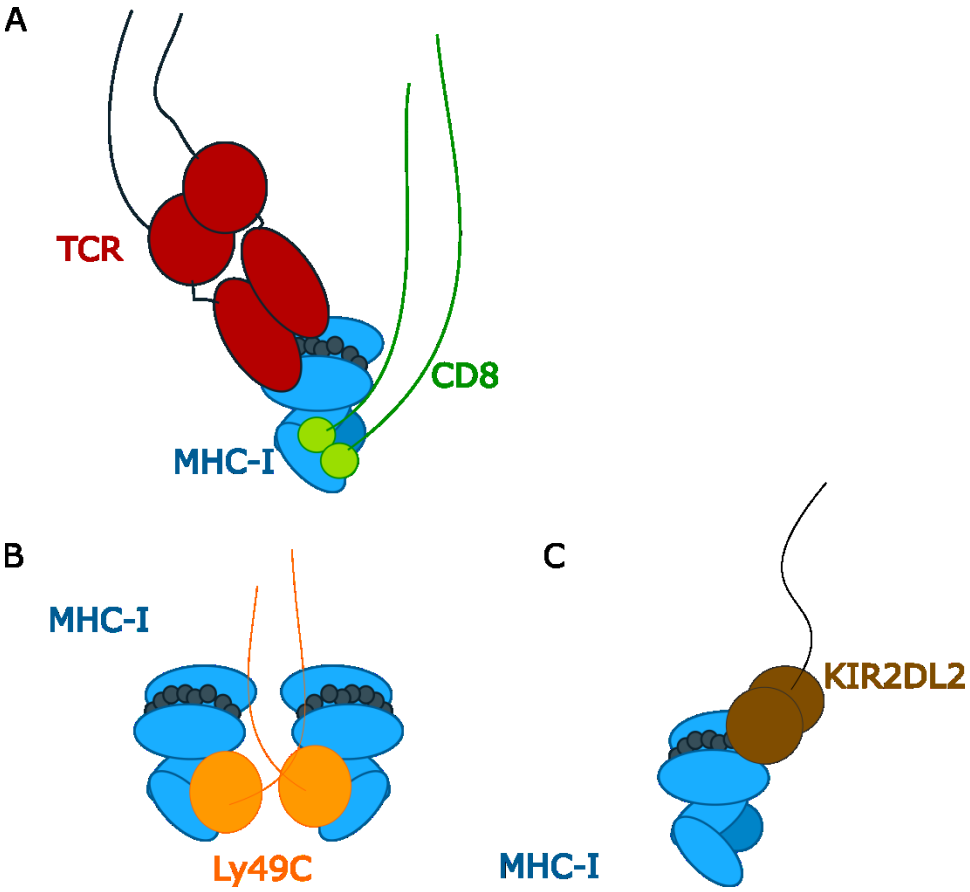

Figure 3: MHC-I receptor binding sites. (A) The TCR (in red) is responsible for peptide recognition upon binding to MHC-I (blue), and so engages MHC-I such that it is in contact with the presented peptide directly (slate). The CD8 dimer (green) helps to stabilize this interaction by binding the MHC-I molecule away from the peptide binding site. (B-C) NK cell receptors, including Ly49 (B) in mice and KIR (C) in humans, also directly bind to MHC-I. However, Ly49 receptors (orange) do not make contact with the presented peptide, while KIR (brown) do. Note that each monomer in the Ly49 homodimer can bind to an MHC-I chain independently, as depicted.

the MHC-I structure, which Ly49C can detect. Of note, human KIR are also somewhat peptide selective[76,77]; however, this is less mysterious, since KIR do engage directly with the peptide (figure 3C)[78].

1.2: New Facets of Natural Killer Cells

The role of NK cells in immune surveillance, in particular through missing-self recognition, has been well studied. Nevertheless, there are still mysteries surrounding these NK cell functions. As mentioned above, the mechanism behind NK cell licensing is still unclear. In a similar vein, a recent paper has cast some doubt on the previous model of Ly49 expression. While the findings of that paper have also been called into question, it is possible that other mechanisms contribute to Ly49 regulation than simple stochastic competition at promoter 1 for the TATA-binding complex. One focus of this thesis is on how nucleosome positioning across Ly49 promoters could affect their expression pattern, which might play a role in better understanding Ly49 gene expression.

The other new facet of NK cells that has emerged in the past decade is the mounting evidence that NK cells can perform a variety of functions previously ascribed to the adaptive immune system, including forming and executing responses based on powerful, long-lived, antigen-specific memories. The main focus of this thesis has been to uncover what role, if any, Ly49 receptors play in adaptive NK cell responses. Both of these new facets will be introduced in greater detail below.

1.2.1: Nucleosomal regulation of gene expression

The nucleosome is the fundamental unit of genomic organization. Each nucleosome consists of ~147 bp of DNA wound around a histone core[79], forming the 'beads' in the 'beads-

on-a-string' model of DNA structure[80]. Nucleosomes are critical for DNA stability and higher-order organization of chromatin, allowing decimeters of DNA to package into a micrometer-scaled cell[81]. Beyond this role in packaging, however, the nucleosome—specifically, the histone core—plays a central role in encoding the epigenome. Myriad post-translational modifications on the histone subunits affect chromatin accessibility, act as protein interacting platforms, and overall dictate gene expression within the cell[82–84].

The epigenome has rightly received a great deal of attention in our attempt to understand genes and how they are expressed. However, comparatively little focus has been on a much simpler method by which nucleosomes might impact gene expression. As a large protein complex with very high affinity for DNA[85], histones could easily play a steric role in limiting access to DNA for other proteins[86–88]. While initial beliefs considered nucleosomes to be positioned every 200 bp—150 bp of DNA wound into the nucleosome itself, and 50 bp of open DNA as the linker—we now know that this is only true for most nucleosomes[89]. This is known as statistical positioning, in which a nucleosome's position is determined only by the other, neighboring nucleosomes. Others, however, are positioned specifically, either by histone remodeling enzymes[90–92] or by genomic regions of particularly high histone affinity[89,93–95].

While each remodeling enzyme likely has a unique target depot site for nucleosomes, the genomic affinity is based on sequence patterns, and is therefore computationally predictable. These sequence patterns appear to be based on dinucleotides repeating every 10 bp. Periodic tracts of A/T oligonucleotides are associated with stronger nucleosome affinity, likely due to the relative flexibility of these A/T tracts allowing for the DNA helix to bend and fit easily to the histone surface[95–98]. Thanks to the identification of these patterns in yeast[94,99], drosophila[100], and worms[101], it is possible to computationally map the affinity-based nucleosome landscape of a

given genome sequence. These maps combine the histone affinity with the physical characteristics of a nucleosome (ie: two nucleosomes cannot be positioned on top of each other) to draw a picture of what the default nucleosome landscape would look like, without the intervention of histone remodeling enzymes (Figure 4).

There are many computational models available for predicting nucleosome positions[83,93,102,103]. In this thesis, the nucleosome map was drawn using the NuPoP algorithm[102], which uses a hidden markov model of variable nucleosome-free regions (the nucleosome linker) to predict nucleosome-bound regions. This model has been shown to be more accurate in predicting real nucleosomes than either the N-score prediction method (where nucleosome predictions are made solely based on periodic dinucleotide patterns)[104] or a markov model trained from an *in-vitro* nucleosome-assembled yeast map[105]. In general, a markov model is a simple probabilistic model where a given number of states have defined probabilities of transitioning to a different state, taking into consideration only the current state and the future state to determine that transition probability[106]. In other words, it is a model without memory, since the previous states occupied by the system do not impact the current probability of a transition. In this case, the states are simply 'nucleosome-bound' and 'nucleosome-free', and are modeled for each nucleotide ± 73 bp (for determining probability of nucleosome-bound) or ± linker length, which is species-specific.

All of the above is only predictive, however; I sought to demonstrate a correlation between nucleosomal steric hindrance and gene expression in an experimental setting. To do this, I took advantage of the unique features of the Ly49 gene cluster—namely, their proximal clustering and homologous promoters, but independent expression—to allow an unbiased investigation of whether nucleosome occupancy at specific transcription factor binding site

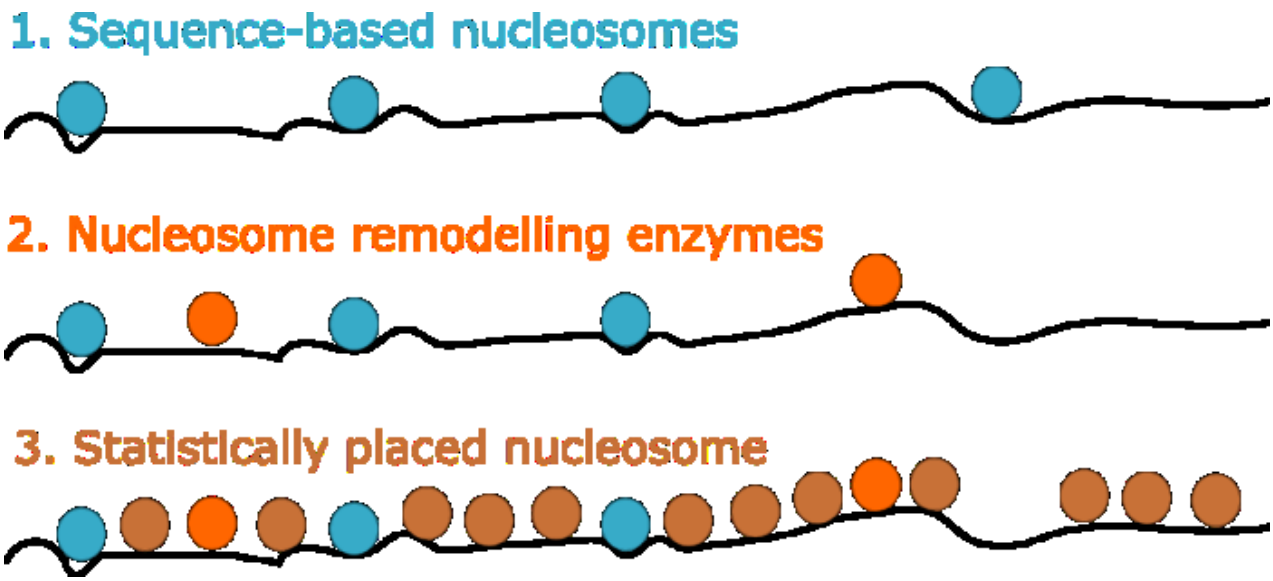

Figure 4: Nucleosome position can be specific or statistical. In the first instance, the genome is covered in nucleosomes based purely on sequence-based nucleosome affinity. Second, nucleosome remodeling enzymes can specifically place or remove nucleosomes, based on the enzyme's own targeting sequences. Finally, other nucleosomes are placed statistically—that is, are placed only with regard to the position of the nearest nucleosomes, and not with regard to sequence signals at all. In this way, the genome is wound into nucleosomes largely at random, but key sites can be selectively covered or exposed either by genomic affinity or by nucleosome remodeling enzymes.

(TFBS) correlates with expression of that Ly49. This also stood to potentially answer one question about Ly49 regulation. Unlike KIR, Ly49 promoters lack CpG islands, and so do not have such a clear method for maintaining an active or inactive state after the bidirectional promoter 'decided' whether a given Ly49 was expressed or not. DNA methylation in promoter 2 has been reported to be chiefly responsible for maintaining a silenced state in unexpressed Ly49[107]. However, that report also identified histone acetylation (H3K9Ac) as indicative of active Ly49. If histone acetylation—known to loosen DNA-histone interactions[108]—is involved in maintaining Ly49 expression, it is possible that tight histones can impede Ly49 expression, which is the question under study in chapter 3.

1.2.2: NK cell memory

A decade ago, the surprising discovery that T and B cell-deficient mice possessed long-lived, adaptive immunity mediated by NK cells launched a nascent field dedicated to determining whether, how, and why this novel adaptive immune system exists. A number of advances since then have provided mounting evidence that NK cells participate in a number of adaptive-like immune responses, giving rise to three separate phenomena collectively known as NK cell memory[109].

One form of NK cell memory was discovered in Ly49H$^+$ NK cells reacting to mouse cytomegalovirus (MCMV)[110]. These NK cells were described to undergo a T cell-like expansion in response to the Ly49H ligand, m157[111], then contract and form a memory pool. These memory cells then displayed stronger reactivation upon subsequent challenge with MCMV, and better ability to protect mice from MCMV exposure on adoptive transfer. Later work from this same group confirmed that NK cells expressing Ly49D, another activating receptor, could likewise

expand and form a memory pool in response to their target antigen, the H-2^d MHC-I haplotype[112].

This memory NK cell population appears to have a human counterpart in NKG2C$^+$ NK cells, which are also significantly expanded in CMV positive individuals and correlate with enhanced protection from a number of diseases[113–115]. These human memory NK cells are also correlated with a CD16$^+$ FcεRγ1$^-$ Syk$^-$ Eat-2$^-$ phenotype known as a 'g negative (g-)' NK cell phenotype[114,115]. These g- NK cells are marked by an extreme responsiveness to antibody-coated target cells through their CD16 activating receptor[116]. This reactivity to any antibody might explain why these CMV-reactive memory cells are not observed to be specific for CMV reactions: a memory pool of these cells is correlated with improved outcomes in leukemia[117], HIV[118], and may be helpful in cancer therapeutics[119].

Around the same time, it was reported that NK cells pre-activated with two cytokines, IL12+IL18, were more readily activated by future stimulus, and that this 'memory' of their previous activation was stable across several generations of daughter NK cells[120]. These became known as 'memory-like' NK cells, due to their marked lack of antigen specificity. These 'memory-like' cells were more responsive than naïve cells against Ly49H or NKR-P1C crosslinking[120] or co-culture with YAC-1 cancer cells[121]. Nevertheless, this represented a true cellular memory of a prior activation state, since it was observed to be stable for weeks and after two to three generations of daughter NK cells[120,122], and to be associated with distinct epigenetic changes resulting in a more T cell-like methylation profile[123].

1.2.3: Adaptive hepatic NK cell memory

The above two forms of NK cell memory represent exciting frontiers in our understanding of NK cell biology, but are distinguished from this third form of memory by their

fundamentally non-adaptive nature. CMV-reactive memory cells in mice are initially formed by a germline-encoded reaction between Ly49H and m157, and so lack the antigen diversity observed in a T cell or B cell pool. The cytokine-induced memory-like NK cells, conversely, appear to lack the tight antigen specificity that is also a hallmark of a specific pool of memory T or B cells. This third type of NK cell memory possesses both of these traits, and so will be referred to here as adaptive NK cell memory.

In the original report of NK cell memory, mice lacking T and B cells were found to display robust contact hypersensitivity responses to chemical haptens—small antigenic molecules that can pierce the skin and form immunogens by modifying self-proteins in the sensitized organism[124]. Conventional contact hypersensitivity responses are mediated by $CD8^+$ T cells[125], but in this study, all the mice that were used lacked the recombination-activating gene (RAG) which is required for T and B cell development, and therefore had no T cells of any kind. Instead, liver NK cells were identified as the memory cell enabling contact hypersensitivity responses. These memory NK cells were observable 4 months after initial exposure, and could be transferred into naïve hosts to transfer the hypersensitivity as well. In every case, the adaptive nature of this response was revealed in its antigen specificity: mice sensitized to one hapten would only react to that hapten and no other. This work was later expanded to include responses to virus-like particles[126], and to be demonstrated in zebrafish[127] and primates[128] as well as mice.

How this adaptive NK cell memory functions is still a mystery. The only receptor described to date with a direct role in adaptive NK cell memory is the chemokine receptor CXCR6, which in mice is responsible for homing the memory cell to the liver[126]. CXCR6 expression is correlated with reduced NK cell activity, suggesting that it puts the NK cell in a resting state and possibly accounts for the remarkable longevity of these adaptive NK cell

memory responses. Adaptive NK cells were also identified as expressing Thy1, NKG2D, L-selectin, and Ly49C or Ly49I (both of which are recognized by the same antibody)[124]. Unfortunately, none of these receptors alone explain how adaptive NK cell memory works, since in mice, only liver NK cells are capable of performing adaptive memory responses, but all of these receptors are well-represented on splenic, non-memory NK cells.

Nevertheless, Ly49C/I being correlated with adaptive NK cell memory cells has intriguing possibilities. These NK memories appear to be very T cell-like, in that they can form against antigens such as HIV[126] peptides or the hapten dinitrofluorobenzene (DNFB)[124], neither of which likely have a germline receptor encoded in the mouse genome. The parallels between $CD8^+$ T cell and NK cell memory suggests that MHC-I presentation, required for T cell memory, may also be involved in NK cell memory. If it is, Ly49C/I, as MHC-I receptors, may play a central role in NK cell memory. Additionally, these studies have all been performed in C57BL/6 mice, and so Ly49C/I involvement may be due to their role as licensing receptors. Resolving this question has been the central focus of this thesis, and will be discussed further in chapter 4.

1.3: Hypotheses

1 - Nucleosome presence at specific transcription factor binding sites within the bidirectional Ly49 promoter inversely correlates with Ly49 expression.

2 - Ly49 expression is directly required for adaptive NK cell memory responses.

2: Materials and Methods

2.1: Nucleosome project

2.1.1: Nucleosome predictions

Genomic sequences for C57BL/6[22], 129S6[129], BALB/c[130], and NOD[131] mice were obtained from previous publications. Nucleosomes were predicted using NuPoP[102], a publicly available algorithm available from bioconductor.org, set to a 4th-order hidden Markov model with a stringent false-discovery rate. Viterbi output (where a given base is either occupied or not) was used to calculate the center for each nucleosome, which was stored in a BED file for subsequent analysis.

2.1.2: Transcription factor predictions

Transcription factor binding sites were predicted on the four different Ly49 gene clusters by obtaining each position-weight matrix (PWM) from the TRANSFAC or JASPAR public databases. These PWMs were located on the reference sequences using MATCH or FIMO algorithms; in both cases, cut-off values were selected to minimize false positives. A list of the transcription factors used, and their PWMs, can be found in Figure 5. The genomic coordinates of each predicted TFBS were recorded in a second BED file.

2.1.3: Nucleosome:TFBS histogram generation and kurtosis calculation

The spatial relationship of each TFBS with its nearest nucleosome center was analyzed using BEDtools to first find the nearest nucleosome to each TFBS using the CLOSEST command. Distance was calculated from the center of the TFBS to the center of the nearest nucleosome. These distances were used to generate a histogram for each class of TFBS, using

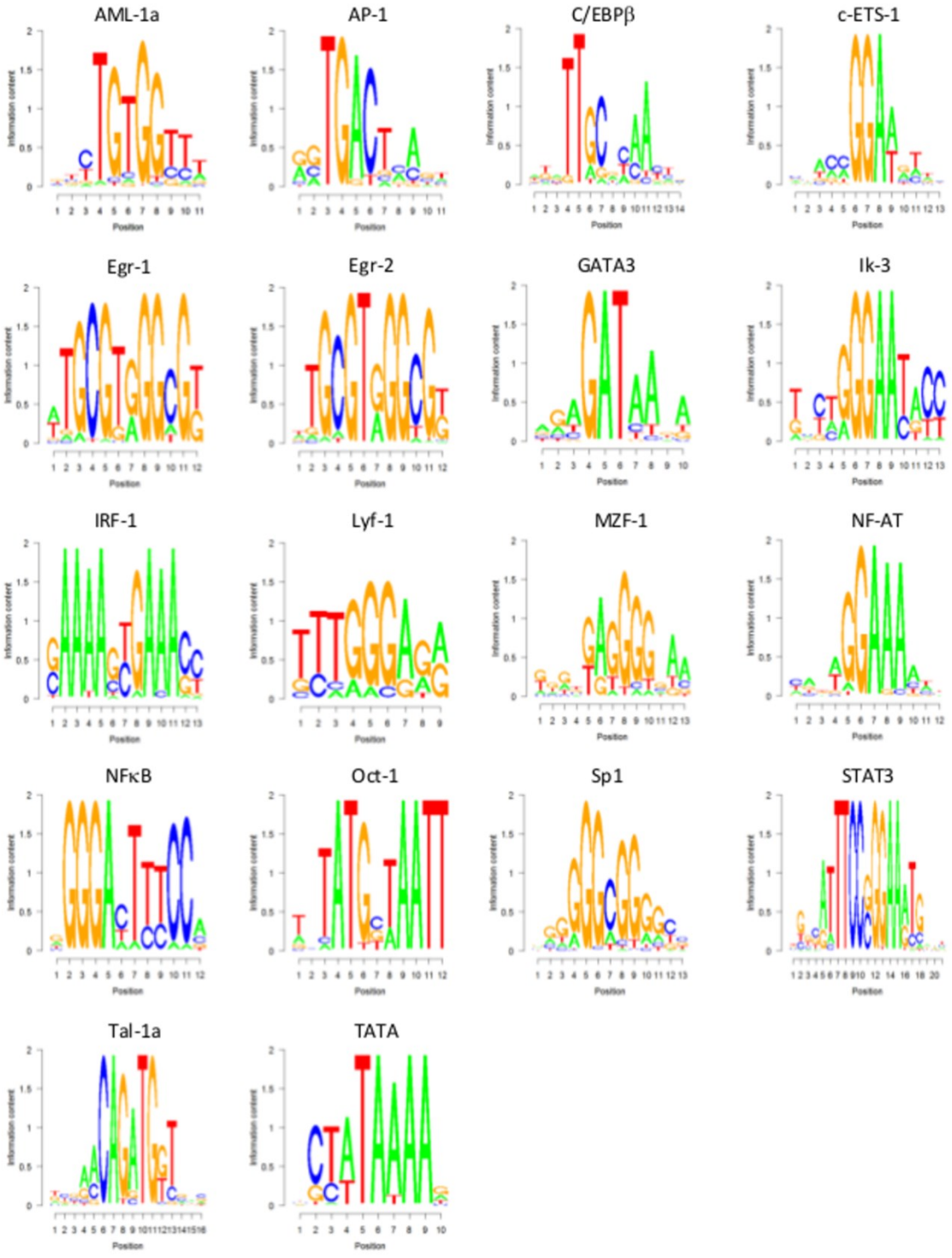

Figure 5: Transcription factor binding site (TFBS) consensus sequences. Sequences were generated from the JASPAR database.

Kernel Density Estimation in R, the statistical computing language. Each histogram was analyzed by Microsoft Excel to determine the kurtosis of the resulting curve.

2.1.4: Fourier Analysis

R was used to perform a fast fourier transform to compute the spectral density of each period within the pooled transcription factor amalgam and each resulting amalgam from removing one class of TFBS. Periodgrams were compared between the baseline and each leave-one-out amalgam, where a reduction in a given periodicity when compared to the pooled amalgam indicates that the left-out factor contributes to the overall spectral density of that specific periodicity, and an increase indicates that the left-out factor lacks that specific periodicity.

2.1.5: Flow Cytometry

Cells were collected for flow cytometry following standard cell culture in RPMI-1640 supplemented with 10% fetal bovine serum, 55 μM 2-mercaptoethanol, 100 U/mL Penicillin, and 0.1 mg/mL Streptomycin, or isolated from mouse spleens or livers by mechanical separation or blood by saphenous puncture. Staining was performed using antibodies against NKR-P1C (NK1.1), NKp46, TCRβ, Ly49A/D (4E5), Ly49D, Ly49C/I (5E6), Ly49E/F, Ly49G (4D11), and Ly49H (3D10) after blocking Fc receptors using anti-CD16/CD32 unlabeled antibodies. Samples were acquired on a CyAN-ADP (Beckman Coulter), LSR-Fortessa (Beckton Dickenson), or a FACS-Celesta (Beckton Dickenson) and analyzed using FlowJo software (FlowJo LLC) or Kaluza (Beckman Coulter).

2.1.6: MNase Digest and Nucleosome Mapping

MNase-Seq was performed as previously described[132]. Briefly, mononucleosome DNA was isolated by crosslinking nucleosomes to DNA with formalin for 10 minutes, then snap-freezing and lysing the cells using Triton X-100 and complete protease inhibitors (Roche) to isolate nuclei and then nuclear DNA. DNA was treated with micrococcal nuclease (MNase, from New England Biolabs) for 15 minutes. Formalin crosslinks were reversed overnight at 65 degrees, then protein contamination was digested with proteinase K. DNA was analysed on an agarose gel, and 150 bp fragments were isolated by cutting the relevant band and extracting the DNA-containing liquid phase with centrifugal force. Library preparation was done by Genome Quebec, and next-generation sequencing was performed using a MiSeq sequencer (Illumina). Intersections between predicted and actual nucleosomes were determined using the UCSC table browser and tabulated to determine the overall accuracy by comparing the accuracy at each TFBS, presented as a heat-map.

2.1.7: Chi Square Analysis

Chi square analysis was performed on the accuracy at each class of TFBS compared to the expected true-positive counts generated by each Ly49's observed overall accuracy. A heat-map of each TFBS class' contribution to the overall chi-square statistic is presented to allow evaluation of each factor's contribution to the overall chi-square statistic.

2.1.8: Asymmetry Analysis

R, the statistical computing language, was used to perform logistic regression of each indicated class of TFBS vs AML-1, comparing the state (true vs false positive nucleosome coverage) at each predictor TFBS to the nearest reporter TFBS in the Ly49 cluster, after eliminating any comparisons where the two TFBS are more than 147 bp apart. A higher

estimated odds ratio indicates a stronger predictor. Symmetric factors have similar odds ratios when each is the other's predictor, asymmetric factors do not.

2.1.9: Chromatin Immunoprecipitation

Micrococcal nuclease (MNase) digestion was used to prepare a fragmented genome. Chromatin was enriched by incubation with a rabbit polyclonal anti-AML-1 antibody (AbCam) or pooled IgG as an isotype control overnight, then collected using protein G beads. DNA was purified from this mixture by high pH chelation and proteinase K digestion. The Ly49A promoter was detected by quantitative PCR using the following primers:

Ly49A promoter:

Forward: AGGCCAGGGAAACCTGGTGTA

Reverse: AAGAGGTGGGGCACTGGACTG

Ly49A 6 kb up (negative control):

Forward: ACAGAACTCAGAGGGCAAAGGAAA

Reverse: TGGGCCACTTGGCCATTTATCT

2.2: NK cell memory

2.2.1: Animals

Rag1$^{-/-}$ (B6.129S7-*Rag1*^{tm1Mom}/J) and *Cd8a*$^{-/-}$ (B6.129S2-Cd8a^{tm1Mak}/J) mice were purchased from the Jackson Laboratory. H-2K^{b} H-2D^{b} double knockout (H-2K$^{b-/-}$D$^{b-/-}$) mice were purchased from Taconic. Ly49-deficient Ly49^{KD} mice or Ly49^{KD} mice expressing Ly49I on a transgene (Ly49^{KD}-I^{tg}) have been described before[133]. Rag-deficient mice were generated by crossing our Ly49^{KD} or Ly49^{KD}-I^{tg} mice, or H-2K$^{b-/-}$D$^{b-/-}$ mice with Rag1$^{-/-}$ mice. All animal breeding was performed in-house to minimize the impact of microbiota differences on these

studies. All animal housing and manipulations were performed according to the Animals for Research Act and were approved by the University of Ottawa Animal Care Committee. Initial experimental manipulations were performed when mice were 6-7 weeks old, and littermates were used for every comparison between Rag1$^{-/-}$ mice, between the various H-2K$^{b-/-}$D$^{b-/-}$ mice, between *Cd8a*$^{-/-}$ mice, and between *Rag1*$^{-/-}$Ly49^{KD} mice and *Rag1*$^{-/-}$Ly49^{KD}-I^{tg} mice.

2.2.2: Ear Swelling

The mouse ear swelling test was performed as previously described[124]. Briefly, mice were sensitized to haptens by topical administration of 0.5% 2,4-dinitrofluorobenzene (DNFB) in acetone or 1% oxazolone (OXA) in 1:1 acetone and methanol on the shorn abdomen once per day for two days. After the time indicated in each figure, mice were challenged on one ear with 0.2% DNFB or 0.5% OXA in vehicle (acetone/methanol), and vehicle alone on the unchallenged ear. Alternatively, mice were sensitized to peptides or whole protein by hock injection (a humane alternative to the footpad injection) of an oil-in-water preparation of 25 nM peptide or the molar equivalent of whole ovalbumin emulsified in complete Freund's Adjuvant, then challenged with a 1 nM peptide solution in sterile 1x phosphate-buffered saline (PBS) in one ear by subcutaneous injection, and PBS alone in the unchallenged ear.

Ear thickness was measured daily starting on the day of the challenge (before administering challenge) using an engineer's micrometer (Mitutoyo), and ear swelling was calculated as the thickness of the challenge ear minus the thickness of the control ear.

2.2.3: Histology

Following euthanasia, ears or tumours were collected, formalin-fixed for 48 hours, embedded in paraffin blocks, and cut into 4 μm sections. For hematoxylin and eosin (H&E)

staining, ear sections were deparaffinized and stained using a Leica Autostainer XL and a Leica CV5030. This staining was performed by the University of Ottawa Histology Core. Slide identities were masked, then images were acquired using a Zeiss AxioImager A2 or a Zeiss Mirax MIDI scanner. Unlabeled image files were counted for cellular infiltrates using ImageJ. Median cell counts from seven fields for each ear are reported.

For immunohistochemistry, ear or tumour sections were deparaffinized as above, and antigens retrieved in a histos5 rapid microwave processor at pH 6.0. These steps were performed by the Histology Core as before. Endogenous peroxidases were blocked with 3% hydrogen peroxide in sterile water for 10 minutes, protein blocked with Background Sniper (biocare), and stained with anti-NKp46 (AbCam BAF2225) or anti-CD3 (Santa Cruz M20) goat polyclonal antibodies. Staining was developed using a goat-on-rodent HRP-polymer kit and betazoid DAB (biocare), followed by hematoxylin counter-staining as above. Slides and then images were blinded as before, and NK cells were counted. Counts were pooled from 5 individual fields for each ear or tumour.

2.2.4: Antibody Purification

Hybridomas producing anti-NKR-P1C (PK136), anti-CD4 (GK1.5), anti-Ly49C/I (5E6), anti-Ly49G (4D11), or anti-interferon gamma (XMG1.2) were cultured for two weeks in DMEM supplemented with 10% FBS, 100 U/mL Penicillin, 0.1 mg/mL Streptomycin, 55 μM 2-mercaptoethanol, 10 mM HEPES, 1X non-essential amino acids, and 1 mM sodium pyruvate. Antibody-containing supernatants were then harvested, purified over a protein G column, concentrated in an amicon centrifuge filter (100 kDa cutoff), and quantified using spectrophotometry and an anti-IgG ELISA.

2.2.5: Antibody Depletions

Two days before sensitization or challenge, as appropriate, mice were injected intraperitoneally with 200 μg of depleting antibody in sterile PBS (specific antibodies indicated). Injections with 100 μg antibody were repeated every two days, alternating injection sites to avoid adverse reactions. Antibody depletions were confirmed by flow cytometry using blood samples.

2.2.6: F(ab')$_2$ Formation

Antibodies prepared as above were digested with pepsin in 50 mM citrate buffer, pH 4.0 (40:1 antibody to pepsin ratio) for 10 hours at 37 degrees Celsius. Cleft Fc portions were removed by protein A beads, and the resulting F(ab')$_2$ fragments were concentrated using an amicon centrifuge filter (50 kDa cutoff) and analyzed by SDS-PAGE to confirm loss of Fc region.

2.2.7: Cancer Vaccine

B16F10 cells and B16F10-Ova cells[134] were kind gifts from Drs. Subash Sad and Jean-Simon Diallo (University of Ottawa and Ottawa Hospital Research Institute). Cells were cultured in DMEM supplemented with 10% FBS and antibiotics. B16F10-Ova cells were grown with 400 μg/mL G418 to maintain Ovalbumin expression. Mice were sensitized to Ovalbumin (Invivogen), Bovine Serum Albumin (NEB), SIINFEKL (GenScript), or SIYRYYGL (GenScript) as above using complete Freund's adjuvant, then challenged by subcutaneous flank injection of 1x10^5 B16F10 cells per mouse. Mice were monitored daily for tumour growth, and tumour size was measured using calipers. Mice were euthanized when tumours ulcerated, or when any one dimension exceeded 10 mm. Tumour volume was calculated as 1/2 length x width x least of (length, width), as previously described[20].

2.2.8: Statistical Analysis

For ear swelling comparisons, statistics were calculated by two-way (ear swelling and time), repeated-measures ANOVA followed by a Bonferroni post-hoc test. In all other cases with only a single variable, comparisons were performed using Student's t test or a one-way ANOVA followed by a Bonferroni post-hoc comparing experimental groups to the naive control, as appropriate.

3: Nucleosomal Interference with Ly49 Gene Expression[1]

As mentioned above, nucleosome positioning has been hypothesized to interfere with gene expression by physically limiting transcription factor access to their binding sites. We investigated whether this nucleosomal hindrance could be impacting Ly49 gene expression. We had two underlying goals for this line of inquiry. First, there has been some suggestion that the current Ly49 gene expression model may be incomplete. An understanding of what role—if any—nucleosomes play in Ly49 gene regulation could help better understand the entire Ly49 expression model. Second, the hypothesis that nucleosomes have a physical effect on DNA accessibility has been difficult to test, because nucleosome position and gene expression are both affected by many different factors. This project would also demonstrate the advantages of the Ly49 gene family as a model for studying nucleosome positions, thanks to each gene's independent expression but homologous promoter.

---

[1]The results presented in this section have been published as a manuscript in PLoS Computational Biology[171], and are reproduced here under that publication's creative commons license. I was personally involved in generating and analyzing the data in every figure presented here, but I am indebted to the co-authors of that paper for their assistance. In particular, the predictive results presented in Figures 6 to 11 were a joint effort between me and my co-author Doo Yang. To acknowledge this fact, I will use 'we' throughout section 3.1, returning to "I" in section 3.2, which consists of work for which I was the principal agent.

3.1: In silico model of nucleosome:Ly49 interactions

3.1.1: Computational prediction of nucleosome binding sites in Ly49 promoter regions

To investigate the potential involvement of nucleosomes in Ly49 gene expression, we first prepared a model of nucleosome binding sites across the Ly49 gene cluster in C57BL/6 mice. This map was generated using the NuPoP hidden markov model described in the introduction, resulting in predicted nucleosome-occupied regions and nucleosome-free regions (Figure 6). These predictions were then validated in two ways. First, since the predictions are based on dinucleotide patterns, we evaluated whether the nucleosome predictions favoured areas with altered GC percentages, which could impact downstream comparisons of nucleosome-bound vs nucleosome-free regions (Figure 7A). We observed only a very slight enrichment for GC-rich areas in the nucleosome-bound regions when compared to the entire sequence of mouse chromosome 6 (where the Ly49 family is located). Second, we compared our predictions to a published, experimentally-derived nucleosome map (Figure 7B), resulting in an overall prediction accuracy of 48.8%. The prediction accuracy is relatively low; however, these predictions do not consider the extensive action of nucleosome remodeling enzymes. Moreover, this relative inaccuracy is taken into account when we later analyze our data for specific nucleosome depletion events.

Having generated and validated the nucleosome occupancy map, we analyzed the relative nucleosome coverage at promoter 1—in both the forward and the reverse positions—and promoter 2, for each Ly49 with annotated promoters in the C57BL/6 (Figure 8A), 129 (Figure 8B), Balb/c (Figure 8C), and NOD (Figure 8D) mouse Ly49 clusters. From these data, an overall pattern emerged in which most Ly49 genes have a nucleosome-free reverse promoter 1 and a nucleosome-bound forward promoter 1. Promoter 2 is less clear in an overall preference for

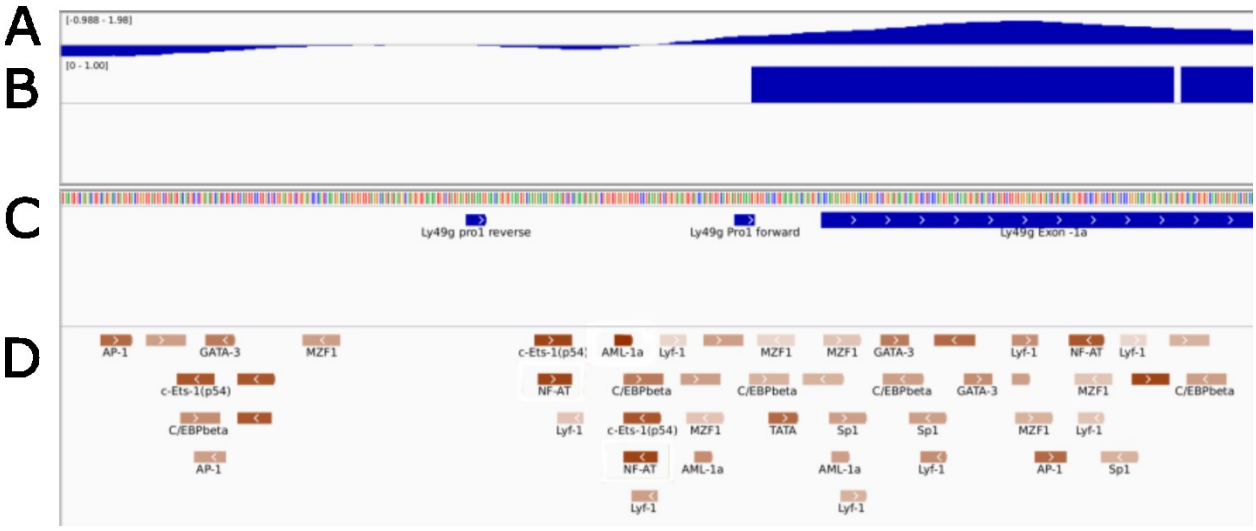

Figure 6: Example nucleosome and transcription factor binding site predictions. Using the NuPoP prediction algorithm, a DNA sequence-based affinity score was generated (A). Using the aggregate affinities and a defined width of 147 bp for a nucleosome, a binary occupied/free model of nucleosome positioning was prepared (B). These predicted nucleosomes were aligned to the annotated genome (mm10) (C). Transcription factor binding sites were predicted using FIMO, a component of the MEME Suite, taking experimentally-derived position-weight matrices from the public TRANSFAC or JASPAR databases. These were similarly aligned to the annotated mouse genome (D).

A

Region	G+C	Total Bases	%GC
Chromosome 6	60606617	146336545	41.42%
Nucleosome-bound regions	43344070	94657763	45.79%

B

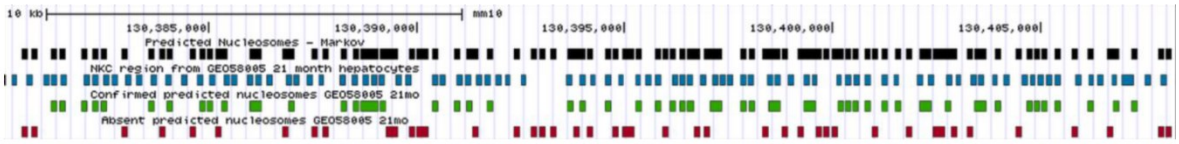

Confirmed Predictions: 48.8%

Figure 7: Quality control of nucleosome predictions. (A) Because these nucleosome predictions are based on dinucleotide patterns present in the genomic sequence, it was possible that the predicted nucleosome-bound regions would have an altered %GC from the rest of the chromosome. A slight increase in %GC was observed for predicted nucleosome-bound regions, but this was deemed not potent enough to bias downstream transcription factor binding predictions. (B) Nucleosome predictions were compared to previously published, experimentally derived nucleosome positions determined by MNase digestion (GEO accession number GEO58005). For the purpose of this quality control, predicted nucleosomes with at least 50% overlap with an actual nucleosome were considered to be confirmed predictions. Note that the prediction cannot account for nucleosome remodeling enzymes, and so is not expected to approach 100% accuracy when compared to a real dataset.

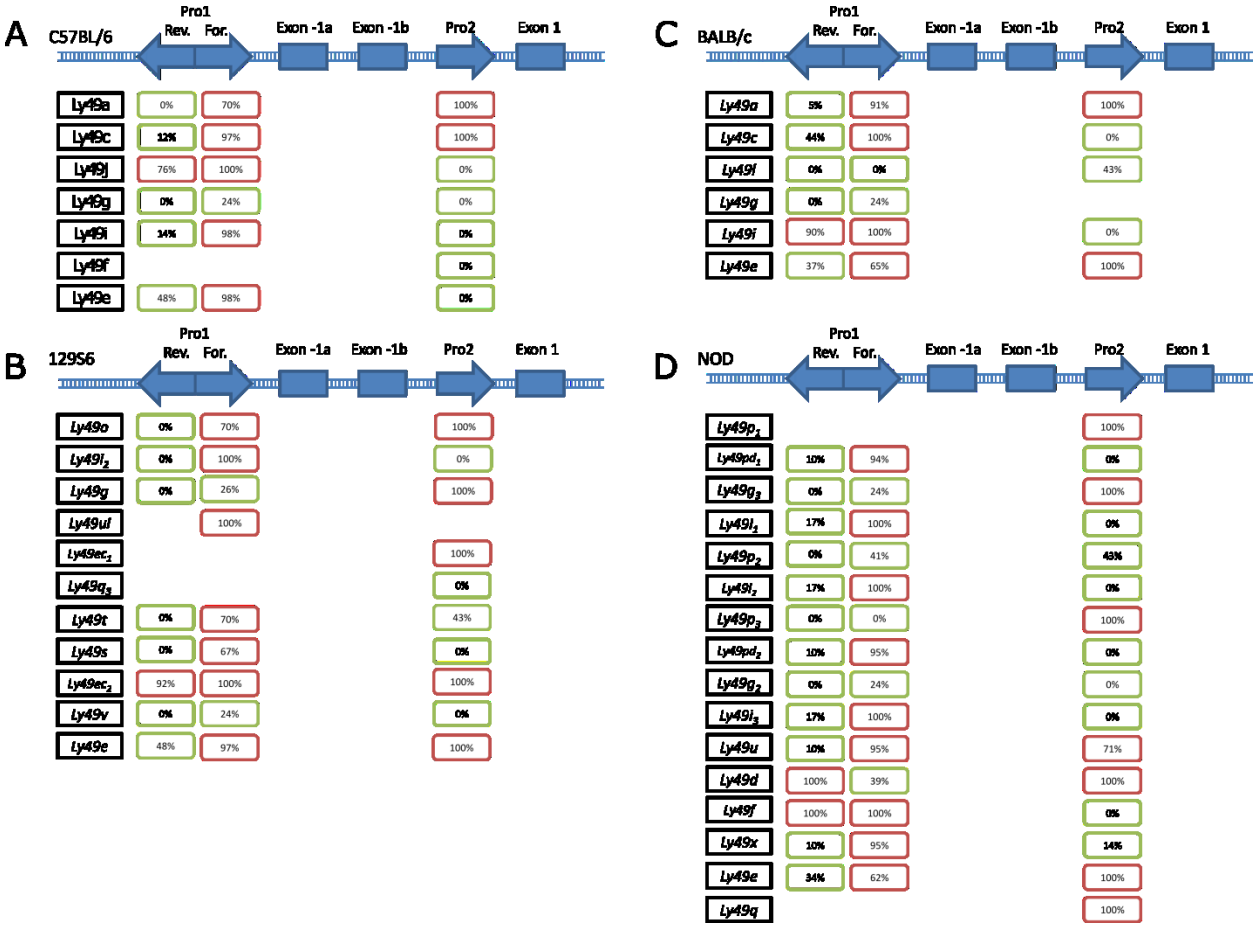

Figure 8: Nucleosome occupancy at Ly49 promoters. For each Ly49 with an annotated promoter in the (A) C57BL/6, (B) 129S6, (C) BALB/c, and (D) NOD genome, nucleosome occupancy was predicted as described. The percentage of nucleotides covered by a predicted nucleosome for promoter 1 in both forward (Pro1 For) and reverse (Pro1 Rev), as well as for promoter 2, is indicated, with boxes coloured green if that region is under 50% covered and red otherwise.

nucleosome occupancy. These data suggest that, if nucleosomes are impacting Ly49 expression, they are doing so by influencing promoter 1, which is consistent with the known role for promoter 1 in determining the lifelong expression state of each Ly49.

3.1.2: Computational prediction of lymphocyte transcription factor binding sites

We hypothesized that if nucleosomes are influencing gene expression, they would likely do so by covering specific transcription factor binding sites. To evaluate this, we first predicted the positions of 17 transcription factor binding sites (TFBS) with a known role in lymphocyte biology (Figure 5) in the promoter and enhancer regions (15000 bp upstream and 1000 bp downstream of the transcription start site) of each Ly49 gene in the C57BL/6 genome. For each transcription factor with at least 300 putative binding sites in all the regions analyzed, we then determined the distance from each TFBS to the center of its nearest nucleosome (Figure 9). Based on the kurtosis (pointedness) of the resulting histograms, we classified the TFBS into one of three categories. Those with relatively flat distributions (low kurtosis) were described as preferentially nucleosome-avoiding, those with relatively peaked distributions (high kurtosis) as preferentially nucleosome-localizing, and those with relatively normal distributions as having no nucleosome preference. Of note, TBP, which is known to preferentially avoid nucleosomes, was indeed found to have a low kurtosis indicative of its anticipated nucleosome-avoiding tendency.

3.1.3: Transcription factor binding site periodicity analysis

We expected the TFBS that displayed a high kurtosis—and consequently high nucleosome coverage—to be optimal sites for potential nucleosome interference. However, one further complication first needed to be analyzed. Nucleosome-associated DNA completes one turn approximately every 10 bp, giving rise to the possibility that TFBS with 10 bp periodicity can

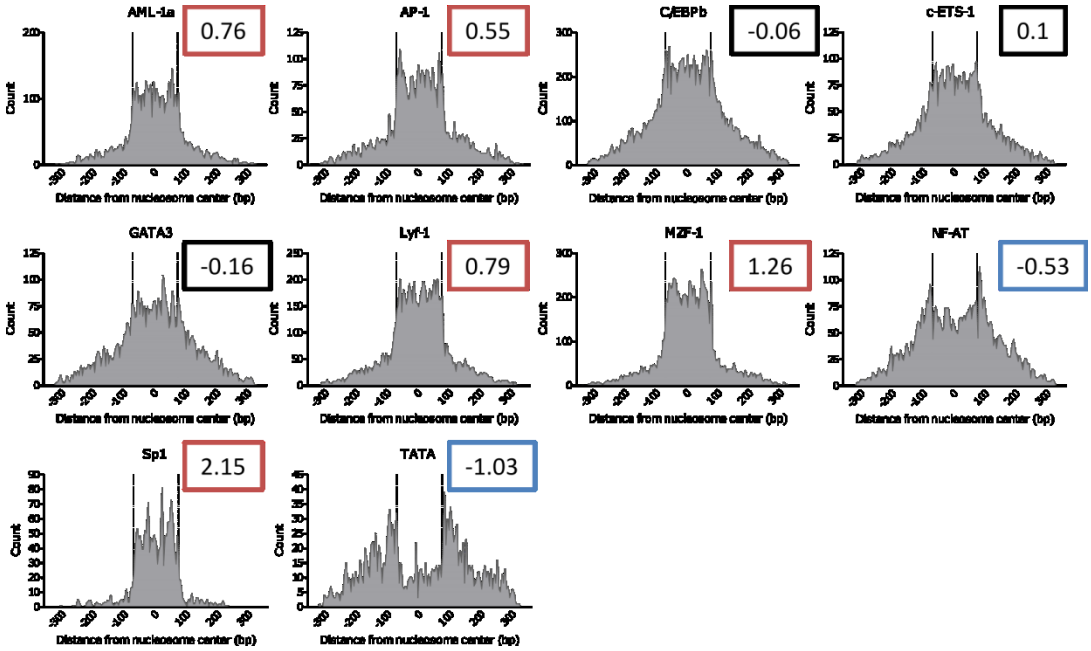

Figure 9: Predicted transcription factor binding site proximity to nucleosome centers within the C57BL/6 Ly49 gene family. Histograms show the distance from the TFBS center to the nearest nucleosome center, determined using the predicted TFBS and nucleosome positions as described. Nucleosome boundaries are identified by dotted lines. Factors with at least 300 putative binding sites within the Ly49 gene family are shown. The kurtosis is indicated for each histogram, with flat distributions (kurtosis less than -0.5) indicated in blue, tight distributions (kurtosis greater than 0.5) in red, and normal distributions (kurtosis between -0.5 and 0.5) in black. Those with flat distributions are taken as preferentially nucleosome-avoiding, while those with tight distributions are taken as preferentially nucleosome-co-localizing.

orient themselves in such a way as to always face 'outward' even when wound around a nucleosome, making them still accessible to their transcription factor even if nucleosome-bound (Figure 10). To account for this possibility, we performed a fourier analysis on the predicted TFBS to determine their periodicity (Figure 11). We selected a leave-one-out approach to this analysis—where all factors are pooled, and then each individually removed to measure its impact on the overall periodicity—to mitigate bias from the different numbers of TFBS present between the different transcription factors. Remarkably, of all the TFBS tested, only those for AML-1 displayed a marked increase in the 10 bp periodicity when removed, indicating that AML-1 uniquely had reduced 10 bp periodicity.

Since AML-1 sites were both preferentially covered by nucleosomes and lacked the 10 bp periodicity needed to orient themselves in-phase with the covering nucleosome, we hypothesized that AML-1 was key to the nucleosome regulation of Ly49 transcription. To confirm that these nucleosome-related features were unique to AML-1 sites within the Ly49 gene cluster, I repeated the transcription factor to nucleosome distribution analysis (Figure 12) and fourier analysis (Figure 13) across the entirety of chromosome 6, and observed that most of the TFBS analyzed displayed preferential nucleosome coverage and marked loss of 10 bp periodicity. Factors such as MZF-1 and Egr-1 did so with a much greater magnitude than AML-1, indicating that this unique propensity for nucleosomal disruption observed for AML-1 in the Ly49 promoter regions is not generalizable to the entire chromosome.

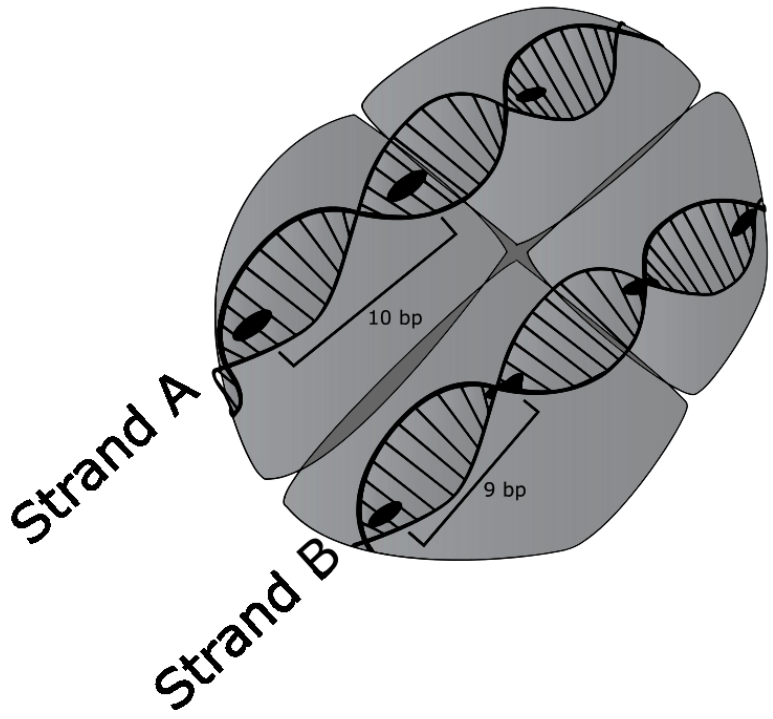

Figure 10: Diagram of the impact of DNA twisting on nucleosome-TFBS interactions. Due to DNA's twisting every 10 bp, it is theoretically possible for a given genetic element such as a series of TFBS to be oriented 'outward' from the nucleosome surface and thus be accessible even if nucleosome-bound. Strand A contains a factor with a repeating 10 bp periodicity that matches the 10 bp turning of the DNA, and so can perform this repeating outward orientation. Strand B contains a factor lacking the 10 bp periodicity, and so it is disrupted by the twisting of the DNA strand.

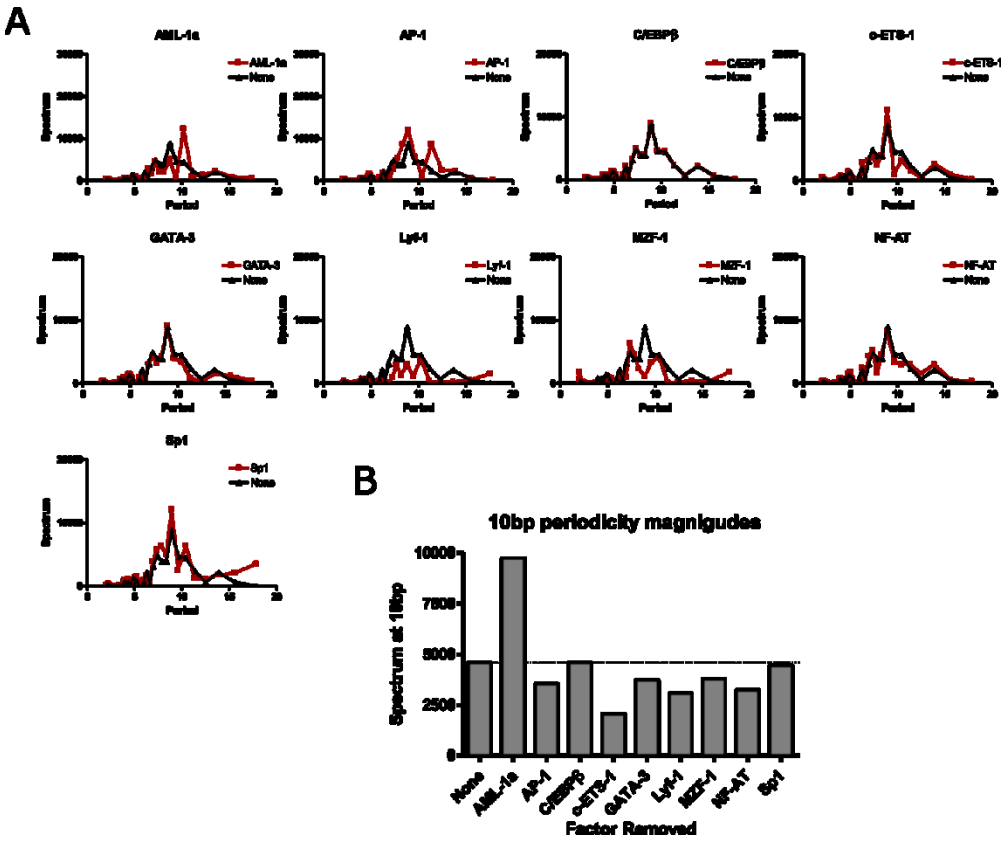

Figure 11: Fourier analysis of TFBS periodicity within nucleosome-bound regions of the Ly49 gene family. Note that only those factors with sufficient signal to generate histograms in Figure 9 (not including the TATA control) are shown, although all were used in generating these data. (A) Fourier analysis was performed on all 18 classes of TFBS for nucleosome-bound regions of the Ly49 gene family, either as an amalgam of all 18 classes (black line "none" in every graph) or by removing the indicated factor (red line in each graph) in a leave-one-out analysis. As this is a leave-one-out analysis, an increase in the red line over the black line indicates that the removal of that factor improves the periodic nature of the series, and so the removed factor specifically lacks periodicity at that period; conversely, a decrease in the red line compared to the black ultimately indicates that the removed factor specifically possesses periodicity at that period. (B) Summary of the leave-one-out analysis for 10 bp periodicity. The dotted line indicates the baseline magnitude of 10 bp periodicity possessed by the amalgam.

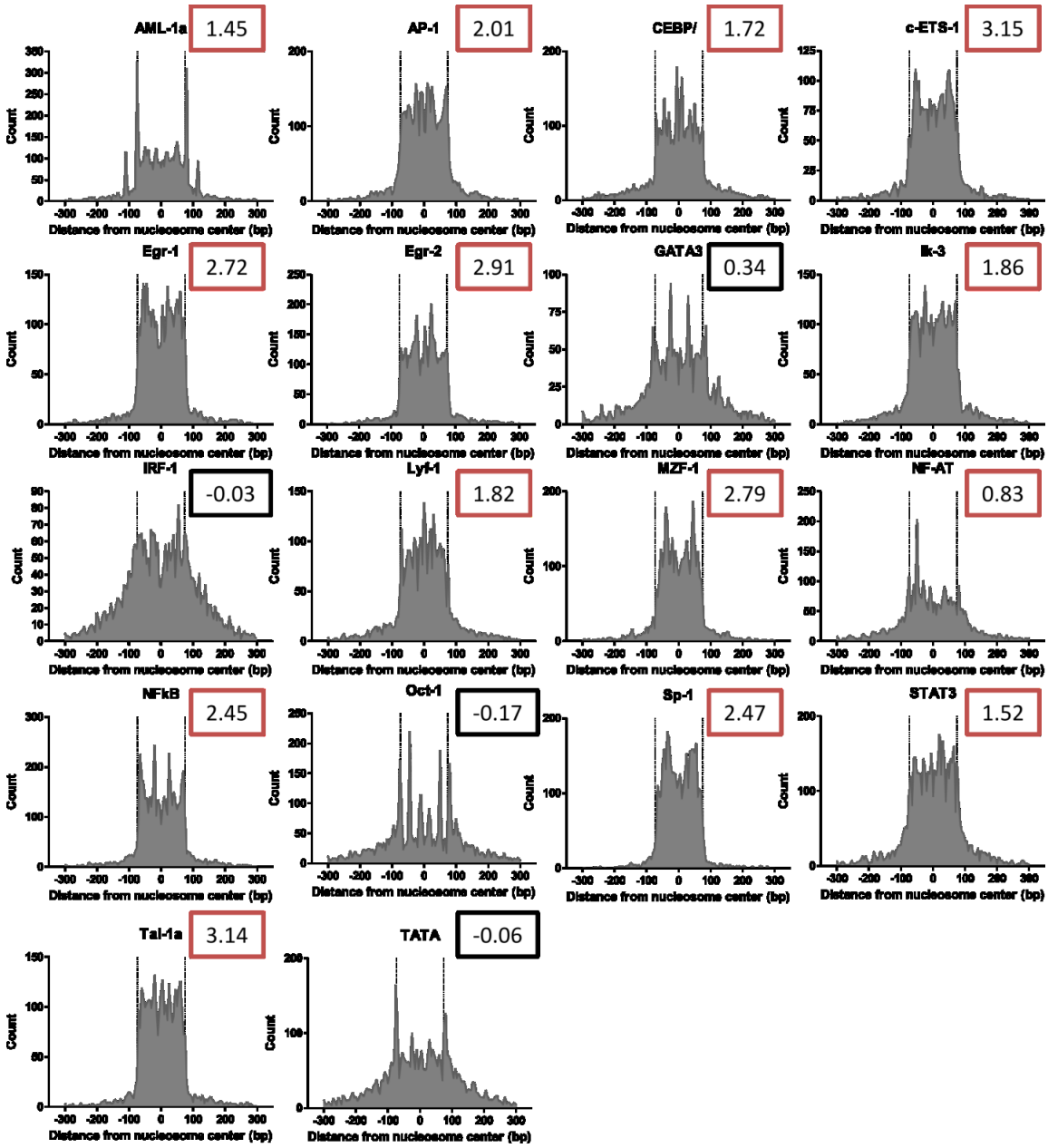

Figure 12: Predicted TFBS-Nucleosome proximity distributions across all of mouse chromosome 6. Histograms were generated as in Figure 9, this time using the entire chromosome 6 sequence. Note that most factors in this whole chromosome analysis appear to co-localize with nucleosomes, in contrast to the predictions on Ly49 promoters alone.

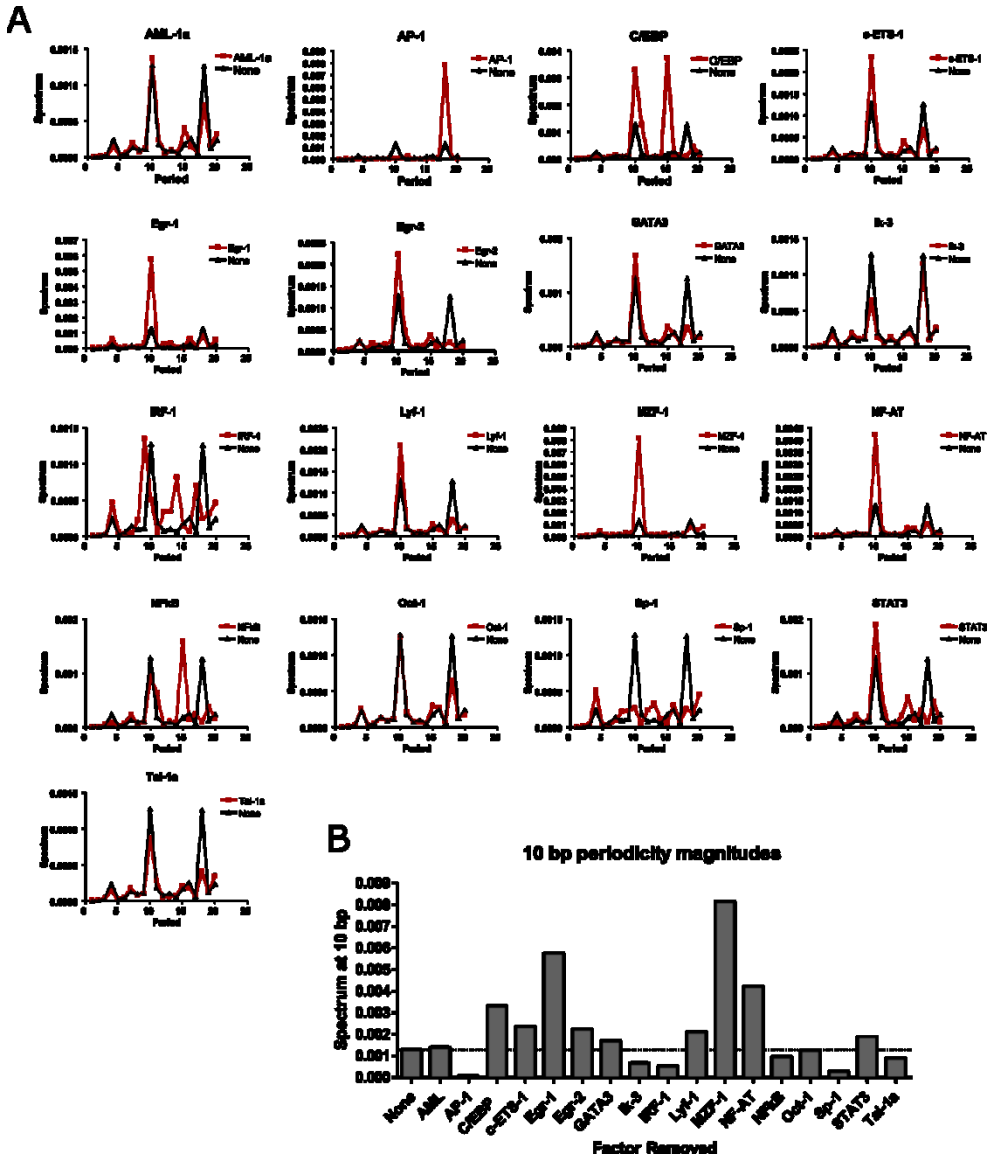

Figure 13: Fourier analysis of all nucleosome-bound TFBS in mouse chromosome 6. Fourier analysis was performed as in Figure 11. Note that many factors specifically lack 10 bp periodicity in nucleosome-bound regions of chromosome 6, with greater magnitude than AML-1, indicating that the observed lack of 10 bp periodicity for this factor within the Ly49 cluster is not a general feature of AML-1 binding sites.

3.2: Laboratory validation of AML-1 as a nucleosome target

The computational predictions generated thus far indicated that AML-1 binding sites were prime targets for nucleosome regulation in the Ly49 gene cluster. As mentioned above, however, one of the driving forces behind this investigation was the Ly49 gene cluster's aptitude as a model system in which to test hypotheses about nucleosome binding. I therefore sought to confirm these predictions in a laboratory setting, by comparing nucleosome occupancy maps between expressed and non-expressed Ly49 genes.

3.2.1: Mapping nucleosomes in RMA cells

The complex nature of Ly49 expression in primary NK cells presented a challenge in preparing nucleosome maps for the various Ly49 genes. Fortunately, RMA cells, an NK-T cell line used extensively in laboratory settings, is known to naturally express Ly49A, and not any other Ly49 for which a detecting antibody exists. I first confirmed this fact by flow cytometry, indicating that RMA cells do indeed express Ly49A alone (Figure 14), compared to primary splenic NK cells, which displayed normal Ly49 expression patterns.

I then prepared a nucleosome map of the RMA genome using MNase digestion to isolate nucleosome-bound DNA followed by next-generation sequencing (Figure 15). The resulting genomic map of nucleosome positions has been deposited to the Gene Expression Omnibus, available online under accession number GSE71863. From this map, I compared actual nucleosome-bound sites to our predicted sites to determine the accuracy of our prediction. I hypothesized that, since gene expression involves active chromatin rearrangement events, expressed Ly49 genes (in this case, Ly49A) should display more divergence between the predicted and actual nucleosome map (ie: less accuracy), since these genes are more likely to

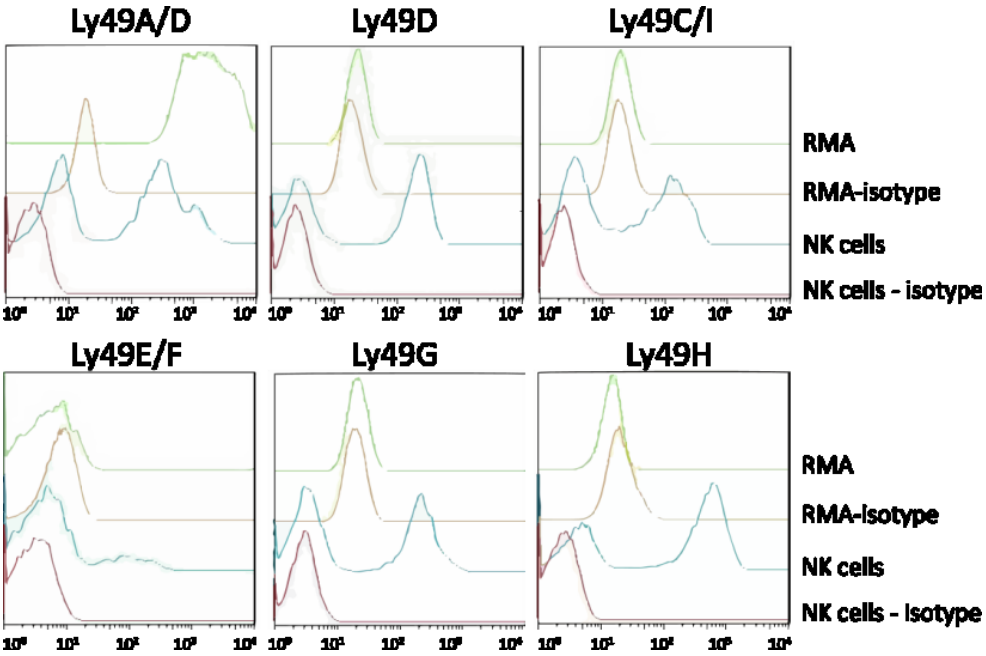

Figure 14: Ly49 expression on RMA cells. Flow cytometry revealed that RMA cells were successfully stained with an antibody recognizing Ly49A and Ly49D, but not with antibodies recognizing Ly49D alone, or Ly49C/I, Ly49E/F, Ly49G, or Ly49H, indicating that RMA homogeneously expresses Ly49A and not other Ly49 receptors. In contrast, NK cells isolated from mouse spleens display a complex expression pattern for all of the antibodies used.

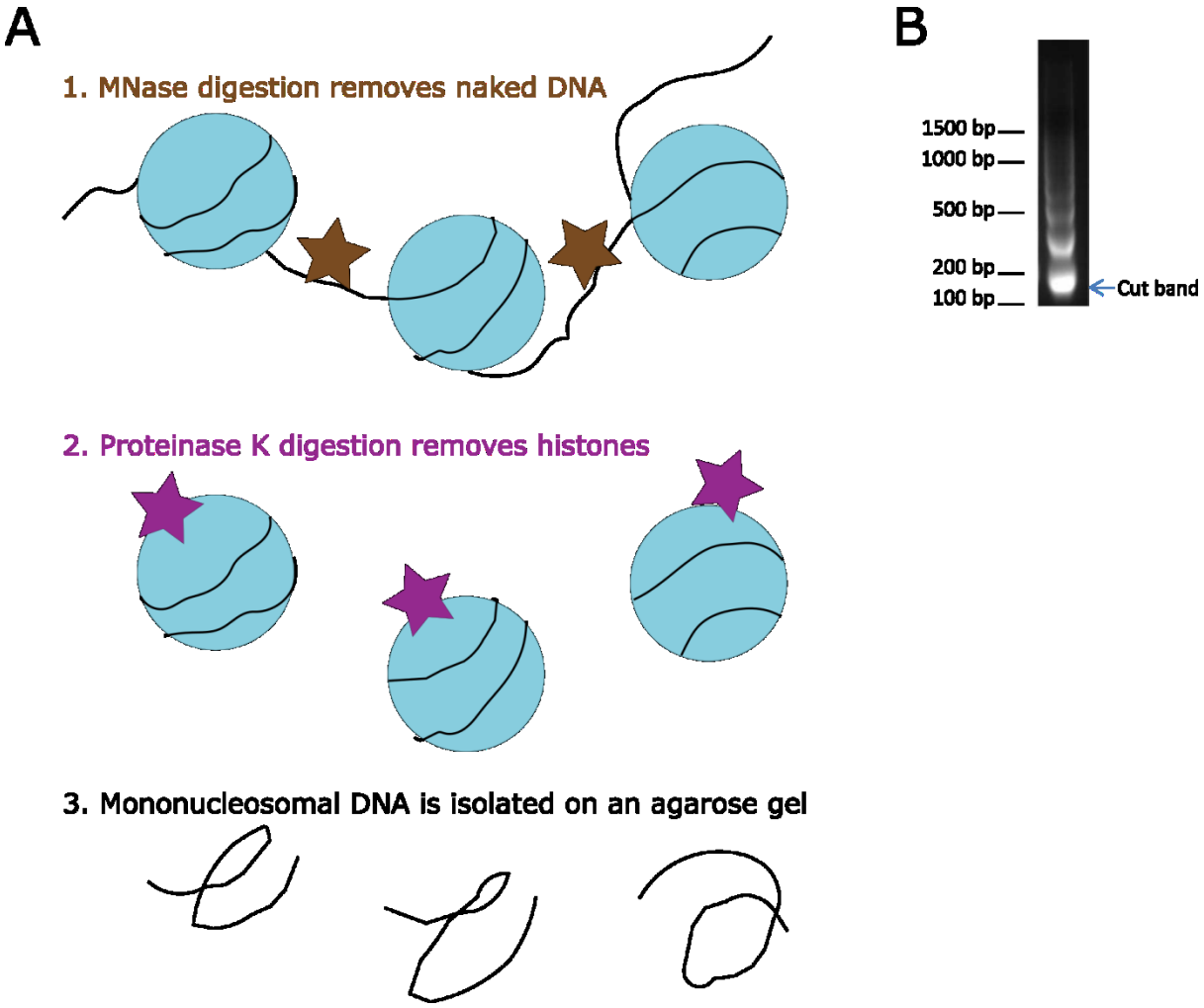

Figure 15: MNase digestion and isolation of mononucleosome DNA. (A) Following formalin cross-linking, DNA fragments are digested by micrococcal nuclease (MNase), resulting in a pool of short DNA fragments that are tightly associated with histones. These histones are then removed by proteinase K digestion, leaving only small fragments of DNA consisting of mononucleosomes, dinucleosomes, and so on. (B) These fragments are separated on an agarose gel, giving rise to a characteristic ladder with bands at approximately 150 bp, 300 bp, 450 bp, etc. Mononucleosomes (the band corresponding to ~150 bp) were excised and purified from the gel, and used for all downstream sequencing.

have active chromatin remodelling taking place. Indeed, Ly49A had less accuracy than any other Ly49 across its entire promoter and enhancer region (Figure 16, first column).

To directly test the hypothesis that nucleosome positioning at specific transcription factor binding sites inversely correlates with gene expression, I investigated each set of TFBS individually for their nucleosome coverage accuracy. Again, Ly49A was among the least accurate at almost every TFBS (Figure 16). In particular, it displayed the lowest accuracy (28%) at AML-1 sites.

3.2.2: Interpreting the nucleosomal depletion at TFBS in Ly49 promoters

I sought to determine whether this apparent depletion of nucleosomes at transcription factor binding sites in Ly49A was statistically meaningful. To this end, I performed a chi-square analysis comparing the observed number of accurately predicted nucleosomes at each TFBS for each Ly49 gene (the same counts that gave rise to the proportions presented in Figure 16) to the 'expected' accuracy obtained for the entirety of each Ly49 gene (the counts from Figure 16, first column). Taking the overall accuracy of each Ly49 gene individually allowed me to correct for the inherent inaccuracy present in our prediction, as discussed above in Figure 7. This enabled me to determine whether the depletion I observed at a given TFBS was specific to that TFBS, or whether it was simply indicative of the depletion for that specific promoter. Of all the promoters tested, only Ly49A and the pseudogene Ly49K had significantly divergent TFBS compared to the rest of their promoters (Figure 17, last two columns). While there is no post-hoc analysis for this chi-square test that would allow a statistical determination of which TFBS were most significant, I have summarized the relative contribution each TFBS had to its promoter's overall chi-square statistic (Figure 17). As indicated, AML-1, c-ETS-1, Lyf-1, and MZF-1 had the strongest

	Whole	AML-1	AP-1	C/EBPb	c-ETS-1	GATA3	Lyf-1	MZF-1	NF-AT	Sp1
Ly49A	39%	26%	31%	33%	24%	43%	27%	27%	35%	22%
Ly49C	47%	50%	56%	42%	41%	58%	37%	36%	35%	38%
Ly49J	46%	49%	37%	45%	43%	38%	44%	50%	55%	53%
Ly49G	44%	39%	39%	36%	27%	28%	43%	40%	38%	42%
Ly49I	42%	37%	42%	41%	48%	39%	38%	44%	48%	36%
Ly49H	42%	30%	41%	41%	44%	45%	39%	39%	38%	42%
Ly49K	44%	38%	47%	38%	25%	37%	38%	30%	34%	27%
Ly49D	40%	34%	25%	32%	36%	35%	31%	32%	34%	27%
Ly49F	48%	54%	49%	45%	43%	38%	44%	46%	45%	36%
Ly49E	42%	34%	34%	34%	40%	41%	34%	34%	39%	43%
Ly49Q	42%	32%	29%	41%	46%	36%	33%	33%	46%	41%

Figure 16: Heatmap showing the confirmed predicted nucleosome binding sites compared to the actual MNase-digested sequence taken from RMA cells. The first column shows the degree of confirmed predicted nucleosomes for the whole enhancer and promoter 1 region of each Ly49 (defined as 10,000 bp upstream and 1000 bp downstream of exon -1a). Each subsequent column indicates the degree of confirmed predicted nucleosomes for each TFBS presented in Figure 11. Red shading indicates relatively low confirmation rates—and blue relatively high—on a column-by-column basis.

	AML-1	AP-1	C/EBPb	c-ETS-1	GATA3	Lyf-1	MZF-1	NF-AT	Sp1	Total	P value
Ly49A	3.3	0.7	1.4	3.3	0.3	4.0	3.6	0.2	1.278	18.0	*
Ly49C	0.1	0.8	0.8	0.3	1.3	2.4	2.3	1.2	0.003	9.4	ns
Ly49I	0.2	0.9	0.0	0.1	0.6	0.1	0.3	0.9	0.813	4.0	ns
Ly49G	0.4	0.4	1.9	3.4	3.6	0.0	0.2	0.4	0.05	10.4	ns
Ly49I	0.4	0.0	0.0	0.5	0.1	0.3	0.2	0.4	0.034	2.0	ns
Ly49H	3.6	0.0	0.1	0.0	0.1	0.3	0.3	0.3	0.077	4.8	ns
Ly49K	0.8	0.2	1.2	4.8	0.6	1.2	6.0	1.2	1.134	17.0	*
Ly49D	1.0	3.3	3.2	0.3	0.4	3.1	2.0	0.6	1.512	15.3	ns
Ly49F	0.5	0.0	0.3	0.2	1.1	0.3	0.1	0.1	0.035	2.6	ns
Ly49E	1.3	1.5	2.8	0.1	0.0	2.4	2.0	0.1	0.147	10.3	ns
Ly49Q	1.9	2.4	0.0	0.3	0.6	2.7	2.2	0.3	0.049	10.4	ns

Figure 17: Chi-Square analysis of nucleosome depletion at TFBS for each Ly49 enhancer/promoter 1. Chi-square tests were performed for each Ly49 individually by considering the actual nucleosome accuracy (the first column, 'whole', in Figure 16) as the expected value for that Ly49, and comparing this to the observed accuracy at each TFBS. Of all the Ly49 tested, only Ly49A and Ly49K were significantly divergent at their TFBS compared to the overall accuracy of that Ly49. The relative contribution of each TFBS to this overall TFBS divergence is indicated by the individual chi-square values, with stronger shading showing a larger contribution to that Ly49's divergence, on a row-by-row basis. * p-value <0.05.

contribution to the chi-square statistic in Ly49A, indicating that these four factors accounted for most of the significant depletion observed at this Ly49 promoter's TFBS.

Unfortunately, these TFBS all exist in close proximity to one another—it was therefore possible that the observed depletion at one site was in fact non-specific, and only caused by specific depletion at a nearby site covered by the same nucleosome. In particular, AML-1, Lyf-1, and MZF-1 are all preferentially nucleosome-covered TFBS, making their co-localization and shared nucleosome depletion even more likely. I hypothesized that, if one TFBS was driving the depletion at other sites, there would be a predictor-response asymmetry between the two. That is to say, if factor 1 was causing the depletion at factors 2 and 3, then knowing the depletion state of factor 1 would be a better predictor of the depletion at 2 or 3 than knowing the depletion of 2 or 3 would be at predicting the depletion of factor 1 (Figure 18).

I performed a logistic regression analysis of each of these factors, and confirmed that knowledge of AML-1's depletion status was a better predictor of the status of Lyf-1 or MZF-1 than either of these factors were at predicting AML-1 (Figure 19). Of note, AML-1 and c-ETS-1 were roughly symmetrical as each other's predictor, indicating that neither one is likely causative of the other's depletion. This agrees nicely with the fact that, while AML-1, Lyf-1, and MZF-1 are all preferentially nucleosome-covered, c-ETS-1 is not; it is therefore less likely to be affected by AML-1 depletion and vice-versa, since it is less likely to be located near AML-1 sites. Therefore, it is likely that the specific nucleosome depletion observed in expressed Ly49 genes is driven by a need to expose AML-1 binding sites. This agrees with the current model of Ly49 expression, which holds that the AML-1 binding site contained within pro1 is essential for promoter function.

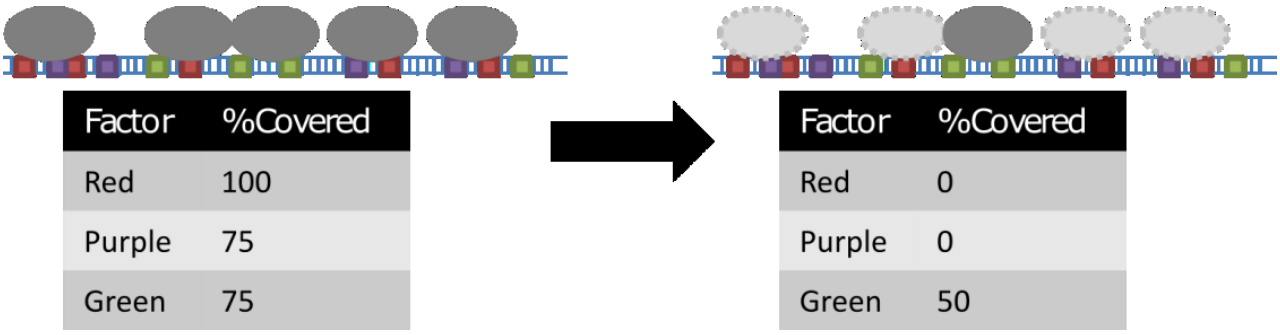

Figure 18: Diagram of the co-depletion problem. Because many of the TFBS studied here are preferentially nucleosome-covered, and because nucleosomes are large, nucleosome depletion at one TFBS will naturally deplete all neighboring TFBS as well. In this example, a nucleosome depletion event causes red coverage to go from 100% to 0%, purple to go from 75% to 0%, and green from 75% to 50%. Using nucleosome depletion as the readout, it is impossible to determine whether red or purple was the 'intended' factor to be exposed. However, if red depletions always correlate with purple depletions, while purple depletions only occasionally correlate with red depletions, it is likely that red is driving the nucleosome depletion event.

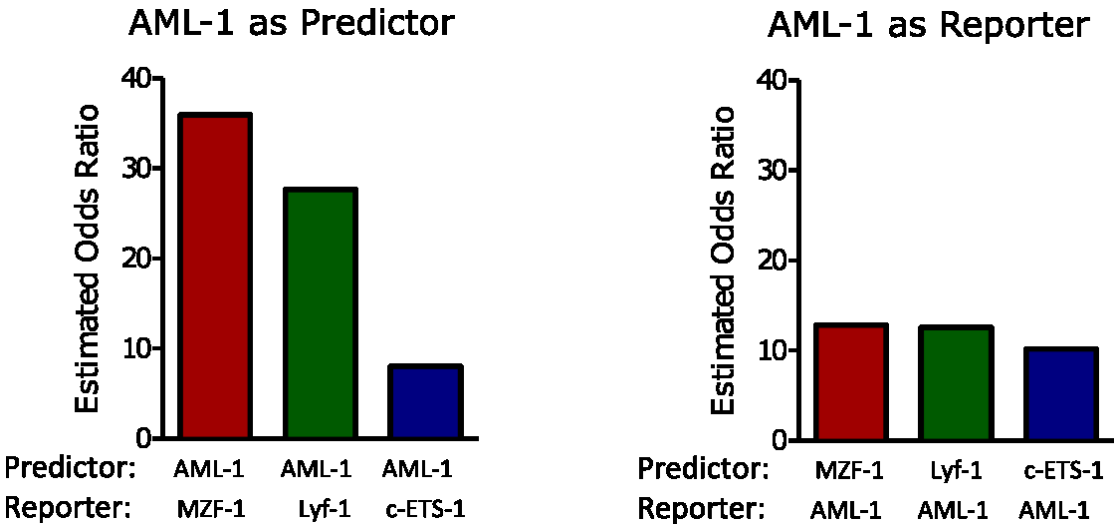

Figure 19: Predictor asymmetry study of AML-1 co-depletion. Logistic regression analysis was performed to determine (A) the ability for AML-1 depletions to predict the nearest MZF-1, Lyf-1, and c-ETS-1 depletion, as well as (B) the ability for each of these factors to predict the depletion of the nearest AML-1 TFBS. AML-1 is a better predictor of MZF-1 and of Lyf-1 than either of these are of AML-1, indicating that the depletion observed at MZF-1 and Lyf-1 sites are likely caused by an intended depletion of a neighboring AML-1 site. Conversely, AML-1 and c-ETS-1 do not share this asymmetric relationship, indicating that they are not likely influencing each other's nucleosome depletions.

I performed two final controls for this finding. First, although we lacked the resources to perform chromatin immunoprecipitations (ChIP) on all tested transcription factors to confirm their predicted binding sites, I did perform a ChIP on AML-1 to confirm that it is indeed bound to the Ly49A promoter in RMA cells (Figure 20). Second, we had originally dismissed pro2 as uninvolved in nucleosomal regulation, based on the lack of a clear nucleosome signal present at this promoter. Nevertheless, I evaluated the prediction accuracy at pro2 and at the hypothetical pro3 region of each Ly49, and found that there is no correlation between nucleosome accuracy and gene expression at either of these promoters (Figure 21), unlike the significant correlation found in pro1.

Overall, the experimental results support our computational predictions that identified AML-1 binding sites as key points for nucleosomal regulation of Ly49 expression. The overall significance of this finding, both for NK cell immunology and nucleosome bioinformatics, will be discussed in chapter 5.

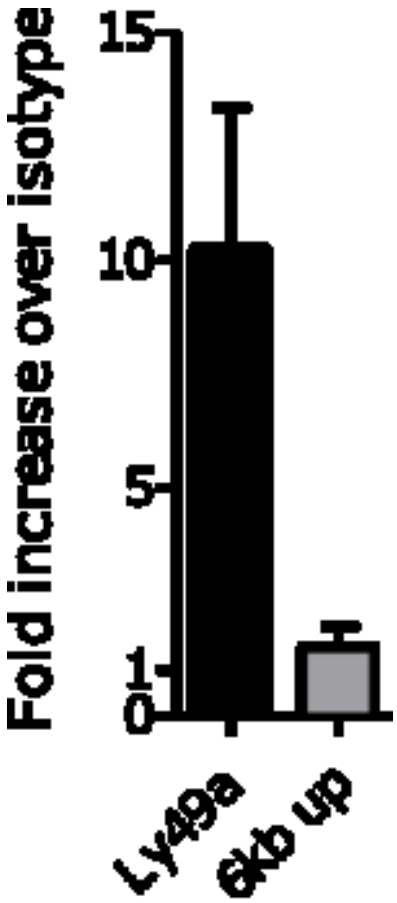

Figure 20: Chromatin immunoprecipitation on AML-1 binding to the Ly49A promoter in RMA cells. Sheared chromatin was prepared as for MNase-seq above, but then immunoprecipitated using anti-AML-1 or an isotype control and PCR amplified to detect either the Ly49A promoter or an irrelevant region 6 kb upstream (6kb up) of this promoter. The Ly49A promoter sequence was enriched 10-fold when compared to immunoprecipitation with the isotype control, indicating that AML-1 is bound to this region of the RMA genome.

Gene	Pro2	Pro3
Ly49A	80%	29%
Ly49C	67%	57%
Ly49J	100%	0%
Ly49G	20%	33%
Ly49I	0%	43%
Ly49H	33%	43%
Ly49D	22%	33%
Ly49F	100%	50%
Ly49E	50%	13%
Ly49Q	100%	20%

Figure 21: Nucleosome prediction correspondence at promoters 2 and 3. Although the heatmapping analyses in figures 14 and 15 could not be performed for the much smaller genomic regions of promoter 2 and 3, the correspondence between predicted and actual nucleosomes was still calculated for this area. Unlike in promoter 1, no correlation was observed between expression state and nucleosome correspondence for either of these promoter regions.

4: Adaptive NK Cell Memory Requires Self-Reactive Ly49 Receptors

In the decade since its discovery, the idea that NK cells can display adaptive memory-like behaviour has been steadily gaining support. We now have evidence that NK cells can respond to specific chemical haptens[124] and viral proteins[126]. Moreover, NK cells can mediate the protective effects of several anti-viral vaccines, with antigen-specific protection observed in mice, primates[128], and zebrafish[127]. Recent studies have also identified a population of NK cells in the pleural fluid from human TB patients that respond stronger than normal NK cells when challenged with tuberculosis peptides, hinting that this surprising function of NK cells might be active in humans as well[135].

Nevertheless, for all these results solidifying the existence of adaptive NK cell memory, we still do not understand how NK cells can generate these specific memories. To this end, I began the work presented in this thesis in an effort to determine what role—if any—self-reactive Ly49 receptors played in the adaptive NK cell response. Ly49C and Ly49I (Ly49C/I) had been previously identified as markers of NK cell memory cells—Ly49C/I^{+} NK cells were able to transfer memories to naive hosts, while Ly49C/I^{-} cells could not[124]. However, no attempt was made to understand why Ly49 receptors were correlated with NK cell memory. It was possible that they were merely markers of memory NK cells and were not directly involved, although the fact that Ly49 receptors are stochastically expressed, yet present on all memory cells, implied that these receptors had some function for NK cell memory. It was more likely that NK cell memory was dependent on Ly49C/I for their role in NK cell licensing—that is, only licensed NK cells could become memory cells. Finally, because Ly49C/I directly interact with the MHC-I

antigen presentation platform, it was possible that these Ly49 receptors were directly involved in NK cell antigen recognition. I undertook this study to test these possibilities.

4.1: Ly49 expression is required for adaptive NK cell memory

Testing adaptive NK cell memory in the lab required two components: a relevant mouse model, and a readout of a memory response. Fortunately, our lab had previously generated two key mouse lines for this study. $Ly49^{KD}$ mice have dramatically reduced expression of the entire Ly49 gene family due to a concatameric insert introduced into the genome upstream of the Ly49 locus[133]. This disruption results in about 80% loss of Ly49 expression in all NK cells, as well as a less marked reduction in several downstream genes. To control for this somewhat non-specific loss of Ly49, the lab had also previously generated $Ly49^{KD}$ mice that had been transgenically complemented with the Ly49I gene ($Ly49^{KD}$-I^{tg})[133,136]. The generalized experimental design was to test whether $Ly49^{KD}$ mice lacked adaptive NK cell memory responses. If they did, I would then test whether $Ly49^{KD}$-I^{tg} mice had no defect in NK cell memory: if so, the defect observed in $Ly49^{KD}$ mice could be ascribed to the loss of Ly49I alone. Of note, I did not have access to an Ly49C-transgenic mouse, but I hypothesize that Ly49C would also be sufficient for memory responses, since both Ly49C and Ly49I share functions and binding targets.

I crossed each of these mouse lines onto a Rag1-deficient background ($Rag1^{-/-}$)[137]. Without Rag1, the mouse cannot generate T or B cells, resulting in T and B cell-deficient mice. This allowed me to study NK cell memory without T cell interference masking the observed responses (Figure 22).

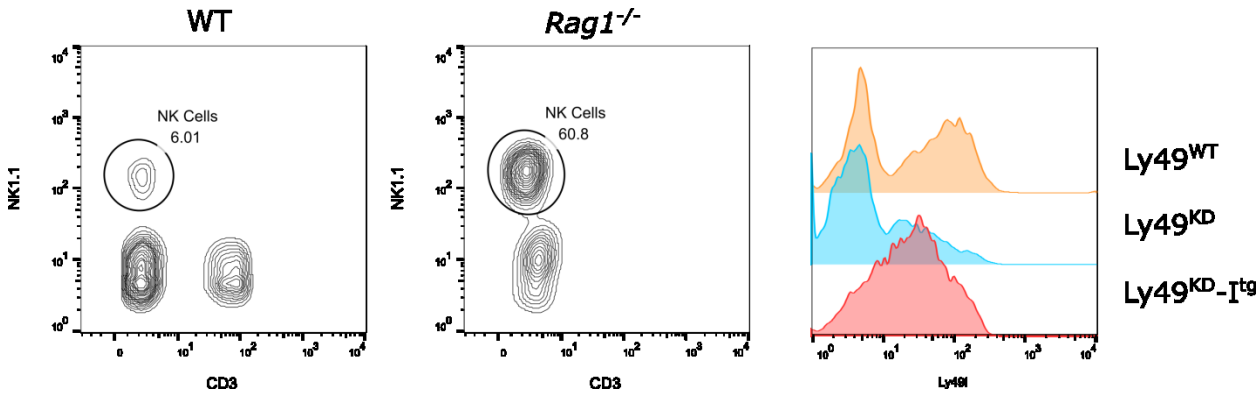

Figure 22: Flow cytometry demonstration of Ly49-modulated mice on the Rag1-deficient background. (A) Rag1-deficient mice lack T cells ($CD3^+$ $NK1.1^-$), and have a proportional increase in NK cells ($CD3^-$ $NK1.1^+$) in the spleen when compared to WT mice. (B) Mice with normal Ly49 expression ($Ly49^{WT}$, yellow graph) have roughly 50% $Ly49I^+$ NK cells in the spleen. The expression of Ly49I (and all other Ly49)[133] is markedly reduced both in percentage of cells expressing it and in the magnitude of their expression ($Ly49^{KD}$, blue). Conversely, in the $Ly49^{KD}$-I^{tg} rescue model, since Ly49I is expressed by the Thy1 promoter, virtually all NK cells express Ly49I (red).

For an experimental readout, much of my work is based on the initial studies in NK cell memory, using the classic mouse ear-swelling test. In this study, mice are sensitized to a relevant antigen or left in a naive state. Sometime later (as indicated in each figure), all the mice are challenged with the same antigen in one ear and not in the other, and ear thickness is recorded daily. Memory responses cause the challenged ear to perceptibly swell when compared to the unchallenged ear, before returning to normal after four days, resulting in a characteristic ear swelling curve (Figure 23).

4.1.1: Genetic disruption of Ly49C/I eliminates adaptive NK cell memory

The simplest evaluation of Ly49C/I's involvement in NK cell memory was to repeat the original NK cell memory experiment, sensitizing my various mouse models to the chemical hapten dinitrofluorobenzene (DNFB), challenging them, and then recording ear swelling data. $Rag1^{-/-}$ mice were able to demonstrate ear swelling responses to DNFB provided they had been previously exposed to the chemical as previously shown. These responses were lost in $Rag1^{-/-}$ $Ly49^{KD}$ mice, and completely rescued in $Rag1^{-/-}$ $Ly49^{KD}$-I^{tg} mice, in both short-term (Figure 24A) and long-term (Figure 24B) memory experiments. Moreover, this response was antigen specific: DNFB could not elicit a memory response from mice sensitized to another hapten, oxazolone (OXA), but OXA-sensitized mice readily responded to OXA challenge, again in an Ly49I-dependent manner (Figure 25).

Figure 23: Schematic of the mouse ear swelling test. Mice are sensitized to the antigen in question either by cutaneous application (for skin-reactive haptens) or hock injection (for peptides), then boosted as indicated. After a rest phase, mice are challenged in one ear, with the control ear given vehicle alone in a mock challenge, and ear thickness is measured daily. Ear swelling is calculated as the thickness of the challenge ear minus the thickness of the control ear.

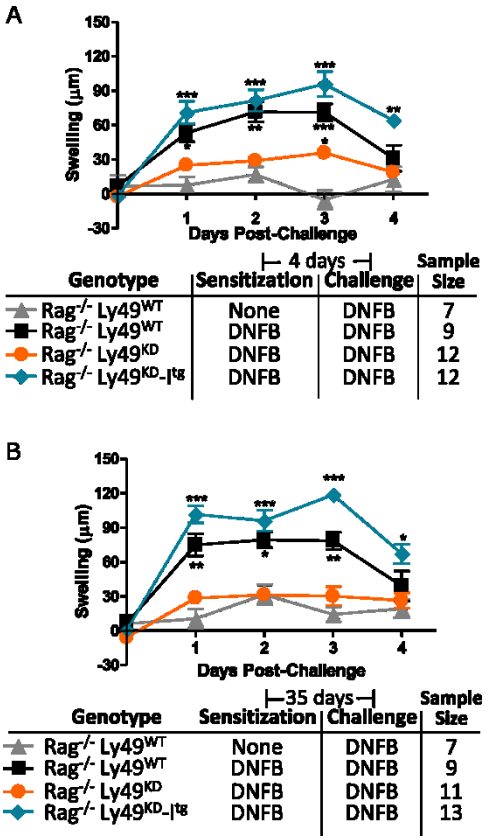

Figure 24: Ly49I is required for memory to dinitrofluorobenzene (DNFB) in Rag1-deficient mice. The mouse ear swelling test was performed, challenging mice after 4 days (A) or 35 days (B) as indicated. Naive Rag1-deficient mice (grey lines) did not respond to the ear challenge, while sensitized littermates of these mice (black lines) displayed robust ear swelling for three days post-challenge, indicative of an immunological memory. Rag1-deficient mice lacking Ly49 expression had a significantly impaired response to the ear swelling, but Ly49I transgenic rescue was sufficient to completely rescue the ear swelling phenotype. Statistics were calculated using a two-way ANOVA followed by the Bonferroni post-hoc test comparing all means to the naive control. Significance is indicated with * $p<0.05$, ** $p<0.01$, *** $p<0.001$.

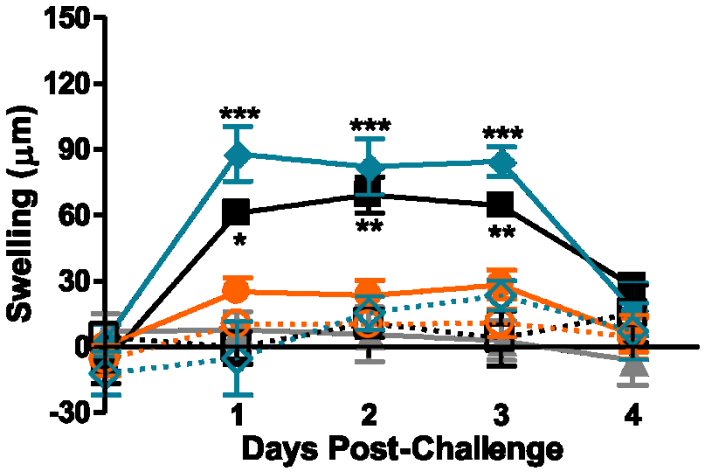

Genotype	Sensitization	4 days Challenge	Sample Size
Rag$^{-/-}$ Ly49^{WT}	None	OXA	5
Rag$^{-/-}$ Ly49^{WT}	OXA	OXA	6
Rag$^{-/-}$ Ly49^{KD}	OXA	OXA	11
Rag$^{-/-}$ Ly49^{KD}-I^{tg}	OXA	OXA	6
Rag$^{-/-}$ Ly49^{WT}	OXA	DNFB	5
Rag$^{-/-}$ Ly49^{KD}	OXA	DNFB	8
Rag$^{-/-}$ Ly49^{KD}-I^{tg}	OXA	DNFB	6

Figure 25: Ly49I-dependent memory to chemical haptens is antigen specific. The mouse ear swelling test was repeated as in Figure 24, but this time mice were sensitized to an unrelated hapten, oxazolone (OXA). Mice challenged with OXA displayed the same ear swelling as those in Figure 24—ear swelling required prior exposure to the antigen and expression of at least Ly49I. Mice sensitized to OXA did not react to DNFB, regardless of Ly49 expression, indicating antigen specificity. Statistics were calculated using a two-way ANOVA followed by the bonferroni post-hoc test comparing all means to the naive control. Significance is indicated with * p<0.05, ** p<0.01, *** p<0.001.

Since the mechanism of action for haptens is unclear, and NK cell memory itself still somewhat controversial, I repeated these findings using conventional peptide antigens. SIINFEKL, the highly antigenic MHC-I-restricted peptide from chicken ovalbumin, was similarly able to provoke memory responses in $Rag1^{-/-}$ mice, provided they had been previously exposed to SIINFEKL and expressed at least Ly49I (Figure 26). Additionally, SIYRYYGL, a synthetic peptide fragment with similar MHC-I affinity as SIINFEKL, was able to provoke NK cell memory, but the two antigens did not cross-react (Figure 27).

4.1.2: Confirmation of Ly49I requirement in non-genetic models

The $Ly49^{KD}$ mouse is a powerful tool for investigating the role of Ly49 receptors in NK cell memory, and the ear swelling test is a well-used and robust model of adaptive immunity. Nevertheless, I next sought to confirm these findings using several independent methods, to control for technical or other unforeseen biases in the ear swelling results. First, I repeated the ear swelling experiment, but euthanized the mice on day two of the challenge—the middle of the response phase—and performed H&E staining on their ears (Figure 28). In agreement with the ear swelling data, those ears that displayed an NK cell memory response had significantly more cellular infiltration compared to either control ears from the same mice or challenge ears from non-responding mice.

Along similar lines, to control for the non-specific nature of our $Ly49^{KD}$ model, I repeated the ear swelling test on $Rag1^{-/-}$ mice after treating them with Ly49-depleting antibodies (Figure 29). Depletion of $Ly49C/I^{+}$ cells abrogated the ear swelling response as expected, while depletion of $Ly49G^{+}$ cells (including $G^{+}C/I^{+}$ cells) had no effect. Of note, neither Ly49 depletion had any effect in T cell-sufficient WT mice, indicating that conventional T cell memory does not require Ly49, and is fundamentally different from NK cell memory in this regard.

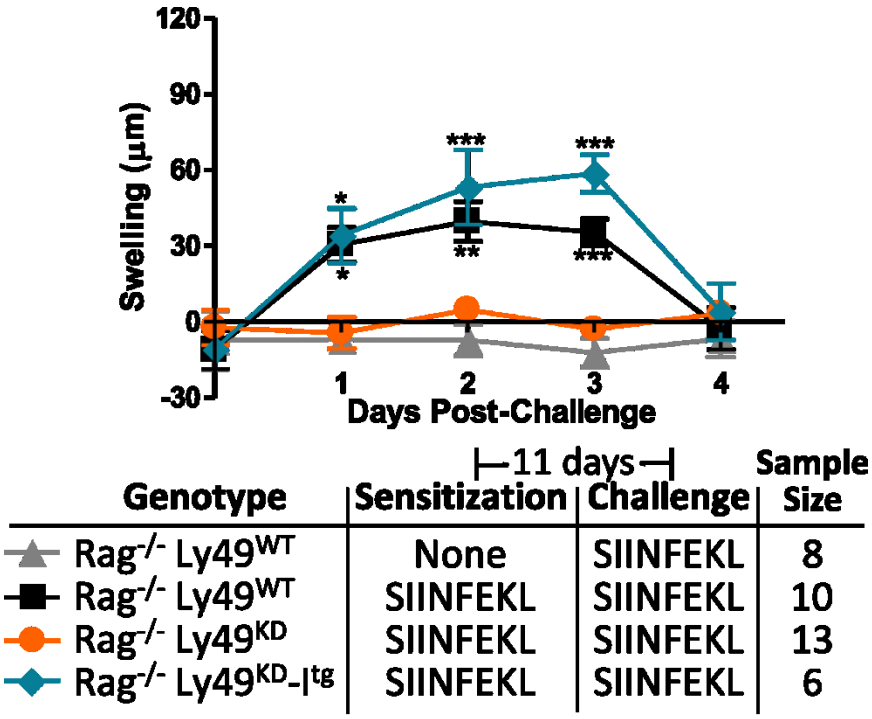

Figure 26: Ly49I-dependent memory functions against conventional peptide antigens. The mouse ear swelling test was repeated in Ly49-modulated, Rag1-deficient mice using SIINFEKL, the MHC-I restricted immunodominant epitope of chicken ovalbumin, confirming that Ly49I is required for conventional immune memory in Rag1-deficient mice. Statistics were calculated using a two-way ANOVA followed by the bonferroni post-hoc test comparing all means to the naive control. Significance is indicated with * $p<0.05$, ** $p<0.01$, *** $p<0.001$.

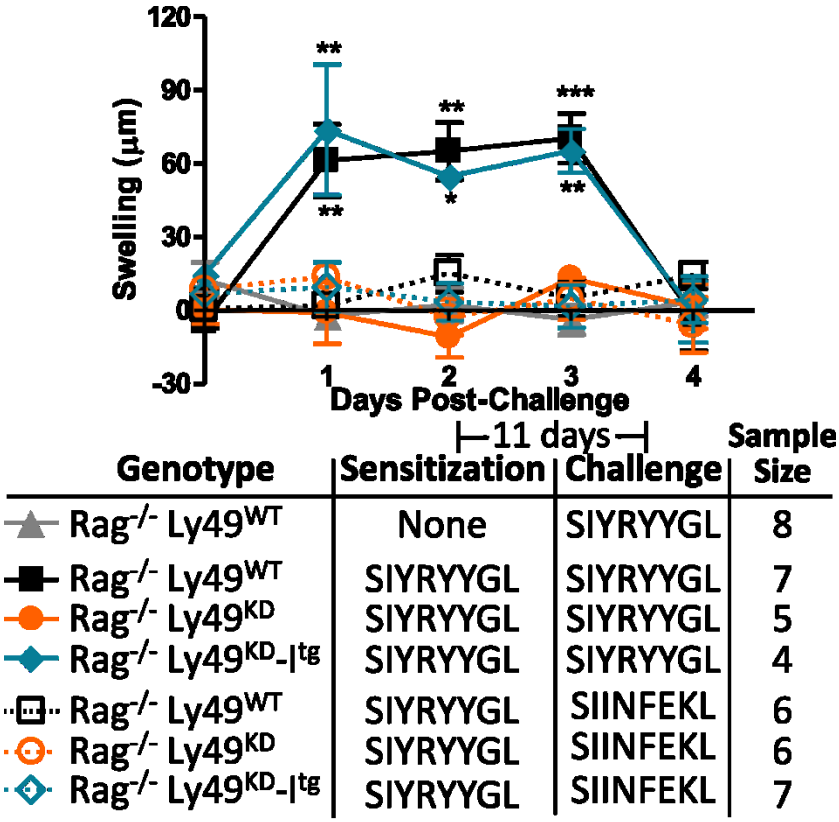

Figure 27: Ly49I-dependent memory is peptide specific. Mice were sensitized to SIYRYYGL, a synthetic antigenic peptide with similar MHC-I affinity as SIINFEKL. Ear swelling revealed an Ly49I-dependent memory to SIYRYYGL in Rag1-deficient mice. Despite its potential to induce NK cell memory responses, SIINFEKL was not able to provoke an ear swelling response in mice sensitized to SIYRYYGL, regardless of their Ly49 expression. Statistics were calculated using a two-way ANOVA followed by the bonferroni post-hoc test comparing all means to the naive control. Significance is indicated with * $p<0.05$, ** $p<0.01$, *** $p<0.001$.

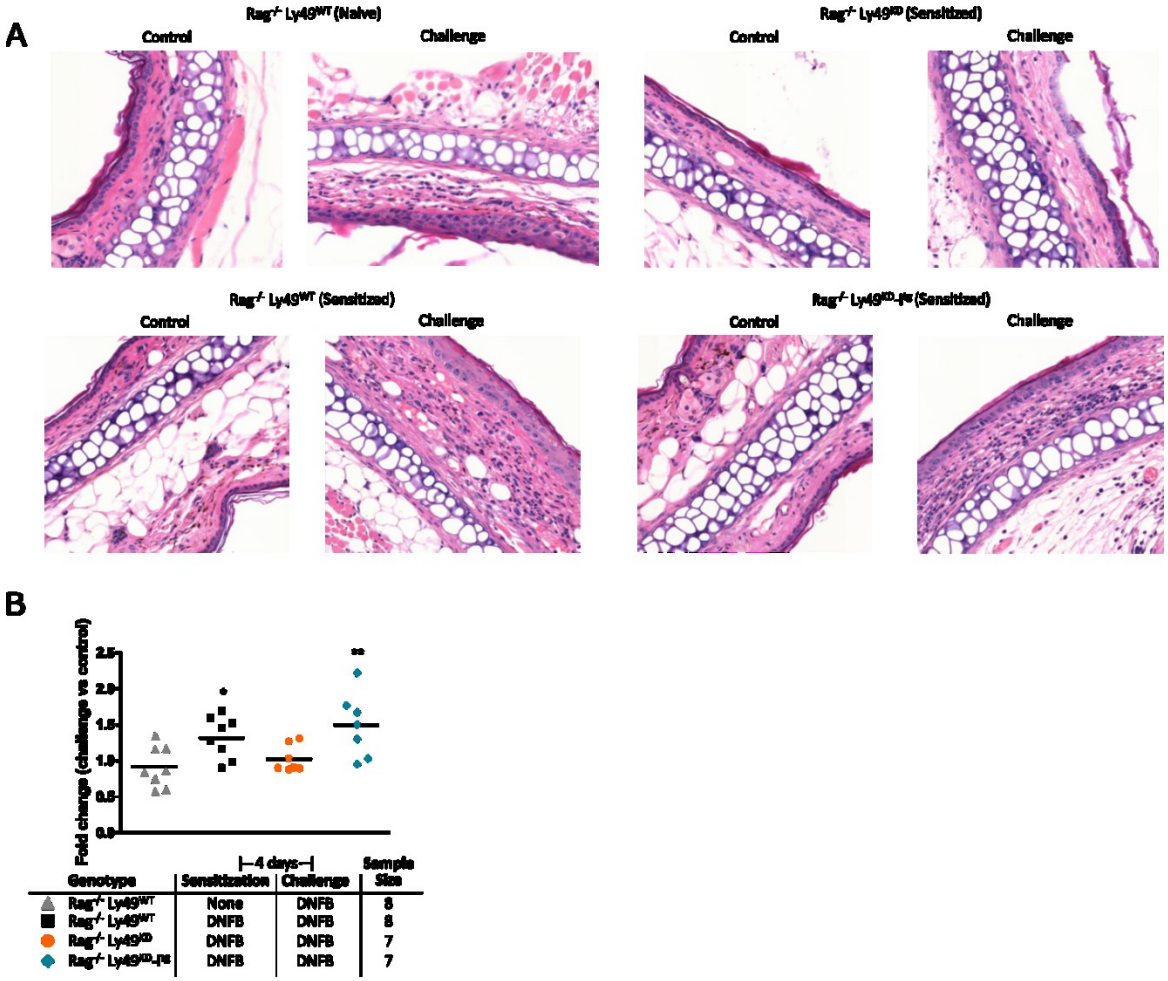

Figure 28: Ear swelling correlates with cellular infiltration in the ear dermis. Mice undergoing the ear swelling test were sacrificed on day 2 of the challenge and ears were analyzed by H&E staining. Infiltration was scored by someone blind to the experimental conditions by defining an arbitrary area of the dermis (the light pink tissue between the darker epidermal layer and the vacuolar central cartilage), counting all nuclei within that area, and calculating the mean number of nuclei per square micrometer. Example fields are shown in (A), and the median counts normalized to the control ear are shown in (B). Statistics were calculated using a one-way ANOVA followed by the bonferroni post-hoc test comparing all means to the naive control. Significance is indicated with * $p<0.05$, ** $p<0.01$, *** $p<0.001$.

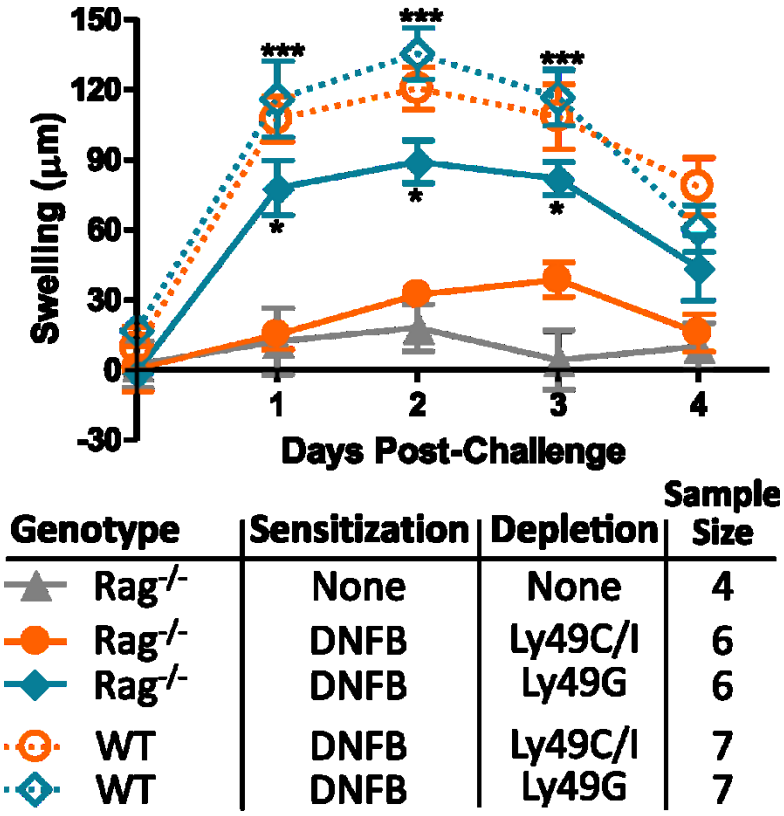

Figure 29: Depletion of Ly49C/I-expressing cells abrogates memory in Rag1-deficient animals. Mice undergoing the ear swelling test were treated with depleting antibodies targeting Ly49C/I (clone 5E6) or Ly49G (clone 4D11) throughout the sensitization and challenge phases of the experiment. Rag1-deficient mice depleted of Ly49C/I-expressing cells did not display a memory response to DNFB, while mice depleted of Ly49G were unaffected. Because Ly49C/I and Ly49G can also be expressed on T cells, I repeated these depletions on WT, T cell-sufficient animals. No effect of Ly49 depletion on memory was observed in these animals, indicating that the Ly49C/I-dependent memory is distinct from classic T cell memory. Statistics were calculated using a two-way ANOVA followed by the bonferroni post-hoc test comparing all means to the naive control. Significance is indicated with * $p<0.05$, ** $p<0.01$, *** $p<0.001$.

4.1.3: NK cells are mediating Ly49I-dependent memory

Ly49I is expressed only on NK cells, and some T cell subsets[136]—so only on NK cells in a $Rag1^{-/-}$ mouse. These results therefore supported the hypothesis that specific memory responses observed in $Rag1^{-/-}$ mice are NK cell mediated. However, to better demonstrate the NK cell mediated nature of this response, I next performed antibody depletions to remove NK cells. The classic allergic response to DNFB is believed to be $CD8^+$ T cell mediated[125]; accounting for NK cell memory, it appears that NK or $CD8^+$ T cells are sufficient to react to DNFB. To confirm this, I depleted NK cells from $Rag1^{-/-}$ mice undergoing the ear swelling test as before using an anti-NKR-P1C (NK1.1) antibody (clone PK136) (Figure 30A). I also sought to confirm the presence of NK memory in a Rag1-sufficient background, and so depleted NK cells in *Cd8a*$^{-/-}$ mice (Figure 30B). These mice lack $CD8^+$ T cells, but otherwise have normal $CD4^+$ T cells and B cells, and are fully capable of antibody responses[138]. In both cases, NK cell depletion was sufficient to disrupt memory responses to DNFB, while $CD4^+$ cell depletion had no effect, confirming that NK cells are responsible for DNFB-reactive memory responses in the absence of $CD8^+$ T cells.

Although the above depletions demonstrate the need for NK cell involvement in this Ly49-dependent memory response, I correlated NK cell involvement in two other ways. First, I repeated the ear sectioning from above and stained for NK cells specifically, using NKp46 as an NK cell marker (Figure 31). In agreement with the increased cellular infiltrate from before, there was a significant enrichment of NK cells in those ears that displayed a positive ear swelling response—namely, challenge ears from sensitized, Ly49I-sufficient mice. Second, I investigated whether interferon gamma (IFNγ) was necessary for NK cell memory. IFNγ is the canonical NK cell cytokine, and mice lacking IFNγ from birth have been shown to lack NK cell memory

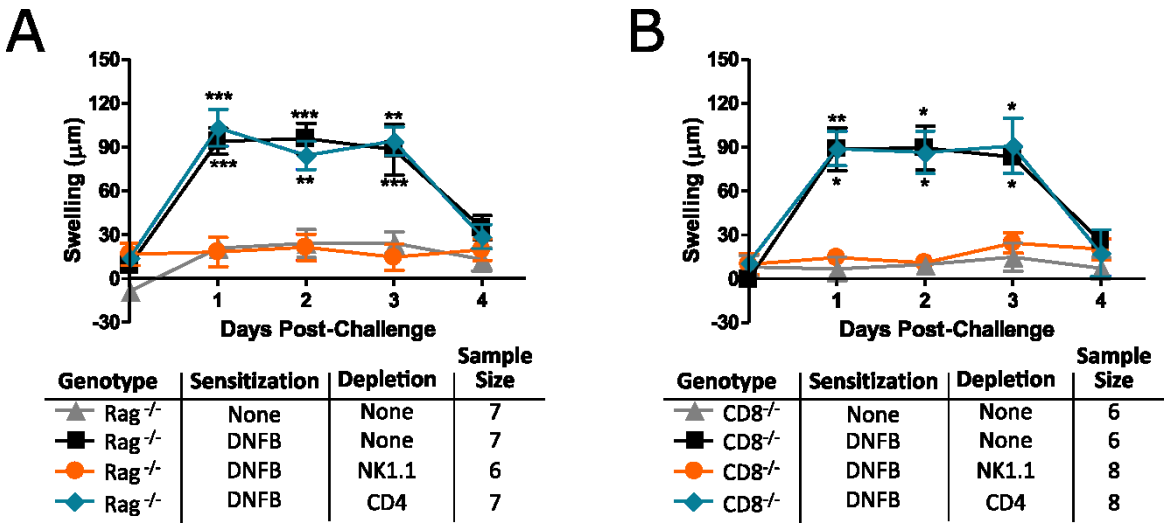

Figure 30: NK cells mediate memory responses in the absence of T cells. (A) Rag1-deficient mice were treated with depleting antibodies targeting either NK1.1 positive cells (clone PK136) or CD4 positive cells (clone GK1.5). NK cell depletion abrogated the memory response in these mice, while $CD4^{+}$ cell depletion had no effect as expected. (B) The above depletion was repeated in *Cd8a*$^{-/-}$ mice, to investigate the memory potential of NK cells in the presence of a normal B cell compartment and a somewhat-intact T cell compartment. Again, depletion of NK cells abrogated memory to DNFB in these mice, while surprisingly, depletion of CD4 positive cells had no effect. Statistics were calculated using a two-way ANOVA followed by the bonferroni post-hoc test comparing all means to the naive control. Significance is indicated with * $p<0.05$, ** $p<0.01$, *** $p<0.001$.

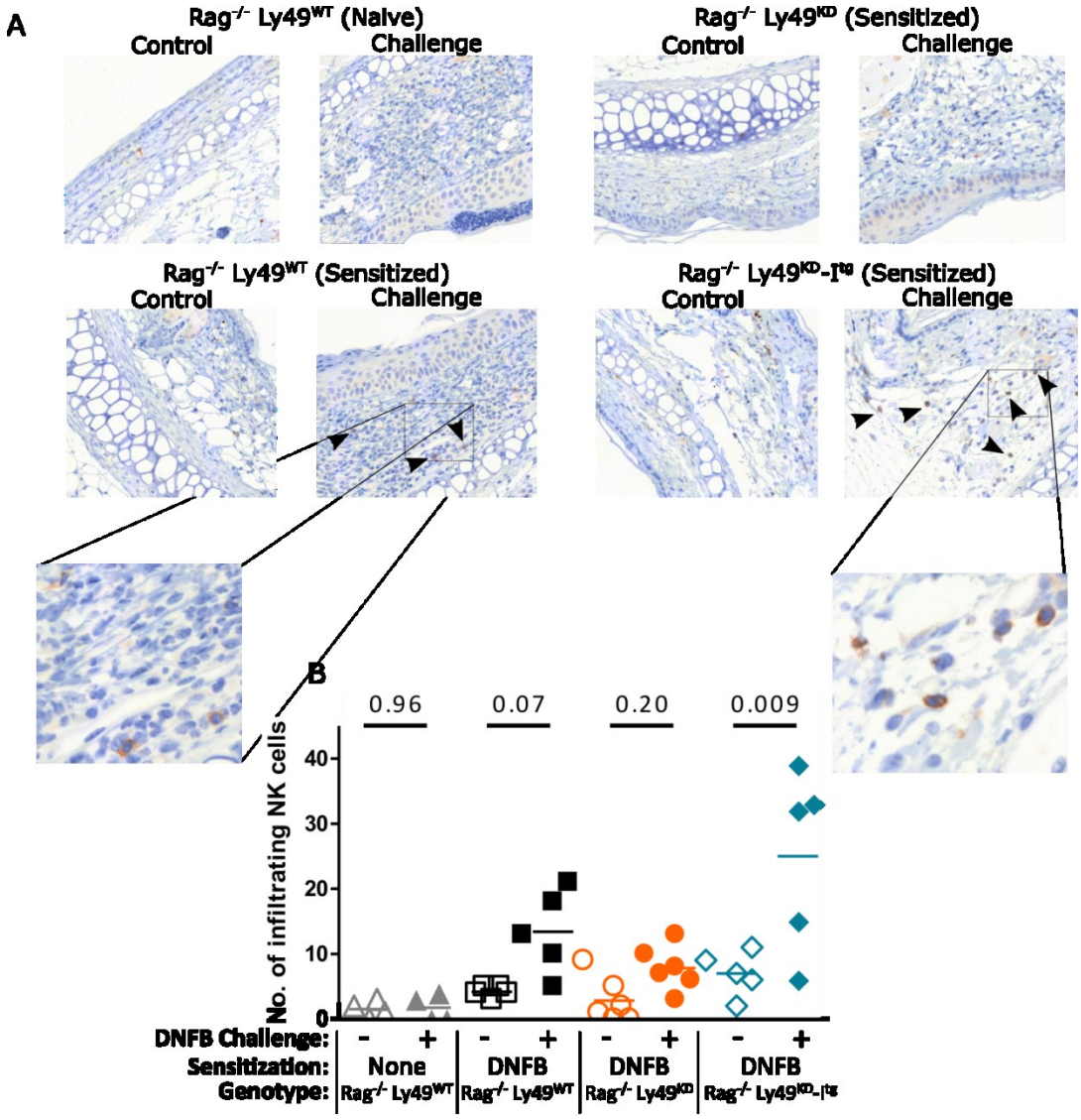

Figure 31: NK cells infiltrate ears that undergo a swelling response. Ear sections were taken as in Figure 28, but this time stained for NK cells using anti-NKp46. Example staining is shown in (A), and counts are summarized in (B), where each dot represents the sum count from five blinded fields. Statistical analysis was performed by paired, two-tailed Student's t-test, comparing each challenge ear to its corresponding control ear. P values are indicated.

responses[139]. In agreement with this, IFNγ neutralization was sufficient to prevent an NK cell memory response (Figure 32). While these results alone do not demonstrate that NK cells are required for the ear swelling reaction, they support the above antibody depletions by implicating NK cell involvement in T and B cell-independent memory responses.

4.2: Ly49C/I receptors are intimately involved in antigen recognition

Above, using both genetic and antibody-based ablations, I demonstrated that Ly49C/I expression is required for adaptive NK cell memory responses. None of these experiments, however, gave any indication as to whether Ly49C/I were acting solely as NK cell licensing receptors, or whether they had a more immediate role in the adaptive NK cell response. Unfortunately, with the mechanisms behind NK cell licensing still poorly understood, it was not possible to devise a direct test of the licensing requirement for NK cell memory. Instead, I focused on testing whether Ly49C/I had another, non-licensing role in the memory response.

4.2.1: Ly49C/I binding activity is required for NK cell memory

The first experiment to determine whether Ly49C/I had some non-licensing role in NK cell memory was to determine whether Ly49C/I binding was required during the memory response. Licensing is a lifelong process within each NK cell, so interfering with Ly49 binding only during the response should leave the licensing status of that NK cell relatively intact. To this end, I prepared $F(ab')_2$ fragments of the antibodies used above: these fragments lack an Fc region, and so will bind to their target and interfere with that target's function, but will not deplete the cell to which they are bound. I then repeated the ear swelling experiment (Figure 33).

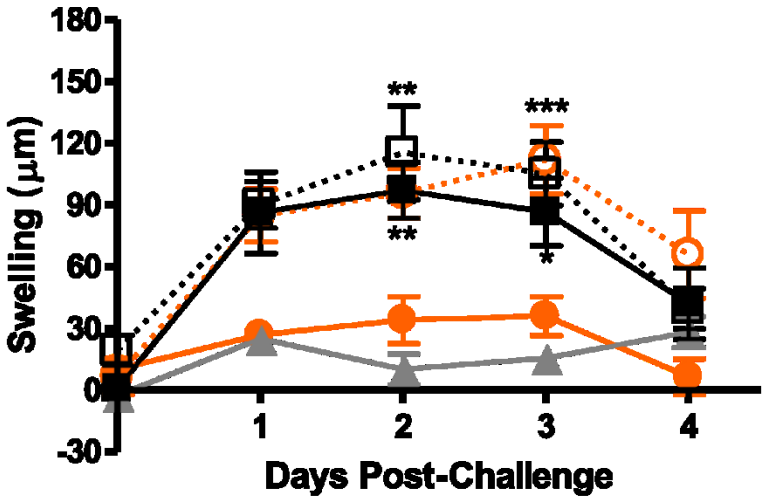

Genotype	Sensitization	Neutralization	Sample Size
$Rag^{-/-}$	None	None	10
$Rag^{-/-}$	DNFB	None	6
$Rag^{-/-}$	DNFB	IFNγ	9
WT	DNFB	None	6
WT	DNFB	IFNγ	10

Figure 32: Interferon gamma is required for NK cell memory to haptens. Rag1-deficient mice undergoing the ear swelling test were treated or not with an IFNγ neutralizing antibody (clone XMG1.2) throughout the sensitization and challenge phases of the experiment, as with the depleting antibodies above. Neutralization of IFNγ (orange line) completely abrogated the ear swelling response. Surprisingly, this neutralization was not effective in WT, T cell-sufficient mice (dashed lines), which displayed normal ear swelling. Statistics were calculated using a two-way ANOVA followed by the bonferroni post-hoc test comparing all means to the naive control. Significance is indicated with * $p<0.05$, ** $p<0.01$, *** $p<0.001$.

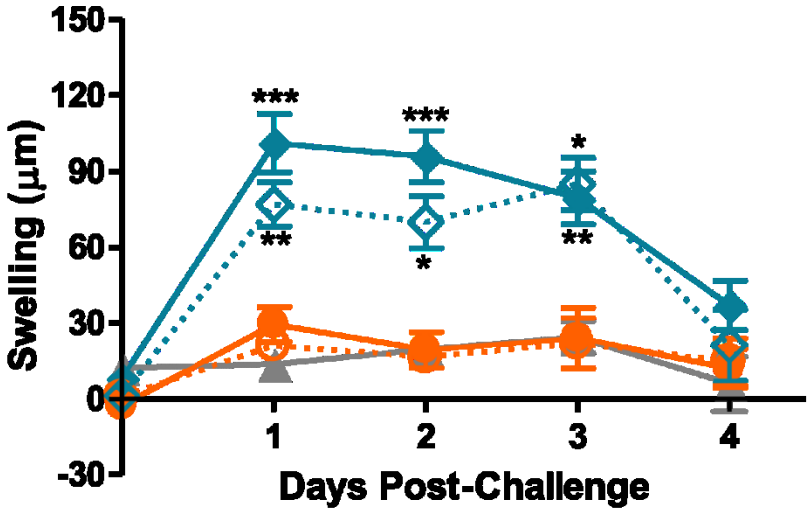

Genotype	Sensitization	Challenge	Sample Size
Rag$^{-/-}$	None	None	5
Rag$^{-/-}$	Ly49C/I	None	7
Rag$^{-/-}$	Ly49G	None	7
Rag$^{-/-}$	None	Ly49C/I	7
Rag$^{-/-}$	None	Ly49G	7

Figure 33: Ly49C/I binding activity is required in-situ for memory in Rag1-deficient animals. Rag1-deficient mice undergoing the ear swelling test against DNFB were treated with 200 μg every 48 hours of F(ab')$_2$ non-depleting antibody fragments targeting Ly49C/I or Ly49G, during either the sensitization phase alone or the challenge phase alone, as indicated. Non-depleting blockade of Ly49C/I during either sensitization or challenge (orange lines) was sufficient to disrupt NK cell memory, while blockade of Ly49G (blue lines) had no effect at either time. Statistics were calculated using a two-way ANOVA followed by the bonferroni post-hoc test comparing all means to the naive control. Significance is indicated with * $p<0.05$, ** $p<0.01$, *** $p<0.001$.

Amazingly, interfering with Ly49C/I binding—but again, not Ly49G, which had no effect—either during the sensitization phase or the challenge phase alone was sufficient to eliminate the adaptive NK cell memory response.

4.2.2: MHC-I expression and activity is required for NK cell memory

If Ly49C/I are functionally required during both sensitization and challenge phases of NK cell memory, I hypothesized that their binding partner, MHC-I, was likewise required. To test this, I crossed a mouse model lacking classical MHC-I expression (H-2K$^{b-/-}$ H-2D$^{b-/-}$ mouse) onto the Rag1$^{-/-}$ background, then performed the ear swelling test as before (Figure 34). Mice lacking MHC-I expression were not capable of responding to DNFB, indicating that MHC-I expression is required for NK cell memory responses. Indeed, in agreement with a publication describing CD8^{+} T cell responses to DNFB, these MHC-I-deficient mice displayed no DNFB memory even on a T cell-sufficient background, again reinforcing the notion that NK cells or CD8^{+} T cells are required for DNFB responses.

Unfortunately, this experiment with MHC-I-deficient mice was too coarse to draw useful conclusions about Ly49 receptor involvement in NK cell memory. While it did show that MHC-I was required for the memory response, these mice lack MHC-I from birth and therefore have no licensed NK cells, returning us to the problem of separating licensing from other potential Ly49C/I activities. Fortunately, MHC-I is not the only antigen-presenting platform available to the immune system, so it was possible to directly test whether MHC-I activity—that is, antigen presentation—was required during the NK cell memory response. I repeated the peptide ear swelling test from before, but this time sensitized mice either to SIINFEKL as before, or to a class II MHC (MHC-II)-restricted peptide from ovalbumin, ISQAVHAAHAEINEAGR. In this experiment, then, the NK cells have had normal Ly49 expression throughout life, and likewise

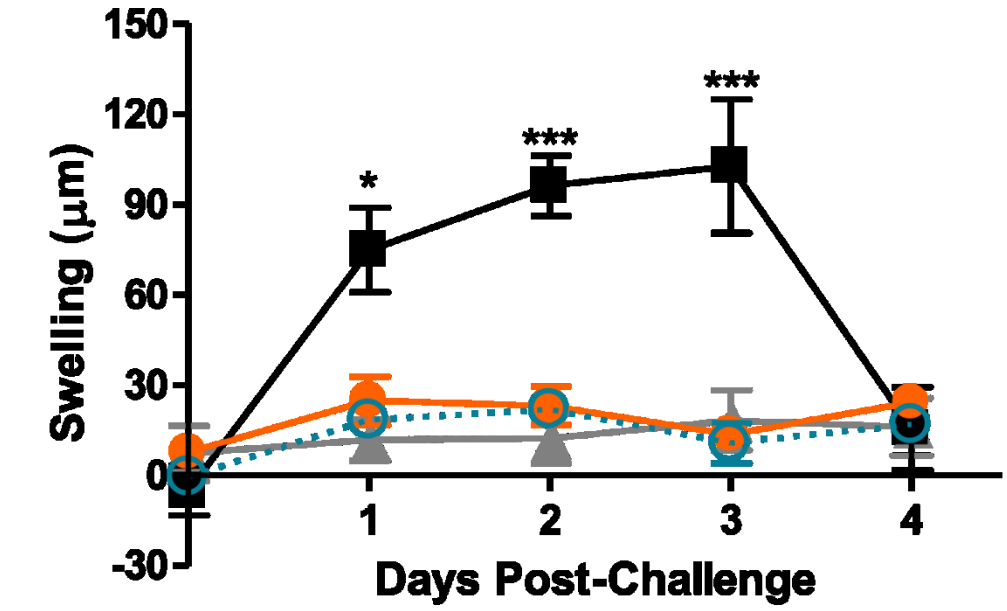

Genotype *Rag1*	Genotype *H-2K^b & H-2D^b*	Sensitization	Sample Size
-/-	WT	None	7
-/-	WT	DNFB	6
-/-	-/-	DNFB	17
WT	-/-	DNFB	12

Figure 34: MHC-I expression is required for memory to DNFB. Rag1-deficient or WT, T cell-sufficient mice undergoing the ear swelling test displayed no memory response if they were genetically deficient for H-2K^b and H-2D^b, the two MHC-Ia molecules expressed in C57BL/6 mice. Statistics were calculated using a two-way ANOVA followed by the bonferroni post-hoc test comparing all means to the naive control. Significance is indicated with * $p<0.05$, ** $p<0.01$, *** $p<0.001$.

all antigen-presenting cells have had normal MHC-I and MHC-II levels. However, the MHC-II-restricted antigen was not capable of provoking an NK cell memory response, even though it could provoke a T cell memory response as normal (Figure 35). This result indicates that MHC-I must actively present antigen during the NK cell memory response: antigen presented in the context of MHC-II, which NK cells do not interact with, cannot provoke NK cell memory.

4.2.3: Ly49C/I are implicated in NK cell antigen recognition

From the above results, I have generated a model in which Ly49 binding is a required component of adaptive NK cell memory responses, as is MHC-I expression and antigen presentation. This suggested that Ly49C/I could be directly recognizing the antigen presented in MHC-I, analogous to how T cell recognition functions. Unfortunately, a typical mass spectrometry or co-immunoprecipitation approach would not likely clarify whether this direct Ly49:MHC-I interaction was involved in memory, since Ly49C/I binds to MHC-I in conventional, non-memory contexts as well. One possible solution to this problem came from the work of Dr. Kevin Kane, who discovered that Ly49C is somewhat sensitive to the antigen presented in MHC-I[75]. In particular, the second and third residues in the presented peptide affect Ly49C binding to the MHC molecule. Based on this finding, I hypothesized that if Ly49C/I were directly involved in antigen recognition, then peptides that shared residues 2 and 3 would be recognized as the same and show NK cell memory cross-reactivity. I had already established that SIINFEKL and SIYRYYGL did not cross-react; I created a third peptide, SIYNFEKL, to test this hypothesis. To my great surprise, sensitization with the hybrid peptide SIYNFEKL was able to provoke NK cell memory against itself or against SIYRYYGL, but not against SIINFEKL, indicating that the antigen specific nature of NK cell memory is dependent on the two Ly49-interacting residues (Figure 36). While this is not firm proof that Ly49C/I are acting

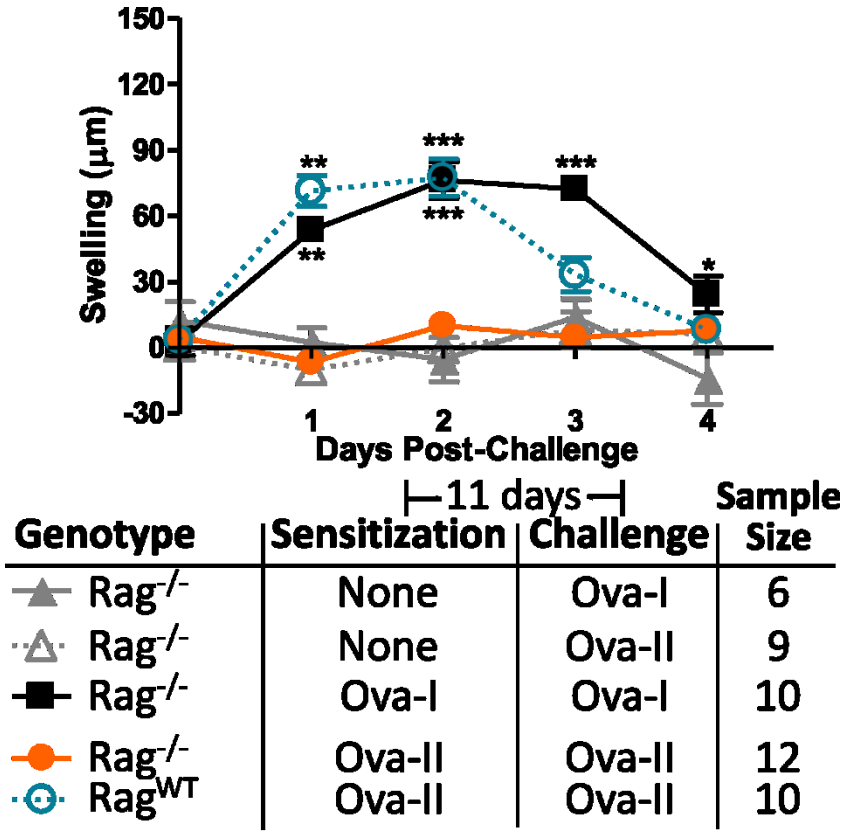

Figure 35: MHC-I antigen presentation is required for memory in Rag1-deficient mice. Rag1-deficient mice were sensitized to SIINFEKL (Ova-I) as before, or to ISQAVHAAHAEINEAGR, the MHC-II restricted peptide from chicken ovalbumin (Ova-II), as indicated. Mice were challenged with the cognate antigen. While Ova-I could provoke a memory response in Rag1-deficient mice as expected (black line), Ova-II could not (orange line), despite the fact that Ova-II was immunogenic in WT, T cell-sufficient mice (dashed blue line). Statistics were calculated using a two-way ANOVA followed by the bonferroni post-hoc test comparing all means to the naive control. Significance is indicated with * $p<0.05$, ** $p<0.01$, *** $p<0.001$.

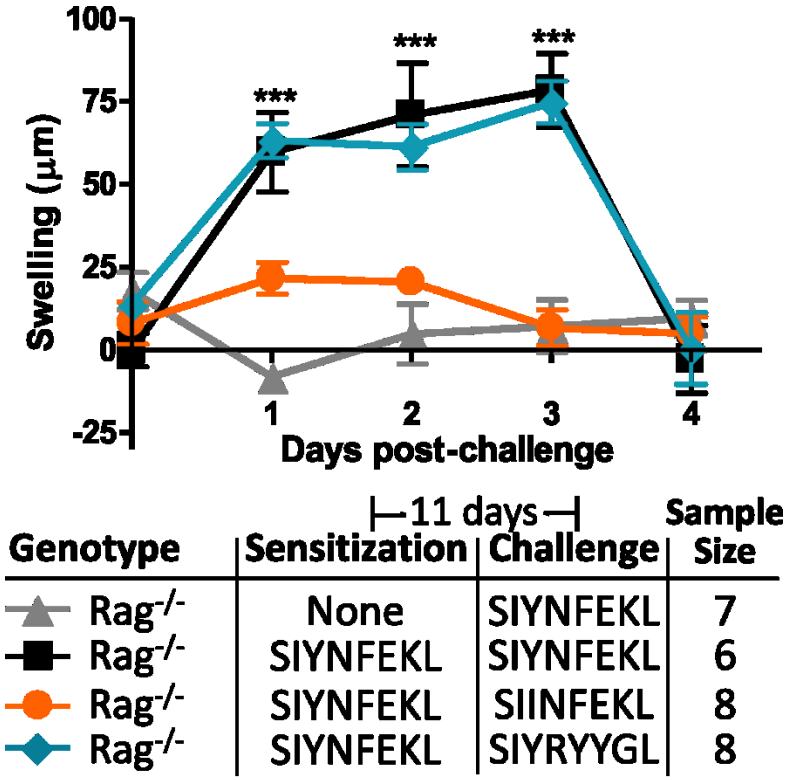

Figure 36: NK cell memory uses the Ly49-interacting residues of a peptide to determine antigen specificity. Rag1$^{-/-}$ mice were entered into the ear swelling test as before. In this experiment, mice were sensitized to a peptide that was a hybrid of SIINFEKL and SIYRYYGL—that is, SIYNFEKL—and then challenged as indicated. This hybrid peptide has the Ly49-binding sequencing from SIYRYYGL and everything else from SIINFEKL, and surprisingly demonstrates that SIYRYYGL but not SIINFEKL will cross-react with the hybrid peptide. Statistics were calculated using a two-way ANOVA followed by the bonferroni post-hoc test comparing all means to the naive control. Significance is indicated with * p<0.05, ** p<0.01, *** p<0.001.

as the antigen-specific NK cell receptor, it provides strong support to the notion that they are intimately involved in NK cell antigen recognition.

4.3: NK cell memory can mediate a model cancer vaccine

Beyond understanding the role of Ly49 receptors in NK cell memory, I was also interested in evaluating the clinical relevance of this adaptive immune response. Additionally, the above findings would be strengthened by evidence that does not involve ear swelling. To these ends, I sought to test NK cell memory through its ability to mediate protective vaccines. Previous work in NK cell memory has shown that it can mediate antiviral protection[126]; however, NK cells are also known to be effective anti-cancer cells. I therefore set out to demonstrate NK cell memory activity in a model cancer vaccine.

4.3.1: NK cells remember whole protein antigens

Before a successful vaccine could be designed, it was first necessary to test whether NK cells could react to whole protein antigens. Thus far, my work has used either haptens or pre-processed peptide antigens to stimulate NK cell memory responses, raising the possibility that an unprocessed protein would not elicit NK cell memory. I therefore sensitized $Rag1^{-/-}$ mice to whole ovalbumin, then challenged them with SIINFEKL—the MHC-I-restricted fragment of ovalbumin—as before. NK cells displayed Ly49I-dependent memory to whole ovalbumin, just as they had with SIINFEKL previously (Figure 37), indicating that protein vaccines could be a viable avenue to pursue for NK-mediated vaccine design.

4.3.2: NK cell memory protects against aggressive melanoma

With the success of ovalbumin in provoking NK cell memory, I next devised a cancer challenge using ovalbumin as a surrogate tumour-specific antigen. In this model, mice would be

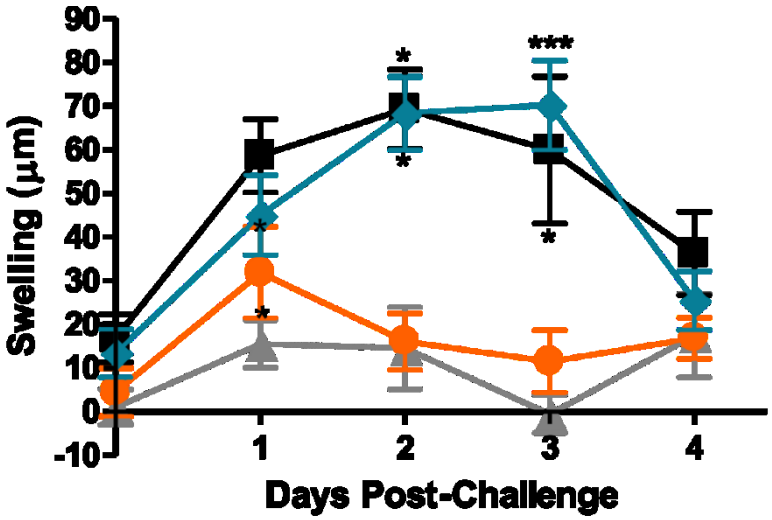

Genotype	Sensitization	Challenge (11 days)	Sample Size
Rag$^{-/-}$ Ly49^{WT}	None	SIINFEKL	7
Rag$^{-/-}$ Ly49^{WT}	Whole Ova	SIINFEKL	6
Rag$^{-/-}$ Ly49^{KD}	Whole Ova	SIINFEKL	12
Rag$^{-/-}$ Ly49^{KD}-I^{tg}	Whole Ova	SIINFEKL	12

Figure 37: NK cell memory functions against whole protein antigens. Rag1-deficient mice were sensitized as before, but this time with a molar equivalent of whole ovalbumin instead of SIINFEKL. Mice were then challenged with SIINFEKL in one ear, and ear swelling responses again indicated an Ly49I-dependent memory response. Statistics were calculated using a two-way ANOVA followed by the bonferroni post-hoc test comparing all means to the naive control. Significance is indicated with * $p<0.05$, ** $p<0.01$, *** $p<0.001$.

vaccinated using ovalbumin or the irrelevant bovine serum albumin as a negative control, then challenged with B16F10 melanoma either expressing ovalbumin or not[134]. Remarkably, 50% of the ovalbumin-vaccinated $Rag1^{-/-}$ mice enjoyed complete protection from this cancer, while none of either the control-vaccinated or those challenged with non-ovalbumin B16F10 cells survived (Figure 38). This indicates that the NK cell memory present in $Rag1^{-/-}$ mice possesses potent anti-cancer potential.

I repeated the above vaccine study using only SIINFEKL as the vaccine antigen (and SIYRYYGL as the control). Unfortunately, SIINFEKL alone was not nearly as protective as whole ovalbumin: none of the vaccinated mice survived, although they did show a modest but significant reduction in the cancer growth rate compared to the other groups (Figure 39). This indicates that SIINFEKL may not be the ideal antigen for NK cell memory like it is for $CD8^+$ T cell memory. It is also possible that the short peptide is insufficient as a vaccine antigen for technical reasons, or that the whole protein immunization is more successful because it gives many options for NK cell epitopes, increasing the chance of specific ovalbumin recognition. In any case, the fact that the vaccinated mice also developed tumours in this experiment meant that I could repeat the NK cell histological examination from above to investigate whether the vaccine induced NK cell enrichment in the tumour bed. Although all tumours had noticeable NK cell infiltration—consistent with the NK cell's role as an anti-cancer lymphocyte—the vaccinated mice that were challenged with ovalbumin-expressing tumours showed significantly more NK cell infiltration (Figure 40). Why this infiltration was insufficient to protect these mice is not known, particularly because the protected mice from the whole ovalbumin vaccine did not develop tumours at all, and so cannot be compared to these groups.

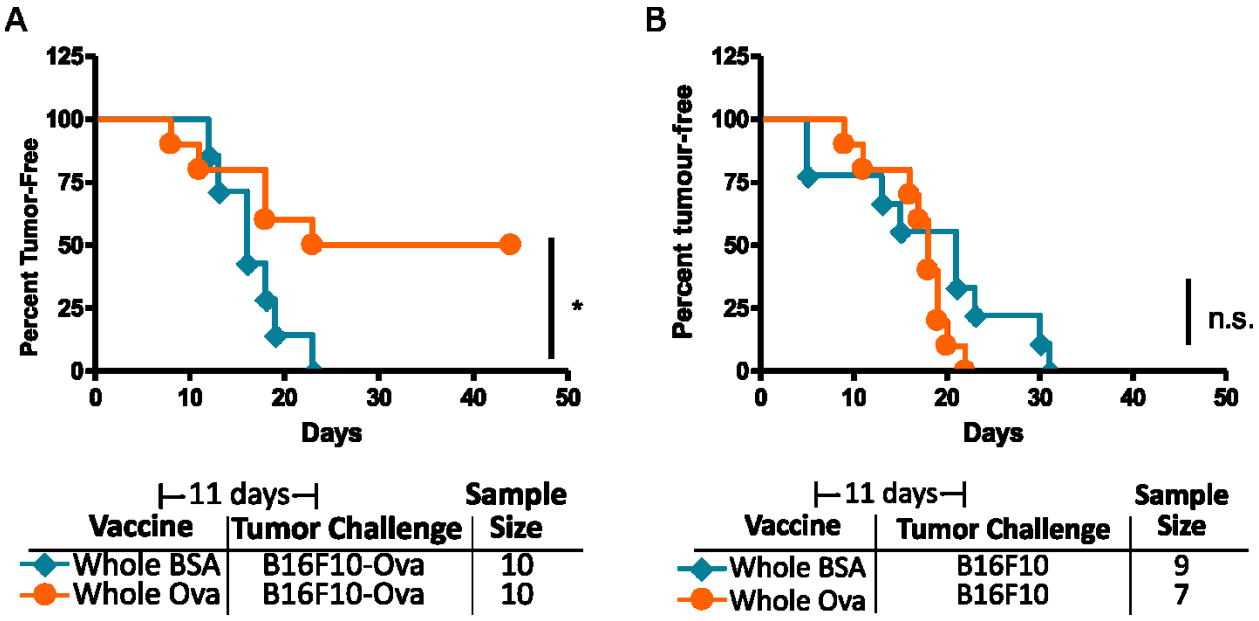

Figure 38: NK cell memory can mediate a protective cancer vaccine. Rag1$^{-/-}$ mice were sensitized to whole ovalbumin as in Figure 37 or to bovine serum albumin as a negative control. Instead of an ear swelling test, mice were then challenged with 1x10^5 B16F10 congenic melanoma cells, either in the parental state or expressing ovalbumin as a surrogate tumour antigen. Mice were observed daily for tumour appearance. The percent tumour-free mice is reported in a kaplan-meyer survival plot for mice challenged with B16F10-Ovalbumin (A) or B16F10-parental (B). Statistical analysis was performed by the log-rank test, with significance indicated as * p<0.05.

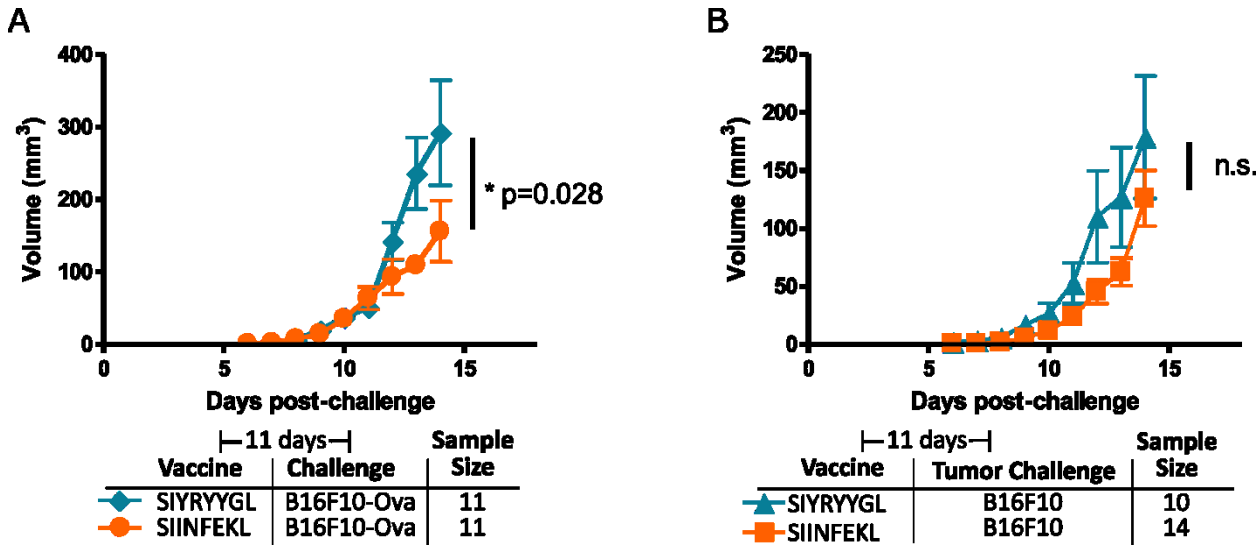

Figure 39: Peptide vaccines are not as effective as whole protein in inducing NK cell memory to B16F10. The cancer vaccine trial was repeated as in Figure 38, but this time, mice were sensitized to SIINFEKL or SIYRYYGL as previously described. Mice were again observed daily, and tumour volume recorded each day. Unfortunately, no mice were tumour-free after 10 days, so tumour volume is plotted instead. A modest but statistically measureable reduction in tumour growth rate was observed for mice vaccinated with SIINFEKL and challenged with B16F10-Ova (A), but no vaccine benefit was observed in those challenged with parental B16F10 cells (B). Statistical analysis was performed by a two-tailed Student's t test comparing the mean tumour sizes at endpoint, with significance indicated as * $p<0.05$.

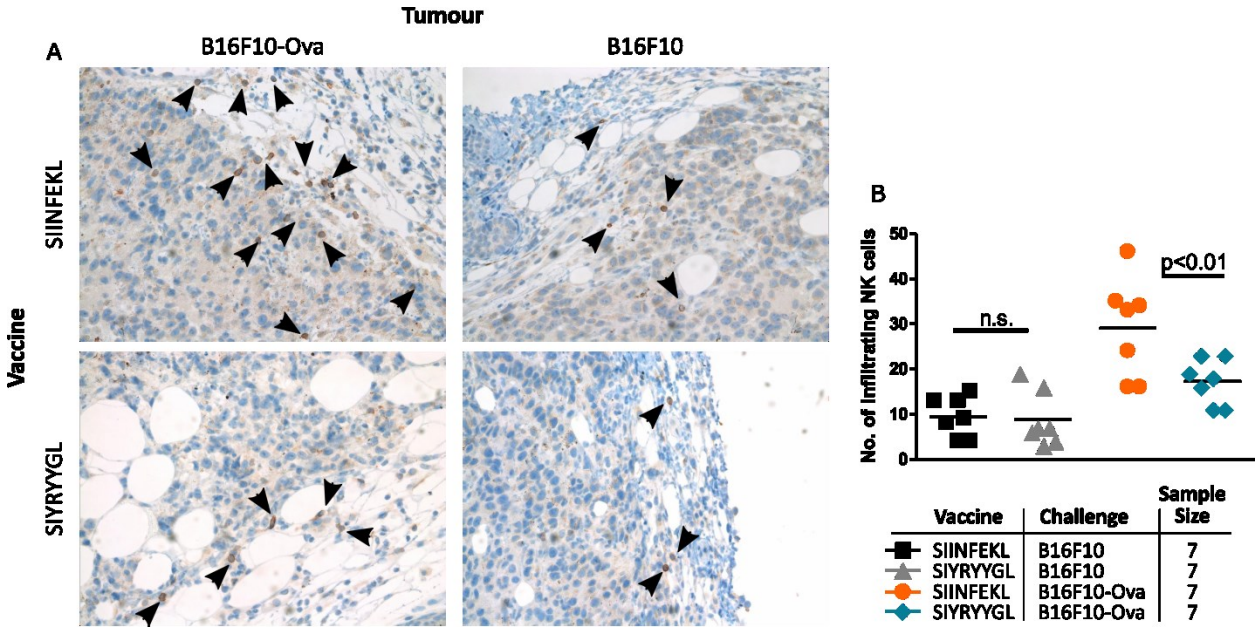

Figure 40: Increased NK cell infiltration into tumours of vaccinated Rag1-deficient mice. Although no mice showed tumour-free survival in Figure 39, the fact that they all presented tumours allowed histological comparisons of those tumours. NK cells were stained and quantified as in Figure 31, with representative images shown in (A) and quantifications shown in (B). Note the presence of NK cells in all four tumour groups, consistent with the NK cell's role as a tumour-fighting lymphocyte. Statistical analysis was performed by a one-way ANOVA followed by a bonferroni post-hoc analysis comparing the two vaccines within each challenge group, as indicated with black bars. P values are indicated.

In all, I have shown that Ly49C/I expression is critical for the development of adaptive NK cell memory responses. More than this, I have shown that Ly49C/I is intimately involved in the antigen recognition process these cells employ: Ly49 expression and MHC-I-restricted antigen presentation are both critical components of the memory response, and NK cell memory relies on the Ly49-sensitive residues to determine antigen specificity. Finally, I have shown that adaptive NK cell memory is not simply a theoretical NK cell response, but can mediate significant protection against an aggressive melanoma. While a great deal of work is still required to understand NK cell memory, this represents a first step toward appreciating the mechanisms by which NK cells generate antigen specificity, and by which NK cell memory might one day be employed in the clinic.

5. Discussion

This research has examined new frontiers in Ly49 research, studying how their expression is regulated by nucleosome positioning, and in turn how they regulate adaptive natural killer cell memory responses. I have found evidence that nucleosome positioning on AML-1 binding sites within the promoter 1/enhancer region of an Ly49 gene inversely correlates with Ly49 expression, which may explain one layer of transcriptional control for these genes. I have also discovered evidence that Ly49 receptors themselves are central and indispensable receptors involved in adaptive NK responses, and specifically that they are implicated in the adaptive NK cell's antigen specific recognition. This chapter will consider the broader context of these findings, as well as the shortcomings and future directions this project ought to take.

5.1: Ly49 Regulation by Nucleosomes

5.1.1: Shortcomings and future directions

The results presented in chapter 3 indicate that specific nucleosome positioning may play an underappreciated role in regulating Ly49 expression. Of course, these are preliminary findings, and more work must be undertaken before definitive conclusions can be drawn about this nucleosome occlusion of AML-1 binding sites. In particular, my work has used the RMA cell line to avoid several complications that would arise from using primary NK cells, chief of which is the extremely heterogeneous expression of Ly49 receptors within the NK population. Any signal indicating an inverse correlation between nucleosome positioning and gene expression would be buried by the inherent randomness present within a bulk population of NK cells. Sorting NK cells based on specific Ly49 expression would solve some of this difficulty, but the field still lacks antibodies for several Ly49 receptors, meaning the best a cell sorting

approach could achieve is to enrich—but not isolate—NK cells with a defined Ly49 expression pattern. In contrast, the RMA cell line naturally expresses only Ly49A (that is, we did not alter or induce these cells to express Ly49A), which I have confirmed using antibodies. A previous report indicates that RMA expresses transcripts encoding Ly49A and Ly49G only, eliminating the antibody deficit problem[140]. In that report, robust Ly49A and weak, heterogeneous Ly49G surface expression was described—using the RMA at hand, I was able to show that these cells express Ly49A and not Ly49G, likely due to clonal divergence. This natural expression of Ly49A suggests that the same processes that control Ly49 expression in primary NK cells may be comparably at work in RMA cells.

Nevertheless, analyzing primary NK cells is necessary: as a cancer cell line, RMA may have dysregulated gene expression, and only primary NK cells can confirm whether this nucleosomal regulation occurs in a normal Ly49 context. Fortunately, advances in nucleosome mapping and single-cell sequencing may soon make this feasible. Already, a nucleosome footprinting technique known as ATAC-Seq, where a highly active transposable element is used to insert next-generation sequencing adapter signals into nucleosome-free DNA sequences, can be performed with as few as 500 cells for input material[141]. With advances in single-cell sequencing for both ATAC-Seq and conventional RNA-Seq, it could soon be possible to sort single NK cells based on Ly49 expression, then assemble both a nucleosome map and an RNA transcription profile to correlate nucleosome position with Ly49 gene expression.

Such an approach—single-cell nucleosome mapping and RNA-seq—would enable a deeper investigation into the role that nucleosomes play in Ly49 regulation. Another shortcoming of the present report is that I have only been able to investigate Ly49A; with primary NK cells, however, it would be possible to compare many different Ly49 receptors to

determine whether this nucleosome effect is generalizable to the entire gene family. Admittedly, Ly49 genes have remarkably similar promoters, making a generalization from Ly49A plausible, but in particular, it would be of interest to compare classes of Ly49 genes—such as inhibitory receptors versus activating ones, or framework genes versus variable ones—to evaluate whether nucleosomes regulate each of these equally.

On the subject of inhibitory and activating genes, a single-cell approach would also allow comparisons between NK cells and T cells. Some T cell populations also express Ly49 receptors; however, these Ly49-expressing T cells only express inhibitory Ly49 receptors[46]. Intriguingly, in humans, NK and T cells require different regions of the KIR promoter for gene expression[142]. It would be of interest to determine whether T cells and NK cells have different nucleosome positioning patterns in the same, expressed Ly49 or KIR genes, which may shed light onto why T cells acquire Ly49 or KIR and whether different TFBS are required for their function in T cells and in NK cells.

Finally, moving away from future laboratory experiments, it would also be of interest to extend the bioinformatic approach taken in this manuscript to identify other patterns of nucleosome-sensitive transcription factors. I found that AML-1 binding sites were the most likely site of nucleosomal inhibition in Ly49 promoters, which correlated nicely with our finding that AML-1 binding sites were uniquely nucleosome covered and non-10 bp-periodical. That this pattern was not extended to the entire chromosome 6 suggests that this covered, non-periodical state is specific to Ly49 promoter AML-1 sites, and raises the intriguing possibility that other promoters have other key factors that display this nucleosome-sensitive trait. A bioinformatic approach to identify the nucleosome-sensitive factor(s) in each annotated promoter followed by a gene ontology approach could discover patterns of genes related by their nucleosome-sensitive factor.

For example, perhaps AML-1 is the nucleosome-sensitive factor for a number of genes related to lymphocyte development or function, while another factor might enrich for cell death genes, metabolic genes, etc. If a number of genes use different nucleosome-sensitive factors, this analysis could provide a novel way of understanding gene networks and may identify hidden connections between individual genes.

5.1.2: Ly49 as a model bioinformatic system

Although these findings raise new possibilities for NK cell gene regulation, another goal of this work has been to highlight the Ly49 gene family as a model bioinformatic system. Gene regulation is an unfathomably complex process, making correlative analyses difficult to interpret. The direct action of specific transcription factors on specific genes is only one way in which gene expression is regulated. As mentioned above, epigenetic modifications to specific histones can open or close regions of chromatin, affecting several unrelated neighboring genes. Similarly, chromosome looping allows sequentially distant genetic elements to exist in close spatial proximity and to influence each other's accessibility and transcriptional activity[143]. Of particular note here, these elements that are impacting each other through looping are generally about 1 mb long, meaning that the entire Ly49 locus likely consists of a single looping element, and so each gene at this locus would be impacted by distal looping factors equally[144]. All of this complexity makes it difficult to know if changes in the nucleosome or other epigenetic landscapes are related to the differential gene expression under study, or whether they arose because of any of these nonspecific effects, to say nothing of bias introduced by comparing different cell preparations or results from different sequencing reactions.

For these reasons, the Ly49 gene family represents an attractive candidate for laboratory tests of subtle epigenetic changes. All of the Ly49 family genes are encoded on the same DNA

strand, oriented end-to-end with no intervening genes over a relatively short stretch of DNA. Therefore, effects such as locus control region-induced accessibility changes or interference from chromosome looping would be expected to impact each family member similarly. Better yet, their stochastic expression means that comparisons between expressed and silent genes can be made within the same dataset and between genes with extremely similar promoters, controlling for transcription factor effects as well as technical bias introduced in sequencing. Finally, if the Ly49 genes themselves are too similar for a given comparison, they carry their own outgroup, with another family of c-type lectin-like receptors—the CD94/NKG2 family of proteins—immediately downstream of them, similarly encoded end-to-end and close enough to mitigate large-scale epigenetic impacts on gene expression.

Although these results are preliminary, it is my hope that they reveal nucleosomes as a potential source of answers when investigating factors that influence Ly49 expression and NK cell or T cell self/non-self discrimination. Moreover, these results are of interest beyond Ly49 receptor studies in two ways. First, they raise the possibility that a gene regulation network exists whereby certain transcription factors are selectively nucleosome sensitive in functionally related genes, allowing the whole network to be regulated by nucleosome remodeling enzymes. Second, these results demonstrate the bioinformatic advantages of studies performed in the Ly49 gene system, which will hopefully empower other groups to undertake laboratory tests of epigenetic regulation of gene expression, either by directly observing the Ly49 family for patterns correlated with expression, or by affecting changes within the epigenetic systems of an appropriate cell line such as RMA and observing the results on Ly49A expression.

5.2: Ly49 and Adaptive NK Cell Memory

5.2.1: Speculation on the evolution of adaptive NK cell memory

There are two major questions raised by the possibility of adaptive NK cell memory: first, why would NK cells have memory at all? And second, if NK cells do have adaptive memory, how does it work? Much of the work in this thesis has been toward answering this second question, which will be discussed below. To better understand how NK cell memory might work, however, it is beneficial to first discuss where it might have come from.

NK cells are believed to have evolved earlier than T cells, because NK-like cells are found in urochordates such as *Botryllus schlosseri*, which are the closest relatives to all vertebrates and yet—unlike their vertebrate cousins—do not possess MHC genes, T cells, B cells, and anything resembling a conventional adaptive immune system[145]. These NK-like cells are large granulocytes with a cytotoxic role to play in self/non-self discrimination and which express well-known NK cell markers such as CD94[146]. Without MHC, these NK-like cells do not reject cells based on the presence or absence of MHC-I, but instead reject transplants that could occur when two *B. schlosseri* colonies grow into contact with one another[145]. In a remarkable parallel with NK cell missing-self reactions, the NK-like cells migrate to a point of contact between the two colonies, and then evaluate the 'histocompatibility' of the other colony by probing that colony's expression of the highly polymorphic Fusability/Histocompatibility (Fu/HC) locus[147] using the inhibitory *fester* receptor[148] and the activating *uncle fester*[149] receptor. Colonies that match in at least one Fu/HC allele are tolerated and merge to form a chimeric colony, while colonies that do not match reject one another, rapidly forming melanin scars between the two at the point of contact and then growing away from each other[145].

This sort of natural transplant rejection is believed to be the evolutionary purpose of NK cells, which may have evolved to protect against germline parasitism between transplantable organisms (where the germline cells of one of the two transplant partners completely take over the germline of the other)[150]. As with MHC-I, the ability to generate a polymorphic 'self-signal' and then recognize it as self and everything else as non-self would allow for protection against the germline parasitism of one's neighbours. This system can also readily be co-opted for tumour and viral defense, since both tumours and viruses can be understood as a sort of genetic parasite—that is, a mostly self-like entity seeking to co-opt the host's genome replication for its own replicative purposes.

Whether this germline parasitism defense system active in *B. schlosseri* possesses memory is not known, but in this context, the evolution of NK cell memory begins to make sense. Establishing a self/non-self discrimination pattern based on a polymorphic self signal begins an arms race, where successful germline parasites are capable of evading detection through robust expression of a self marker. Indeed, previous work published by our lab gives an example of this, where licensed, self-reactive NK cells are a liability when clearing virus infections where the virus increases MHC-I expression in a bid to evade NK recognition, as is the case with influenza[38]. In this case, the licensed NK cells are directly inhibited by the increased MHC-I expression, while the unlicensed NK cells—which can still be activated through the inflammatory milieu or through the engagement of their activating receptors—are not, and are able to kill the infected cells without inhibition. Adaptive NK cell memory may have evolved to counteract this NK cell evasion strategy. While inhibited by the increased MHC-I, licensed cells would also develop memory cells specific for the offending virus. Assuming the host survives the virus infection, there would now exist a pool of licensed, memory NK cells that

would not be inhibited upon a repeat infection, and in fact would respond stronger to the virus and aid in rapid viral clearance. It would be interesting to evaluate whether mice that survive the initial infection have considerably higher NK cell activation in a case such as this, and whether NK cell memory-deficient mice such as CXCR6$^{-/-}$ mice are less able to clear repeat influenza infections. Similarly, it would be interesting to study whether *B. schlosseri* colonies possess memories of non-compatible colonies that they have previously encountered. Of course, until the genetic system underlying adaptive NK cell memory is better understood, it is not possible to phylogenetically evaluate whether NK or T cell memory arose first in mammals, but by understanding adaptive NK cell memory as a response to germline parasitism, it is possible to understand why it may have evolved alongside T cell memory.

5.2.2: Challenges to deciphering the mechanisms behind adaptive NK cell memory

The second major question for adaptive NK cell memory as a field is how NK cells acquire their antigen specificity. Both T cell and B cell specificity arises through genomic recombination, giving rise to genetically unique T cell or B cell receptors in each individual T or B cell. NK cells, therefore, might also acquire specificity through genomic recombination. This does not seem likely, however, simply because whole genome sequencing is becoming common-place in immunology, and if there were a recombining receptor in NK cells, it ought to have been detected by sequencing, especially since various research groups have been studying adaptive NK cell memory for a decade now. Moreover, NK cell memory is detectable in mice lacking Rag[124]—required for both T and B cell receptor rearrangement—or mice lacking DNA-PKcs[139]—required for all forms of non-homologous end-joining, including T and B cell receptor rearrangement.

Nevertheless, it may be worthwhile to examine memory NK cells for the presence of the histone variant gamma-H2AX, indicative of double-stranded DNA breaks and therefore of genomic recombination, to more clearly determine whether any NK cell receptors are undergoing recombination during adaptive NK cell memory development[151]. Drawing on my work with nucleosome occupancy, a chromatin immunoprecipitation for gamma-H2AX using commercially available antibodies could identify candidate genes that are undergoing some sort of DNA rearrangement, without needing to guess which double-stranded DNA break-repair mechanism is potentially at play in adaptive NK cells. NK cells would be isolated from the flank tumours of SIINFEKL-sensitized, B16F10-Ova-challenged mice (those in Figures 39 and 40). While this peptide vaccine was ultimately not very protective, it did induce a significant increase in NK cell infiltration when compared to sham vaccinated or Ova-null tumour challenge, and so is currently the most likely source of an NK cell population enriched in memory cells. After confirming that a gamma-H2AX immunoprecipitation can enrich the TCR or BCR as a technical control, these memory-enriched NK cells would be analyzed by chromatin immunoprecipitation followed by next-generation sequencing to identify any genes that were noticeably marked by DNA breaks within the NK population. If successful, this would identify candidate genes involved in antigen-specific NK cell recognition, and if this approach failed to enrich any NK cell genes from the population, it would further support the notion that adaptive NK cell memory is somehow generated without receptor recombination.

Through the course of the present work, I have identified Ly49C/I as directly involved in the antigen specific response. The mechanism behind Ly49C/I's antigen specificity is not currently known, but it is also not likely due to recombination, since no Ly49 receptor has ever been described as a recombining receptor, and because my results with Ly49-dependent antigen

specific memory are functional in the Ly49I^{tg} mouse, in which Ly49I is separated from its natural promoter and so unlikely to undergo recombination even if the native Ly49I gene somehow did do so[136]. Whether Ly49C/I are the sole determinants of antigen specificity in adaptive memory NK cells, or whether another co-receptor is involved, is also not clear.

Unfortunately, the involvement of Ly49C/I at all raises another issue: Ly49C/I are inhibitory receptors, and yet are clearly involved in a process that activates NK cells. Moreover, this cannot be explained by a simple missing-self reaction, since different haptens or peptides do not cross react. If SIINFEKL and SIYRYYGL peptides both could induce a missing-self response, why do NK cells react to them differently, depending on sensitization state? Additionally, the blocking antibody experiments indicate that loss of Ly49C/I signaling inhibits NK cell memory rather than induces it as would be expected in a simple missing-self model.

It is possible that, in the context of memory, at least, Ly49C/I are acting as activating receptors directly. There is precedent for such a possibility: our research group has previously published results indicating that Ly49Q, another inhibitory Ly49 expressed on plasmacytoid dendritic cells, induces cellular activation upon target ligation, and does so in an immunoreceptor tyrosine inhibitory motif (ITIM)-dependent manner[152]. Indeed, the classification of an inhibitory receptor depends on a functional cytoplasmic ITIM domain, which recruits SHP-family and SHIP phosphatases. While phosphatase activation is generally an inhibitory action within a cell, there are cases where phosphorylation is inhibitory, and dephosphorylation activating, such as insulin signaling inactivating glycogen synthase kinase 3 through phosphorylation[153]. Such a mode of action might be occurring in NK cell memory as well. One piece of continuing work on this project would be to identify the downstream signaling events that occur following an NK memory cell's encounter with its target antigen. Although it is not currently possible to sort

antigen-specific NK cells, enriching NK cells from a B16F10 flank tumour as above would allow comparisons between these and naive NK cells to determine differences in signaling molecule phosphorylation states.

It is also possible that Ly49C/I are mediating their activating effects through a similar mode of action as NK cell licensing. Indeed, although my results rule out conventional licensing as the sole purpose for Ly49C/I expression in NK cell memory, I have not ruled out a partial role for licensing in memory. It is conceivable that NK cell memory represents a sort of hyper-licensing: upon target recognition, Ly49C/I rapidly reinforce the licensing state of the NK cell, leading to a potent cell that can act quickly upon target cell recognition in the future, which is one of the hallmarks of memory cells in general. Unfortunately, licensing is not adequately understood, and so direct tests of licensing as it pertains to memory are not possible at this time. Once an Ly49C/I-independent marker of NK cell licensing is discovered, it will be critical to determine how much of Ly49C/I's involvement in NK cell memory is due to their licensing ability, and how much is due to some other aspect of their biology.

5.2.3: A urochordate model of NK cell antigen specificity

The above challenges pose a difficult problem in constructing a model of how NK cell antigen specificity may arise: it is likely not due to genomic recombination, and appears to require the inhibitory Ly49C/I for a stimulatory function, which may or may not be operating through the same mechanisms they use for NK cell licensing, which is also not mechanistically understood. I cannot completely resolve these questions here, but by again returning to the NK-like progenitors in *B. schlosseri*, a fairly parsimonious—albeit completely speculative—model of NK cell antigen specificity can be found.

As mentioned above, *B. schlosseri* NK-like cells perform a type of missing-self recognition through the inhibitory receptor *fester*. Unlike the Ly49 gene family, *fester* is a single gene, but generates a remarkable amount of surface expression diversity through extensive alternative splicing of the protein, such that 64 surface variants and 16 secreted forms are theoretically possible[145]. This system is hypothesized to give rise to exquisite 'self' Fu/HC specificity—ignoring all the similar 'non-self' possibilities in the polymorphic Fu/HC region—by careful microclustering of splice variants of different avidities on the cell surface, such that each microcluster has higher affinity for 'self' than for 'non-self'[145].

Klra genes are not extensively alternatively spliced like *fester*, but another mechanism exists that can fine-tune the avidity of clusters of surface Ly49 receptors. Due to their flexible stalk region, Ly49 receptors can bind to MHC-I molecules expressed on the same cell surface—that is, can interact in a *cis* configuration with MHC-I[154]. This is believed to adjust the *trans*-MHC-I sensitivity of these receptors by forcing them to compete with *cis*-MHC-I molecules, increasing the inhibition threshold of the NK cell in question (i.e. making the NK cell easier to activate[154]. It is therefore conceivable that a memory NK cell learns its target antigen by subtle adjustments to the ratio of surface expressed MHC-I to Ly49C/I. In the context of a memory-favouring cytokine milieu, a naïve adaptive NK cell that has been inhibited by self-MHC-I expressing a foreign antigen either subtly increases its own MHC-I expression or decreases its Ly49C/I expression until its surface MHC-I:Ly49C/I microclusters are unable to bind in *trans* against the foreign peptide, favouring *cis* interactions that can only be broken by a self-MHC-I that also expresses self peptide, and allowing for a sort of hyper-sensitive missing-self reaction.

This model makes several assumptions that must be addressed. First, it assumes that MHC-I presenting self-peptides have higher Ly49C/I affinity than those presenting non-self

peptides. Whether this is true or not is currently unknown, although an immunodominant peptide from LCMV and T cell escape mutants of this peptide were all found to be poor Ly49C interactors, indicating that non-self peptides may have lower affinity for inhibitory Ly49[155]. This could also explain how the adaptive NK cell becomes self-tolerant, since the self-peptides in a target MHC-I would be sufficiently high affinity to always bind Ly49C/I in *trans*.

Second, this model assumes that the *cis* binding of the Ly49 receptors is required to maintain the functional status of the adaptive NK cell. Otherwise, my blocking antibody experiment completely invalidates the model. There is precedent for a model of NK cell activity that requires *cis* binding: NK cells expressing a mutant form of Ly49A that could bind in *trans* but not *cis* could be inhibited by Ly49A signaling, but were found to be unlicensed[156]. Additionally, mice that lacked MHC-I expression only on NK cells displayed unlicensed NK cells, supporting a role for *cis* interactions in generating licensed NK cells[157]. Unfortunately, the role of *cis* binding in licensing is still unclear, since other groups have found that MHC-I-deficient mice with inducible MHC-I expression did not develop licensed NK cells when MHC-I was induced on NK cells, but did when induced on other cell types[158]. Nevertheless, if *cis* interactions are required to develop and maintain a licensed status in NK cells, it is possible that this fine-tuning of Ly49C/I affinity through *cis* interactions could explain the antigen specific nature of the NK cell response, and if the fine-tuning is performed by epigenetic regulation of MHC-I or Ly49 expression, it could even be heritable, allowing for the longevity and transferability of adaptive NK cell responses.

If this *B. schlosseri*-based model of adaptive NK cell responses is correct, it predicts that memory NK cells are not truly antigen-specific, but rather would display a sort of hierarchic antigen recognition, where a memory NK cell would respond to its sensitizing non-self antigen

and all antigens with a lower Ly49C/I affinity. Of particular interest, a study of Ly49 interactions with SIINFEKL and SIYNFEKL, as in Figure 35 above (albeit in a different model), found that Ly49C interacted more strongly with SIINFEKL than with SIYNFEKL[155], making my finding that SIYNFEKL-sensitized mice recognize other SIY-containing peptides but not SII-peptides congruous with this model of adaptive NK cell responses. Experiments are currently underway to examine several different peptides and determine whether a hierarchic pattern of Ly49 affinity dictating NK cell cross-reactivity exists, which will go a long way to supporting or disproving this model.

5.2.3: Future directions in antigen presentation

My work has been focused on understanding NK cell memory though understanding NK memory cells. However, antigen specific memory also depends on antigen presentation, and our lab is currently undertaking a new project in understanding how antigens are presented to NK cells. A recent publication has proposed that macrophages, and particularly macrophages undergoing pyroptosis, are the antigen presenting cell for NK cell memory[159]. Unfortunately, the only antigen tested in that report was a very peculiar hapten, which has the unique property of inducing an anti-melanocyte response in only NK cells, whether or not T cells are present. It is therefore unclear if macrophages are the antigen presenting cell for all antigens, or whether the unique properties of this hapten make it only suitable for presentation through macrophages.

Nevertheless, macrophages are known to be good antigen presenting cells in general, and NK cells are known to participate in reciprocal cross-talk with macrophages, so the hypothesis is consistent with known properties of these cells. More interestingly, memory-like NK cells, characterized by an enhanced recall response to any stimulus given to the NK cell, are induced by IL-12 and IL-18, and may be a prerequisite of developing a complete NK cell memory[120]. IL-

12 is known to be produced by macrophages and dendritic cells when cross-talking with NK cells[160–162], and IL-18 is one of the main cytokines released during pyroptosis. Therefore, an antigen presenting cell such as an IL-12-producing macrophage that is also undergoing pyroptosis and releasing IL-18 would hypothetically be creating an ideal environment for developing NK cell memory, or at least memory-like cells. It would be worthwhile to test whether any of these cells, either macrophages or dendritic cells with or without pyroptosis, can induce NK cell memory *in vitro* to conventional peptide antigens. If macrophages undergoing pyroptosis are still the only antigen-presenting cell that can induce NK cell memory *in vitro*, this would be stronger support that IL18-producing macrophages are indeed the NK cell-interacting antigen-presenting cell.

Aside from the obvious importance of this to understanding NK cell memory, identifying macrophages as the principle antigen-presenting cell (APC) for NK cells has intriguing implications for our understanding of macrophage biology and general MHC-I antigen presentation as well. There has been a great deal of debate as to whether macrophages are capable of cross-presenting antigen to $CD8^+$ T cells at all, or whether this is a unique feature of dendritic cells[163–166]. If macrophages are found to be responsible for presenting antigen to adaptive NK cells, this could present a powerful model in which to study whether and how macrophages cross-present, since we have shown that NK memory responses are functional against exogenous antigen such as ovalbumin, which likely must be cross-presented. Even if macrophages are not the sole agents capable of presenting to NK cells, the ability to study cross-presentation in Rag-deficient mice—away from the complexity introduced by having multiple T cell types responding to direct and cross-presentation and B cells also potentially acting as APCs—could be useful in advancing our understanding of cross-presentation.

5.2.4: Clinical uses of antigen specific NK cell memory

Beyond the academic value in understanding how antigen presentation works for NK cells, this knowledge of NK cell antigen presentation would help in moving NK cell memory into clinically relevant tests. My preliminary results with a model cancer vaccine indicate that NK cell memory can potentially mediate protection against melanoma in the absence of T cells. There are several reasons that NK cells represent an attractive avenue for clinical development. First, NK cell deficiency in the population is virtually nonexistent, while T cell deficiency can arise through congenital conditions such as severe combined immunodeficiency disorder (SCID) or through conditions such as acquired immunodeficiency syndrome (AIDS). The ability to vaccinate people without normal T cell populations could prevent or at least ameliorate the serious complications that arise when such an immunocompromised person gets an infection.

Second, even in T cell-sufficient people, therapies using antigen-specific T cells are risky. T cells are the principal mediators of graft-versus-host disease, and so transfer of antigen-specific T cells into a patient requires autologous T cell expansion to avoid a lethal T cell reaction. Conversely, NK cells do not mediate graft-versus-host responses even in cases of complete mismatch, and in fact may serve to curb any damaging T cell responses[167]. Therefore, adaptive NK cell therapies could be used in cases where expansion of host T cells is not possible, either for technical or patient safety reasons, making these potentially life-saving treatments more available, less expensive, and safer.

Finally, with regard to cancer vaccines in particular, T cell-based cancer vaccines have not been tremendously successful thus far. One of the hallmarks of cancer is a high mutation rate, and if a tumour can successfully mutate away from antigen recognition by an infiltrating T cell, that T cell is no longer functional with regard to cancer rejection. Conversely, if a tumour

mutated away from antigen-specific NK cell recognition, it still must contend with a fully functional, licensed, tumour-killing NK cell. NK cell vaccines may therefore be more effective than T cell vaccines in cancer protection. Indeed, B16F10 is such an aggressive cancer that there are reports where OT-I T cells—a transgenic model where 100% of the T cells are specific for B16F10 cancer expressing ovalbumin—cannot effectively control it[168]. Achieving even 50% protection through NK cell vaccination in the absence of T cells suggests that this may be a very potent anti-cancer response.

Nevertheless, 50% protection is not sufficient for a successful vaccine, and so our lab has recently partnered with a vaccine development company, Immunovaccine Inc., to determine whether this success rate can be improved[169,170]. In the future, it will be important to determine whether novel adjuvanting strategies can improve the success of NK cell-mediated cancer vaccines, as well as to test the ability of an NK-mediated vaccine to protect against a more clinically relevant model, such as C3 cells, which express an endogenous tumour antigen rather than ovalbumin, or one of the Her2-expressing human breast cancer cell lines. Ultimately, another method of developing cancer vaccines can only bolster attempts at improving patient outcomes through immunotherapies.

5.3: Conclusions

Natural killer cells are complex immune cells that are capable of a remarkable range of immune responses, from missing-self recognition and immune surveillance to novel and mysterious forms of immune memory. In this research project, I have pursued two avenues of discovery about how NK cells function, both centered on the Ly49 family of NK cell receptors. I have provided evidence that Ly49 receptor expression is influenced by nucleosome positioning, and furthermore argued that the Ly49 family is itself an ideal system for testing epigenetic

hypotheses. I have also demonstrated that adaptive NK cell memory requires Ly49 expression, and that these MHC-I-receptors may be key to understanding how NK cells gain antigen specificity. While this represents only a first step in deciphering NK cell memory, it is my hope that this finding provides the launching point that eventually leads to uncovering the mechanisms behind adaptive NK cell responses, leading to finally understanding how this novel adaptive immune response functions.

6: References

1. Spits, H. *et al.* Innate lymphoid cells--a proposal for uniform nomenclature. *Nat. Rev. Immunol.* **13,** 145–9 (2013).
2. Zwirner, N. W. & Domaica, C. I. Cytokine regulation of natural killer cell effector functions. *BioFactors* **36,** 274–288 (2010).
3. Adib-Conquy, M., Scott-Algara, D., Cavaillon, J.-M. & Souza-Fonseca-Guimaraes, F. TLR-mediated activation of NK cells and their role in bacterial/viral immune responses in mammals. *Immunol. Cell Biol.* **92,** 256–262 (2014).
4. Smith, H. R. C. *et al.* Recognition of a virus-encoded ligand by a natural killer cell activation receptor. *Proc. Natl. Acad. Sci. U. S. A.* **99,** 8826–31 (2002).
5. Zamai, L. *et al.* Natural killer (NK) cell-mediated cytotoxicity: differential use of TRAIL and Fas ligand by immature and mature primary human NK cells. *J. Exp. Med.* **188,** 2375–80 (1998).
6. Trapani, J. A. & Smyth, M. J. Functional significance of the perforin/granzyme cell death pathway. *Nat. Rev. Immunol.* **2,** 735–47 (2002).
7. Schroder, K., Hertzog, P. J., Ravasi, T. & Hume, D. A. Interferon- : an overview of signals, mechanisms and functions. *J. Leukoc. Biol.* **75,** 163–189 (2003).
8. Smyth, M. J., Kelly, J. M., Baxter, A. G., Körner, H. & Sedgwick, J. D. An essential role for tumor necrosis factor in natural killer cell-mediated tumor rejection in the peritoneum. *J. Exp. Med.* **188,** 1611–9 (1998).
9. Levitt, L. J. *et al.* Production of granulocyte/macrophage-colony-stimulating factor by human natural killer cells. Modulation by the p75 subunit of the interleukin 2 receptor and by the CD2 receptor. *J. Clin. Invest.* **88,** 67–75 (1991).

10. Narni-Mancinelli, E. *et al.* Complement factor P is a ligand for the natural killer cell-activating receptor NKp46. *Sci. Immunol.* **2,** (2017).

11. Leung, W.-H. *et al.* PRL-3 Mediates the Protein Maturation of ULBP2 by Regulating the Tyrosine Phosphorylation of HSP60. *J. Immunol.* **194,** 2930–2941 (2015).

12. Hanke, T. *et al.* Direct assessment of MHC class I binding by seven Ly49 inhibitory NK cell receptors. *Immunity* **11,** 67–77 (1999).

13. McFall, E. *et al.* Optimized Tetramer Analysis Reveals Ly49 Promiscuity for MHC Ligands. *J. Immunol.* (2013). doi:10.4049/jimmunol.1300726

14. Zhang, Q. *et al.* Mouse Nkrp1-Clr Gene Cluster Sequence and Expression Analyses Reveal Conservation of Tissue-Specific MHC-Independent Immunosurveillance. *PLoS One* **7,** e50561 (2012).

15. Karre, K., Ljunggren, H.-G., Piontek, G. & Kiessling, R. Selective rejection of H-2 deficient lymphoma varients suggests alternative immune defence strategy. *Nature* **319,** 675–678 (1986).

16. Ljunggren, H. G., Ohlén, C., Höglund, P., Franksson, L. & Kärre, K. The RMA-S lymphoma mutant; consequences of a peptide loading defect on immunological recognition and graft rejection. *Int. J. Cancer. Suppl.* **6,** 38–44 (1991).

17. Glas, R. *et al.* Recruitment and activation of natural killer (NK) cells in vivo determined by the target cell phenotype. An adaptive component of NK cell-mediated responses. *J. Exp. Med.* **191,** 129–38 (2000).

18. Öberg, L. *et al.* Loss or mismatch of MHC class I is sufficient to trigger NK cell-mediated rejection of resting lymphocytesin vivo– role of KARAP/DAP12-dependent and -independent pathways. *Eur. J. Immunol.* **34,** 1646–1653 (2004).

19. Miletić, A., Krmpotić, A. & Jonjić, S. The evolutionary arms race between NK cells and viruses: Who gets the short end of the stick? *Eur. J. Immunol.* **43,** 867–877 (2013).

20. Tu, M. M. *et al.* Ly49 family receptors are required for cancer immunosurveillance mediated by natural killer cells. *Cancer Res.* **74,** 3684–94 (2014).

21. Dimasi, N. & Biassoni, R. Structural and functional aspects of the Ly49 natural killer cell receptors. *Immunol. Cell Biol.* **83,** 1–8 (2005).

22. Wilhelm, B. T., Gagnier, L. & Mager, D. L. Sequence analysis of the ly49 cluster in C57BL/6 mice: a rapidly evolving multigene family in the immune system. *Genomics* **80,** 646–61 (2002).

23. Smith, K. M., Wu, J., Bakker, A. B. H., Phillips, J. H. & Lanier, L. L. Ly-49D and Ly-49H Associate with Mouse DAP12 and Form Activating Receptors. *J. Immunol.* **161,** 7–10 (1998).

24. Proteau, M.-F., Rousselle, E. & Makrigiannis, A. P. Mapping of the BALB/c Ly49 cluster defines a minimal natural killer cell receptor gene repertoire. *Genomics* **84,** 669–677 (2004).

25. Saleh, A. *et al.* Identification of probabilistic transcriptional switches in the Ly49 gene cluster: a eukaryotic mechanism for selective gene activation. *Immunity* **21,** 55–66 (2004).

26. Anderson, S. K. Probabilistic Bidirectional Promoter Switches: Noncoding RNA Takes Control. *Mol. Ther. - Nucleic Acids* **3,** e191 (2014).

27. Kelley, J., Walter, L., Trowsdale, J., Bryant, S. & Canese, K. Comparative Genomics of Natural Killer Cell Receptor Gene Clusters. *PLoS Genet.* **1,** e27 (2005).

28. Davies, G. E. *et al.* Identification of bidirectional promoters in the human KIR genes. *Genes Immun.* **8,** 245–253 (2007).

29. Mason, L. H. *et al.* Differential tyrosine phosphorylation of inhibitory versus activating Ly-49 receptor proteins and their recruitment of SHP-1 phosphatase. *J. Immunol.* **159,** 4187–96 (1997).

30. Vély, F. & Vivier, E. Conservation of structural features reveals the existence of a large family of inhibitory cell surface receptors and noninhibitory/activatory counterparts. *J. Immunol.* **159,** 2075–7 (1997).

31. Mason, L. H. *et al.* Cutting Edge: Characterization of an Associated 16-kDa Tyrosine Phosphoprotein Required for Ly-49D Signal Transduction 1. *J. Immunol.* **160,** 4148–4152 (1998).

32. Mócsai, A., Ruland, J. & Tybulewicz, V. L. J. The SYK tyrosine kinase: a crucial player in diverse biological functions. *Nat. Rev. Immunol.* **10,** 387–402 (2010).

33. Binstadt, B. A. *et al.* Sequential involvement of Lck and SHP-1 with MHC-recognizing receptors on NK cells inhibits FcR-initiated tyrosine kinase activation. *Immunity* **5,** 629–638 (1996).

34. Olcese, L. *et al.* Human and mouse killer-cell inhibitory receptors recruit PTP1C and PTP1D protein tyrosine phosphatases. *J. Immunol.* **156,** 4531–4 (1996).

35. Wang, J.-W. *et al.* Influence of SHIP on the NK Repertoire and Allogeneic Bone Marrow Transplantation. *Science (80-.).* **295,** (2002).

36. Nakamura, M. C. *et al.* Mouse Ly-49A Interrupts Early Signaling Events in Natural Killer Cell Cytotoxicity and Functionally Associates with the SHP-1 Tyrosine Phosphatase. *J. Exp. Med.* **185,** 673–684 (1997).

37. Long, E. O., Kim, H. S., Liu, D., Peterson, M. E. & Rajagopalan, S. Controlling natural killer cell responses: integration of signals for activation and inhibition. *Annu. Rev.*

Immunol. **31,** 227–58 (2013).

38. Mahmoud, A. B. *et al.* Influenza Virus Targets Class I MHC-Educated NK Cells for Immunoevasion. *PLOS Pathog.* **12,** e1005446 (2016).

39. Tay, C. H., Welsh, R. M. & Brutkiewicz, R. R. NK cell response to viral infections in beta 2-microglobulin-deficient mice. *J. Immunol.* **154,** 780–9 (1995).

40. Orr, M. T., Murphy, W. J. & Lanier, L. L. 'Unlicensed' natural killer cells dominate the response to cytomegalovirus infection. *Nat. Publ. Gr.* **11,** (2010).

41. Garstka, M. A. *et al.* The first step of peptide selection in antigen presentation by MHC class I molecules. *Proc. Natl. Acad. Sci. U. S. A.* **112,** 1505–10 (2015).

42. Cohen, G. B. *et al.* The Selective Downregulation of Class I Major Histocompatibility Complex Proteins by HIV-1 Protects HIV-Infected Cells from NK Cells. *Immunity* **10,** 661–671 (1999).

43. Held, W. & Kunz, B. An allele-specific, stochastic gene expression process controls the expression of multiple Ly49 family genes and generates a diverse, MHC-specific NK cell receptor repertoire. *Eur. J. Immunol.* **28,** 2407–2416 (1998).

44. Tanamachi, D. M., Hanke, T., Takizawa, H., Jamieson, A. M. & Raulet, D. R. Expression of natural killer receptor alleles at different Ly49 loci occurs independently and is regulated by major histocompatibility complex class I molecules. *J. Exp. Med.* **193,** 307–15 (2001).

45. Ortaldo, J. R. *et al.* Ly-49 receptor expression and functional analysis in multiple mouse strains. *J. Leukoc. Biol.* **66,** 512–20 (1999).

46. Coles, M. C., McMahon, C. W., Takizawa, H. & Raulet, D. H. Memory CD8 T lymphocytes express inhibitory MHC-specific Ly49 receptors. *Eur. J. Immunol.* **30,** 236–

244 (2000).

47. Cichocki, F. *et al.* Cutting edge: KIR antisense transcripts are processed into a 28-base PIWI-like RNA in human NK cells. *J. Immunol.* **185,** 2009–12 (2010).

48. Saleh, A., Makrigiannis, A. P., Hodge, D. L. & Anderson, S. K. Identification of a novel Ly49 promoter that is active in bone marrow and fetal thymus. *J. Immunol.* **168,** 5163–5169 (2002).

49. Gays, F., Taha, S. & Brooks, C. G. The Distal Upstream Promoter in Ly49 Genes, Pro1, Is Active in Mature NK Cells and T Cells, Does Not Require TATA Boxes, and Displays Enhancer Activity. *J. Immunol.* **194,** 6068–6081 (2015).

50. McCullen, M. V *et al.* Analysis of Ly49 gene transcripts in mature NK cells supports a role for the Pro1 element in gene activation, not gene expression. *Genes Immun.* **17,** 349–357 (2016).

51. Smith, H. R. *et al.* Nonstochastic coexpression of activation receptors on murine natural killer cells. *J. Exp. Med.* **191,** 1341–54 (2000).

52. Sundback, J., Karre, K. & Sentman, C. L. Cloning of Minimally Divergent Allelic Forms of the Natural Killer (NK) Receptor Ly-49C, Differentially Controlled by Host Genes in the MHC and NK Gene Complexes. *J. Immunol.* **157,** 3936–3942 (1996).

53. Yu, Y. Y. L. *et al.* The Role of Ly49A and 5E6(Ly49C) Molecules in Hybrid Resistance Mediated by Murine Natural Killer Cells Against Normal T Cell Blasts. *Immunity* **4,** 67–76 (1996).

54. Raulet, D. H. *et al.* Specificity, tolerance and developmental regulation of natural killer cells defined by expression of class I-specific Ly49 receptors. *Immunol. Rev.* **155,** 41–52 (1997).

55. Kim, S. *et al.* Licensing of natural killer cells by host major histocompatibility complex class I molecules. *Nature* **436,** 709–13 (2005).

56. Bix, M. *et al.* Rejection of class I MHC-deficient haemopoietic cells by irradiated MHC-matched mice. *Nature* **349,** 329–331 (1991).

57. Höglund, P. *et al.* Recognition of beta 2-microglobulin-negative (beta 2m-) T-cell blasts by natural killer cells from normal but not from beta 2m- mice: nonresponsiveness controlled by beta 2m- bone marrow in chimeric mice. *Proc. Natl. Acad. Sci. U. S. A.* **88,** 10332–6 (1991).

58. Höglund, P. & Brodin, P. Current perspectives of natural killer cell education by MHC class I molecules. *Nat. Rev. Immunol.* **10,** 724–734 (2010).

59. Brodin, P. & Höglund, P. Beyond licensing and disarming: a quantitative view on NK-cell education. *Eur. J. Immunol.* **38,** 2934–37 (2008).

60. Brodin, P., Lakshmikanth, T., Johansson, S., Karre, K. & Hoglund, P. The strength of inhibitory input during education quantitatively tunes the functional responsiveness of individual natural killer cells. *Blood* **113,** 2434–2441 (2009).

61. Brodin, P., Kärre, K. & Höglund, P. NK cell education: not an on-off switch but a tunable rheostat. *Trends Immunol.* **30,** 143–9 (2009).

62. Elliott, J. M., Wahle, J. A. & Yokoyama, W. M. MHC class I–deficient natural killer cells acquire a licensed phenotype after transfer into an MHC class I–sufficient environment. *J. Exp. Med.* **207,** 2073–2079 (2010).

63. Enqvist, M. *et al.* Coordinated Expression of DNAM-1 and LFA-1 in Educated NK Cells. *J. Immunol.* **194,** 4518–27 (2015).

64. Wagner, A. K. *et al.* Expression of CD226 is associated to but not required for NK cell

education. *Nat. Commun.* **8,** (2017).

65. Reits, E. A. J., Vos, J. C., Grommé, M. & Neefjes, J. The major substrates for TAP in vivo are derived from newlysynthesized proteins. *Nature* **404,** 774–778 (2000).

66. Hewitt, E. W. The MHC class I antigen presentation pathway: strategies for viral immune evasion. *Immunology* **110,** 163–9 (2003).

67. Bevan, M. J. Cross-priming for a secondary cytotoxic response to minor H antigens with H-2 congenic cells which do not cross-react in the cytotoxic assay. *J. Exp. Med.* **143,** 1283–8 (1976).

68. Bevan, M. J. Minor H antigens introduced on H-2 different stimulating cells cross-react at the cytotoxic T cell level during in vivo priming. *J. Immunol.* **117,** 2233–8 (1976).

69. Joffre, O. P., Segura, E., Savina, A. & Amigorena, S. Cross-presentation by dendritic cells. *Nat. Rev. Immunol.* **12,** 557–569 (2012).

70. Merwe, P. A. van der & Davis, S. J. Molecular interactions mediating T cell antigen recognition. *Annu. Rev. Immunol.* **21,** 659–684 (2003).

71. Kern, P. S. *et al.* Structural basis of CD8 coreceptor function revealed by crystallographic analysis of a murine CD8aa ectodomain fragment in complex with H-2K. *Immunity* **9,** 519–530 (1998).

72. Tormo, J., Natarajan, K., Margulies, D. H. & Mariuzza, R. A. Crystal structure of a lectin-like natural killer cell receptor bound to its MHC class I ligand. *Nature* **402,** 623–631 (1999).

73. Dam, J. *et al.* Variable MHC class I engagement by Ly49 natural killer cell receptors demonstrated by the crystal structure of Ly49C bound to H-2K(b). *Nat. Immunol.* **4,** 1213–22 (2003).

74. Su, R.-C. *et al.* Ly-49CB6 NK Inhibitory Receptor Recognizes Peptide-Receptive H-2Kb 1. *J. Immunol.* **163,** 5319–5330 (1999).

75. Marquez, E. A. & Kane, K. P. Identities of P2 and P3 Residues of H-2Kb-Bound Peptides Determine Mouse Ly49C Recognition. *PLoS One* **10,** e0131308 (2015).

76. Malnati, M. S. *et al.* Peptide specificity in the recognition of MHC class I by natural killer cell clones. *Science* **267,** 1016–8 (1995).

77. Peruzzi, M., Parker, K. C., Long, E. O. & Malnati, M. S. Peptide sequence requirements for the recognition of HLA-B*2705 by specific natural killer cells. *J. Immunol.* **157,** (1996).

78. Boyington, J. C., Motyka, S. a, Schuck, P., Brooks, a G. & Sun, P. D. Crystal structure of an NK cell immunoglobulin-like receptor in complex with its class I MHC ligand. *Nature* **405,** 537–543 (2000).

79. Kornberg, R. D. & Thomas, J. O. Chromatin structure; oligomers of the histones. *Science* **184,** 865–8 (1974).

80. Luger, K., Mäder, A. W., Richmond, R. K., Sargent, D. F. & Richmond, T. J. Crystal structure of the nucleosome core particle at 2.8 A resolution. *Nature* **389,** 251–60 (1997).

81. Teif, V. B. & Bohinc, K. Condensed DNA: Condensing the concepts. *Prog. Biophys. Mol. Biol.* **105,** 208–222 (2011).

82. Kwon, C. S. & Wagner, D. Unwinding chromatin for development and growth: a few genes at a time. *Trends Genet.* **23,** 403–12 (2007).

83. Roy, S. *et al.* Identification of functional elements and regulatory circuits by Drosophila modENCODE. *Science* **330,** 1787–97 (2010).

84. Talbert, P. B. & Henikoff, S. Histone variants--ancient wrap artists of the epigenome. *Nat.*

Rev. Mol. Cell Biol. **11,** 264–75 (2010).

85. Lowary, P. T. & Widom, J. New DNA sequence rules for high affinity binding to histone octamer and sequence-directed nucleosome positioning. *J. Mol. Biol.* **276,** 19–42 (1998).

86. Wyrick, J. J. *et al.* Chromosomal landscape of nucleosome-dependent gene expression and silencing in yeast. *Nature* **402,** 418–21 (1999).

87. Bai, L. & Morozov, A. V. Gene regulation by nucleosome positioning. *Trends Genet.* **26,** 476–83 (2010).

88. Lickwar, C. R. *et al.* The Set2/Rpd3S Pathway Suppresses Cryptic Transcription without Regard to Gene Length or Transcription Frequency. *PLoS One* **4,** e4886 (2009).

89. Ioshikhes, I. P., Albert, I., Zanton, S. J. & Pugh, B. F. Nucleosome positions predicted through comparative genomics. *Nat. Genet.* **38,** 1210–5 (2006).

90. Ito, T., Bulger, M., Pazin, M. J., Kobayashi, R. & Kadonaga, J. T. ACF, an ISWI-containing and ATP-utilizing chromatin assembly and remodeling factor. *Cell* **90,** 145–55 (1997).

91. Chandy, M., Gutiérrez, J. L., Prochasson, P. & Workman, J. L. SWI/SNF displaces SAGA-acetylated nucleosomes. *Eukaryot. Cell* **5,** 1738–47 (2006).

92. Sadeh, R. & Allis, C. D. Genome-wide 're'-modeling of nucleosome positions. *Cell* **147,** 263–6 (2011).

93. Peckham, H. E. *et al.* Nucleosome positioning signals in genomic DNA. *Genome Res.* **17,** 1170–7 (2007).

94. Segal, E. *et al.* A genomic code for nucleosome positioning. *Nature* **442,** 772–8 (2006).

95. Collings, C. K., Fernandez, A. G., Pitschka, C. G., Hawkins, T. B. & Anderson, J. N. Oligonucleotide sequence motifs as nucleosome positioning signals. *PLoS One* **5,** e10933

(2010).

96. Richmond, T. J. & Davey, C. A. The structure of DNA in the nucleosome core. *Nature* **423,** 145–50 (2003).

97. Ioshikhes, I., Hosid, S. & Pugh, B. F. Variety of genomic DNA patterns for nucleosome positioning. *Genome Res.* **21,** 1863–1871 (2011).

98. Fraser, R. M., Keszenman-Pereyra, D., Simmen, M. W. & Allan, J. High-resolution mapping of sequence-directed nucleosome positioning on genomic DNA. *J. Mol. Biol.* **390,** 292–305 (2009).

99. Albert, I. *et al.* Translational and rotational settings of H2A.Z nucleosomes across the Saccharomyces cerevisiae genome. *Nature* **446,** 572–6 (2007).

100. Mavrich, T. N. *et al.* Nucleosome organization in the Drosophila genome. *Nature* **453,** 358–62 (2008).

101. Salih, F., Salih, B. & Trifonov, E. N. Sequence structure of hidden 10.4-base repeat in the nucleosomes of C. elegans. *J. Biomol. Struct. Dyn.* **26,** 273–82 (2008).

102. Xi, L. *et al.* Predicting nucleosome positioning using a duration Hidden Markov Model. *BMC Bioinformatics* **11,** 346 (2010).

103. Lubliner, S. & Segal, E. Modeling interactions between adjacent nucleosomes improves genome-wide predictions of nucleosome occupancy. *Bioinformatics* **25,** i348-55 (2009).

104. Yuan, G.-C., Liu, J. S., Dura, J., Paro, R. & Loukinov, D. Genomic Sequence Is Highly Predictive of Local Nucleosome Depletion. *PLoS Comput. Biol.* **4,** e13 (2008).

105. Kaplan, N. *et al.* The DNA-encoded nucleosome organization of a eukaryotic genome. *Nature* **458,** 362–6 (2009).

106. Eddy, S. R. What is a hidden Markov model? *Nat. Biotechnol.* **22,** 1315–6 (2004).

107. Rouhi, A., Gagnier, L., Takei, F. & Mager, D. L. Evidence for epigenetic maintenance of Ly49a monoallelic gene expression. *J. Immunol.* **176,** 2991–9 (2006).

108. Eberharter, A. & Becker, P. B. Histone acetylation: a switch between repressive and permissive chromatin. Second in review series on chromatin dynamics. *EMBO Rep.* **3,** 224–9 (2002).

109. Min-Oo, G., Kamimura, Y., Hendricks, D. W., Nabekura, T. & Lanier, L. L. Natural killer cells: walking three paths down memory lane. *Trends Immunol.* **34,** 251–8 (2013).

110. Sun, J. C., Beilke, J. N. & Lanier, L. L. Adaptive immune features of natural killer cells. *Nature* **457,** 557–61 (2009).

111. Brown, M. G. *et al.* Vital Involvement of a Natural Killer Cell Activation Receptor in Resistance to Viral Infection. *Science (80-.).* **292,** (2001).

112. Nabekura, T. & Lanier, L. L. Antigen-specific expansion and differentiation of natural killer cells by alloantigen stimulation. *J. Exp. Med.* **211,** 2455–2465 (2014).

113. Guma, M. *et al.* Imprint of human cytomegalovirus infection on the NK cell receptor repertoire. *Blood* **104,** 3664–3671 (2004).

114. Muccio, L. *et al.* Analysis of memory-like Natural Killer cells in Human Cytomegalovirus-infected children undergoing αβ+T- and B-cell depleted HSCT for hematological malignancies. *Haematologica* (2015). doi:10.3324/haematol.2015.134155

115. Schlums, H. *et al.* Cytomegalovirus infection drives adaptive epigenetic diversification of NK cells with altered signaling and effector function. *Immunity* **42,** 443–456 (2015).

116. Zhang, T., Scott, J. M., Hwang, I. & Kim, S. Cutting edge: antibody-dependent memory-like NK cells distinguished by FcRγ deficiency. *J. Immunol.* **190,** 1402–6 (2013).

117. Cichocki, F. *et al.* CD56dimCD57+NKG2C+ NK cell expansion is associated with

reduced leukemia relapse after reduced intensity HCT. *Leukemia* **30,** 456–463 (2016).

118. Lima, J. F. *et al.* Distinct natural killer cells in HIV-exposed seronegative subjects with effector cytotoxic CD56(dim) and CD56(bright) cells and memory-like $CD57^{+}NKG2C^{+}$CD56(dim) cells. *J. Acquir. Immune Defic. Syndr.* **67,** 463–71 (2014).

119. Sarhan, D. *et al.* Adaptive NK Cells with Low TIGIT Expression Are Inherently Resistant to Myeloid-Derived Suppressor Cells. *Cancer Res.* **76,** 5696–5706 (2016).

120. Cooper, M. A. *et al.* Cytokine-induced memory-like natural killer cells. *Proc. Natl. Acad. Sci. U. S. A.* **106,** 1915–1919 (2009).

121. Keppel, M. P., Yang, L. & Cooper, M. A. Murine NK cell intrinsic cytokine-induced memory-like responses are maintained following homeostatic proliferation. *J. Immunol.* **190,** 4754–4762 (2013).

122. Jin, F. *et al.* The anti-tumor role of NK cells in vivo pre-activated and re-stimulated by interleukins in acute lymphoblastic leukemia. *Oncotarget* **7,** 79187–79202 (2016).

123. Wiencke, J. K. *et al.* The DNA methylation profile of activated human natural killer cells. *Epigenetics* **11,** 363–380 (2016).

124. O'Leary, J. G., Goodarzi, M., Drayton, D. L. & von Andrian, U. H. T cell- and B cell-independent adaptive immunity mediated by natural killer cells. *Nat. Immunol.* **7,** 507–516 (2006).

125. Bour, H. *et al.* Major histocompatibility complex class I-restricted CD8+ T cells and class II-restricted CD4+ T cells, respectively, mediate and regulate contact sensitivity to dinitrofluorobenzene. *Eur. J. Immunol.* **25,** 3006–10 (1995).

126. Paust, S. *et al.* Critical role for the chemokine receptor CXCR6 in NK cell-mediated antigen-specific memory of haptens and viruses. *Nat. Immunol.* **11,** 1127–1135 (2010).

127. Hohn, C. & Petrie-Hanson, L. Rag1-/- mutant zebrafish demonstrate specific protection following bacterial re-exposure. *PLoS One* **7,** e44451 (2012).

128. Reeves, R. K. *et al.* Antigen-specific NK cell memory in rhesus macaques. *Nat. Immunol.* **16,** 927–933 (2015).

129. Makrigiannis, A. P., Patel, D., Goulet, M.-L., Dewar, K. & Anderson, S. K. Direct sequence comparison of two divergent class I MHC natural killer cell receptor haplotypes. *Genes Immun.* **6,** 71–83 (2005).

130. Anderson, S. K., Dewar, K., Goulet, M.-L., Leveque, G. & Makrigiannis, A. P. Complete elucidation of a minimal class I MHC natural killer cell receptor haplotype. *Genes Immun.* **6,** 481–492 (2005).

131. Belanger, S., Tai, L.-H., Anderson, S. K. & Makrigiannis, A. P. Ly49 cluster sequence analysis in a mouse model of diabetes: an expanded repertoire of activating receptors in the NOD genome. *Genes Immun.* **9,** 509–521 (2008).

132. Henagan, T. M. *et al.* Sodium butyrate epigenetically modulates high-fat diet-induced skeletal muscle mitochondrial adaptation, obesity and insulin resistance through nucleosome positioning. *Br. J. Pharmacol.* **172,** 2782–98 (2015).

133. Bélanger, S. *et al.* Impaired natural killer cell self-education and 'missing-self' responses in Ly49-deficient mice. *Blood* 592–602 (2012). doi:10.1182/blood-2012-02-408732

134. Bellone, M. *et al.* Relevance of the Tumor Antigen in the Validation of Three Vaccination Strategies for Melanoma. *J. Immunol.* **165,** 2651–2656 (2000).

135. Fu, X. *et al.* Memory-Like Antigen-Specific Human NK Cells from TB Pleural Fluids Produced IL-22 in Response to IL-15 or Mycobacterium tuberculosis Antigens. *PLoS One* **11,** e0151721 (2016).

136. Liu, J. *et al.* Ly49I NK cell receptor transgene inhibition of rejection of H2b mouse bone marrow transplants. *J. Immunol.* **164,** 1793–9 (2000).

137. Mombaerts, P. *et al.* RAG-1-deficient mice have no mature B and T lymphocytes. *Cell* **68,** 869–877 (1992).

138. Fung-Leung, W. P. *et al.* CD8 is needed for development of cytotoxic T cells but not helper T cells. *Cell* **65,** 443–9 (1991).

139. Majewska-Szczepanik, M., Paust, S., von Andrian, U. H., Askenase, P. W. & Szczepanik, M. Natural killer cell-mediated contact sensitivity develops rapidly and depends on interferon-α, interferon-γ and interleukin-12. *Immunology* **140,** 98–110 (2013).

140. Gays, F. *et al.* The Mouse Tumor Cell Lines EL4 and RMA Display Mosaic Expression of NK-Related and Certain Other Surface Molecules and Appear to Have a Common Origin. *J. Immunol.* **164,** (2000).

141. Tsompana, M. & Buck, M. J. Chromatin accessibility: a window into the genome. *Epigenetics Chromatin* **7,** 33 (2014).

142. Xu, J., Vallejo, A. N., Jiang, Y., Weyand, C. M. & Goronzy, J. J. Distinct transcriptional control mechanisms of killer immunoglobulin-like receptors in natural killer (NK) and in T cells. *J. Biol. Chem.* **280,** 24277–24285 (2005).

143. Kadauke, S. & Blobel, G. A. Chromatin loops in gene regulation. *Biochim. Biophys. Acta* **1789,** 17–25 (2009).

144. Holwerda, S. & de Laat, W. Chromatin loops, gene positioning, and gene expression. *Front. Genet.* **3,** 217 (2012).

145. Taketa, D. A. & De Tomaso, A. W. Botryllus schlosseri allorecognition: tackling the enigma. *Dev. Comp. Immunol.* **48,** 254–265 (2014).

146. Khalturin, K., Becker, M., Rinkevich, B. & Bosch, T. C. G. Urochordates and the origin of natural killer cells: Identification of a CD94ŃKR-P1-related receptor in blood cells of Botryllus. *PNAS* **100,** 622–627 (2003).

147. De Tomaso, A. W. *et al.* Isolation and characterization of a protochordate histocompatibility locus. *Nature* **438,** 454–9 (2005).

148. Nyholm, S. V *et al.* fester, a Candidate Allorecognition Receptor from a Primitive Chordate. *Immunity* **25,** 163–173 (2006).

149. McKitrick, T. R., Muscat, C. C., Pierce, J. D., Bhattacharya, D. & De Tomaso, A. W. Allorecognition in a Basal Chordate Consists of Independent Activating and Inhibitory Pathways. *Immunity* **34,** 616–626 (2011).

150. Buss, L. W. Somatic cell parasitism and the evolution of somatic tissue compatibility. *PNAS* **79,** 5337–5341 (1982).

151. Kuo, L. J. & Yang, L.-X. Gamma-H2AX - a novel biomarker for DNA double-strand breaks. *In Vivo* **22,** 305–9

152. Rahim, M. M. A. *et al.* Ly49Q positively regulates type I IFN production by plasmacytoid dendritic cells in an immunoreceptor tyrosine-based inhibitory motif-dependent manner. *J. Immunol.* **190,** 3994–4004 (2013).

153. Cross, D. A. E., Alessi, D. R., Cohen, P., Andjelkovich, M. & Hemmings, B. A. Inhibition of glycogen synthase kinase-3 by insulin mediated by protein kinase B. *Nature* **378,** 785–789 (1995).

154. Doucey, M.-A. *et al.* Cis association of Ly49A with MHC class I restricts natural killer cell inhibition. *Nat. Immunol.* **5,** 328–336 (2004).

155. Marquez, E. A. Dependency of Ly49 Recognition on Anchor Residues of Peptide Bound

to MHC-I. (University of Alberta, 2015).

156. Chalifour, A. *et al.* A Role for cis Interaction between the Inhibitory Ly49A Receptor and MHC Class I for Natural Killer Cell Education. *Immunity* **30,** 337–347 (2009).

157. Bessoles, S. *et al.* Education of murine NK cells requires both cis and trans recognition of MHC class I molecules. *J. Immunol.* **191,** 5044–51 (2013).

158. Ebihara, T., Jonsson, A. H. & Yokoyama, W. M. Natural killer cell licensing in mice with inducible expression of MHC class I. *Proc. Natl. Acad. Sci. U. S. A.* **110,** E4232-7 (2013).

159. van den Boorn, J. G. *et al.* Inflammasome-Dependent Induction of Adaptive NK Cell Memory. *Immunity* **44,** 1406–1421 (2016).

160. Ebihara, T. *et al.* Identification of a polyI:C-inducible membrane protein that participates in dendritic cell–mediated natural killer cell activation. *J. Exp. Med.* **207,** 2675 (2010).

161. Lucas, M., Schachterle, W., Oberle, K., Aichele, P. & Diefenbach, A. Dendritic cells prime natural killer cells by trans-presenting interleukin 15. *Immunity* **26,** 503–17 (2007).

162. Luu, T. T. *et al.* Independent control of natural killer cell responsiveness and homeostasis at steady-state by CD11c+ dendritic cells. *Sci. Rep.* **6,** 37996 (2016).

163. Melief, C. J. M. Mini-review: Regulation of cytotoxic T lymphocyte responses by dendritic cells: peaceful coexistence of cross-priming and direct priming? *Eur. J. Immunol.* **33,** 2645–2654 (2003).

164. Meredith, M. M. *et al.* Expression of the zinc finger transcription factor zDC (Zbtb46, Btbd4) defines the classical dendritic cell lineage. *J. Exp. Med.* **209,** (2012).

165. Bernhard, C. A., Ried, C., Kochanek, S. & Brocker, T. CD169+ macrophages are sufficient for priming of CTLs with specificities left out by cross-priming dendritic cells. *Proc. Natl. Acad. Sci. U. S. A.* **112,** 5461–6 (2015).

166. Asano, K. *et al.* CD169-Positive Macrophages Dominate Antitumor Immunity by Crosspresenting Dead Cell-Associated Antigens. *Immunity* **34,** 85–95 (2011).

167. Olson, J. A. *et al.* NK cells mediate reduction of GVHD by inhibiting activated, alloreactive T cells while retaining GVT effects. *Blood* **115,** 4293–301 (2010).

168. Xu, Y. *et al.* Optogenetic control of chemokine receptor signal and T-cell migration. *Proc. Natl. Acad. Sci. U. S. A.* **111,** 6371–6 (2014).

169. Weir, G. M. *et al.* Metronomic cyclophosphamide enhances HPV16E7 peptide vaccine induced antigen-specific and cytotoxic T-cell mediated antitumor immune response. *Oncoimmunology* **3,** e953407 (2014).

170. Berinstein, N. L. *et al.* Survivin-targeted immunotherapy drives robust polyfunctional T cell generation and differentiation in advanced ovarian cancer patients. *Oncoimmunology* **4,** e1026529 (2015).

171. Wight, A. *et al.* Nucleosome Presence at AML-1 Binding Sites Inversely Correlates with Ly49 Expression: Revelations from an Informatics Analysis of Nucleosomes and Immune Cell Transcription Factors. *PLOS Comput. Biol.* **12,** e1004894 (2016).

Contributions of Collaborators

Drs. Doo Yang and Ilya Ioshikhes designed and assisted me with the *in silico* analyses presented in figures 6 to 11. Dr. Ahmad Mahmoud prepared the initial batches of hybridoma-derived antibodies, and taught me to continue this antibody production. Drs. Mir Munir Rahim and Megan Tu performed initial animal handling while I was becoming certified for animal use.

Appendix I

Nucleosome Presence at AML-1 Binding Sites Inversely Correlates with Ly49 Expression: Revelations from an Informatics Analysis of Nucleosomes and Immune Cell Transcription Factors

Andrew Wight, Doo Yang, Ilya Ioshikhes, and Andrew P. Makrigiannis

Contributions: A.W. performed an equal share of the *in silico* modeling, all of the laboratory work confirming these results, and spearheaded the writing of the manuscript.

Published: PLoS Computational Biology, April 2016